Mathematical Models Assessing the Importance of Disease on Ecological Invasions

Sally Sue Bell

Submitted for the degree of Doctor of Philosophy

Heriot-Watt University

Department of Mathematics,

School of Mathematical and Computer Sciences.

March, 2010

Abstract

A general understanding of the role that both shared disease and competition may play in ecological invasions is lacking. We develop a theoretical framework to determine the role of disease, in addition to competition, in invasions.

We first investigate the effect of disease characteristics on the replacement time of a native species by an invader. The outcome is critically dependent on the relative effects that the disease has on the two species and less dependent on the basic epidemiological characteristics of the interaction. This framework is extended to investigate the effect of disease on the spatial spread of an invader and indicates that a wave of disease spreads through a native population in advance of the replacement.

A probabilistic simulation model is developed to examine the particular example of the replacement of red squirrels by grey squirrels in the United Kingdom. This model is used to examine conservation strategies employed within red squirrel refuges and compared to observations from Sefton Coast Red Squirrel Refuge. Our findings indicate that culling greys may be effective at protecting red populations from replacement, but none of the conservation strategies currently employed can prevent periodic outbreaks of infection within red squirrel refuges.

ACKNOWLEDGEMENTS

Firstly, and most importantly, I thank my supervisor Andy White for all his help, knowledge and encouragement during my PhD. A big thank-you must also go to Mike Boots for his excellent input to my work over the years. Andy's expertise in maths modelling and Mike's ecological knowledge made them a supervision dream-team for me. My experience of writing this thesis was made much less painful by their patience and excellent proof-reading.

A special thank-you must also go to Jonathan Sherratt for his help and guidance with my work. I really enjoyed working with him on the spatial modelling section and his guidance with mathematical writing was much needed and appreciated.

My work also benefited from discussions with many different people over the years including Matthew Smith, Gabriel Lord and Fiona Whitfield to name but a few. I also recognise the input of editorial board member Mark Lewis and two anonymous referees for the journal Theoretical Ecology, whose valuable comments on a submitted paper improved the content of Chapters 2 and 3. My chats with Katie Russell, Emma Coutts and Jenny Bloomfield may not always have been about work but they were always appreciated and fun!

I acknowledge the support of Heriot-Watt University and also the generous funding provided through an Engineering and Physical Sciences Research Council studentship award.

Thanks also to all at Greenspace, especially Neil, for all their support while I tried to balance a job with writing a thesis.

Last, but definitely not least, a very very big thank-you to Toby for being there with me through the whole thing from start to finish!

Contents

Abstract ii

Acknowledgements iii

List of Tables vi

List of Figures vii

1 Introduction 1
- 1.1 Overview . . . 1
- 1.2 Mathematical modelling of ecological interactions . . . 3
- 1.3 Squirrels in the UK . . . 5
- 1.4 Main objectives . . . 7
- 1.5 Outline of thesis . . . 8

2 Temporal Modelling of Invasion Dynamics 10
- 2.1 Introduction . . . 10
- 2.2 Model . . . 16
- 2.3 Results . . . 17
  - 2.3.1 Disease-induced fecundity loss . . . 21
  - 2.3.2 Disease-induced mortality . . . 23
  - 2.3.3 Recovery from disease . . . 24
  - 2.3.4 Generality of results . . . 24
- 2.4 Discussion . . . 27
- 2.5 Appendix . . . 30
  - 2.5.1 Competition-only model . . . 30
  - 2.5.2 Disease-only model . . . 34
  - 2.5.3 Full model . . . 38

3 Spatial Modelling of Invasion Dynamics 46
- 3.1 Introduction . . . 46
- 3.2 Model . . . 49
- 3.3 Results . . . 49
  - 3.3.1 Critical wave speed . . . 51
  - 3.3.2 Range of spatial spread . . . 60
- 3.4 Discussion . . . 61

4 A Stochastic Framework for Modelling Competition and Disease **65**
4.1 Introduction . . . 65
4.2 Model . . . 66
4.3 Results . . . 70
4.3.1 Competition-only scenario . . . 70
4.3.2 Competition-and-infection scenario . . . 71
4.3.3 Grey-only scenario . . . 73
4.3.4 Model modifications . . . 85
4.4 Discussion . . . 87

5 A Stochastic Model of a Red Squirrel Refuge **90**
5.1 Introduction . . . 90
5.2 Model . . . 95
5.3 Results . . . 96
5.3.1 Buffer zone characteristics . . . 97
5.3.2 Management strategies . . . 100
5.4 Discussion . . . 102

6 Discussion **107**
6.1 The impact of disease on ecological invasions . . . 107
6.2 The spatial spread of invading species . . . 109
6.3 Red squirrels, grey squirrels and squirrelpox . . . 110
6.4 Red squirrel conservation . . . 110
6.5 The future of red squirrels in the UK . . . 112

References **113**

List of Tables

2.1 Invadability criteria 15
2.2 Summary of parameters used in equations (2.3a–d). 17

4.1 Parameters used in Tompkins *et al.* (2003). 67
4.2 Events in the stochastic Tompkins *et al.* (2003) model. 69
4.3 Virus transmission rate (β) 77
4.4 Virus transmission rate (β) with seroprevalence defined as $\frac{I_G^*+R_G^*}{S_G^*+I_G^*+R_G^*}$. . . . 78

List of Figures

2.1 Competition-only replacement . . . 21
2.2 Competition-and-disease-mediated replacement . . . 22
2.3 SIS, SIR and SIRS model frameworks . . . 26

3.1 Fisher-type equation . . . 47
3.2 Spatial replacement . . . 50
3.3 Spatial replacement highlighting competition-only wave, wave of replacement and wave of disease. . . . 52
3.4 Observed and critical wave speeds . . . 60
3.5 Heterogeneous landscape . . . 61

4.1 Tompkins *et al.* (2003) model with and without disease . . . 67
4.2 Tompkins *et al.* (2003) model showing different classes of reds and greys. 68
4.3 Competition-mediated stochastic model with one grey. . . . 70
4.4 Competition-mediated stochastic model with two, five and ten greys. . . . 71
4.5 Competition-and-infection-mediated stochastic model with one grey. . . . 72
4.6 Competition-and-infection-mediated stochastic model with two, five and ten greys. . . . 72
4.7 Competition-and-infection-mediated stochastic model with two greys (time plot). . . . 73
4.8 Grey-only stochastic model with one infected grey. . . . 74
4.9 Effect of varying carrying capacity on grey-only stochastic model. . . . 76
4.10 Effect of varying seroprevalence in the grey-only stochastic model. . . . 77
4.11 Effect of varying recovery on grey-only stochastic model with $K_G = 1500$. 79
4.12 Effect of varying recovery on disease persistence. . . . 79
4.13 Effect of varying recovery in the grey-only stochastic model. . . . 80
4.14 One-dimension grid for spatial stochastic model . . . 80
4.15 Outcomes from one-dimensional spatial stochastic model with carrying capacity of 80 . . . 81
4.16 Effect on different classes in one-dimensional spatial stochastic model with carrying capacity of 80 . . . 82
4.17 Outcomes from one-dimensional spatial stochastic model with carrying capacity of 80 . . . 82
4.18 Effect on different classes in one-dimensional spatial stochastic model with carrying capacity of 80 . . . 83
4.19 Outcomes from one-dimensional spatial stochastic model with carrying capacity of 1500 . . . 83

4.20 Effect on different classes in one-dimensional spatial stochastic model with carrying capacity of 1500 84
4.21 Competition-mediated stochastic model with carrying capacities K_G = 1500 and K_R = 1125. 85
4.22 Competition-only and competition-and-infection spatial stochastic model 86
4.23 Spread of different classes in competition-only and competition-and-infection spatial stochastic model 87

5.1 Sefton Coast Refuge and Buffer Zone map 93
5.2 Population index of Sefton Coast red squirrel refuge 94
5.3 A schematic representation of the refuge, buffer zone and landscape patches. 95
5.4 Population densities in refuge and buffer zone with no conservation strategies in place (baseline scenario) 97
5.5 Population densities in refuge and buffer zone with lowered connectivity between buffer zone and landscape 98
5.6 Population densities in refuge and buffer zone with reduced habitat suitability for squirrels in buffer zone. 100
5.7 Refuge and buffer zone, with culling of greys twice a year. 105
5.8 Population densities in the refuge and buffer zone, with grey squirrel control. 106

Chapter 1

Introduction

1.1 Overview

Ecological invasions, in which new species attempt to establish themselves in non-native environments, are a world-wide problem with major economic repercussions. They are widely acknowledged to be one of the main threats to native biodiversity and ecosystem function (Sala *et al.*, 2000; Kolar and Lodge, 2001). Regardless of this, we continue at an ever increasing rate to introduce alien species into new ecosystems (Pimentel *et al.*, 2001) with potentially devastating consequences for native species. A further concern is the change in species' natural ranges as a result of predicted changes in climate (Dukes and Mooney, 1999; Ims *et al.*, 2008).

Some well-studied invasions, from across the world, include the invasion of Nile perch, *Lates niloticus*, into Lake Victoria (Kolar and Lodge, 2001) and the rapid spread of the European zebra mussel, *Dreissena polymorpha*, through North America (Lodge, 1993). It is unknown how many non-native species are present within the United Kingdom (UK), some well-known examples are highlighted below (further examples are included in later chapters).

Giant hogweed (*Herracleum mantegazzianum*), native in South-West Asia, was introduced to the UK in the 1800s as an ornamental plant but it has rapidly spread and is now common along river banks, roadsides and waste-ground. It produces a large number of seed and long-distance dispersal is possible along waterways (Tiley *et al.*, 1996). The seeds can also be accidentally dispersed when present in soil (Cook *et al.*, 2007). Giant hogweed is seen as a threat to UK biodiversity as it shades out and replaces native flora (Manchester and Bullock, 2000). It is also a danger to human health as it can

cause phytophotodermatitis if contact occurs with the skin, resulting in sensitivity to the sun, pigmentation and blistering for up to six years following contact (Tiley *et al.*, 1996). This threat to human health makes any eradication programme less manageable and due to the large seed base it is believed that any clearance needs to be followed up by seven years of further controls (Manchester and Bullock, 2000). A second invasive plant causing problems in the UK is rhododendron (*Rhododendron ponticum*), which is found in woodland, grassland and heaths and believed to inhibit native woodland regeneration and cause major changes in soils (Manchester and Bullock, 2000). Like giant hogweed, it is difficult and expensive to control with any clearance requiring follow-up controls such as herbicide spraying.

Our third example of a well-known plant invader in the UK is Japanese knotweed, *Fallopia japonica*, it not only displaces native plants but also damages roads and pavements. Following its introduction in the 1800s, it has spread throughout the entire UK with the exception of the islands of Orkney in Scotland (Kidd, 2000). Its control is costly as it requires that all plants and rhizomes, horizontal stems found underground, are killed (Manchester and Bullock, 2000). A consortium of organisations, including DEFRA and Network Rail, have formed the "Japanese Knotweed Alliance" and are currently proposing the introduction of a biological control (Kidd, 2000).

Turning our focus away from plant invasions, the New Zealand flatworm, *Artioposthia triangulata*, was accidentally introduced into the UK relatively recently in plant pots, with the first recorded sightings dating from the 1960s (Cannon *et al.*, 1999). They are believed to replace the native earthworms and potentially reduce them to extinction, hence impacting soil processes (Manchester and Bullock, 2000). There is not a recognised chemical control for New Zealand flatworm and no known biological controls, so current strategies rely on physical and cultural methods (Cannon *et al.*, 1999).

The final two examples, outlined here, are the North American signal crayfish (*Pacifastacus leniusculus*) and the grey squirrel (*Sciurus carolinensis*); both of these species threaten to replace native species (the white-clawed crayfish, *Austropotamobius pallipes*, and the red squirrel, *Sciurus vulgaris*, respectively). Both of the native species have been replaced across much of the UK as a result of the invading species, and are under constant threat of further replacement (Reynolds, 1985; Cerenius *et al.*, 2003). In both cases the invader is a superior competitor and also carries a disease that is much more lethal to the

native than to the invading species.

The crayfish and squirrel examples highlight the importance of disease in ecological invasions. It has become increasingly recognised that disease plays an important part in ecological invasions, although our theoretical understanding of this is lacking and requires further research (Prenter *et al.*, 2004). Within this thesis, we will incorporate the influence of disease and competition, using mathematical modelling to gain an insight into the underlying causes of ecological replacement of a native species by an alien invader.

1.2 Mathematical modelling of ecological interactions

The logistic equation, first proposed for use in ecology by Verhulst in 1838, describes population growth of one species (Begon *et al.*, 1996). It is a simple, but very powerful, continuous-time model:

$$\frac{dH}{dt} = rH\left(1 - \frac{H}{K}\right). \tag{1.1}$$

Here, H represents the density of individuals, r the growth rate (birth rate − death rate) and K is the carrying capacity. The single population is subject to density dependence, with the population reaching a stable equilibrium at its carrying capacity. The logistic equation, although simple, has played a significant role in the development of ecology.

The logistic equation formed the basis for the Lotka-Volterra equations (proposed by Volterra in 1926 and Lotka in 1932), they can be expressed as follows

$$\frac{dH_1}{dt} = r_1 H_1\left(1 - \frac{H_1 + c_2 H_2}{K_1}\right) \tag{1.2a}$$

$$\frac{dH_2}{dt} = r_2 H_2\left(1 - \frac{H_2 + c_1 H_1}{K_2}\right). \tag{1.2b}$$

These equations model two species, species 1 and species 2, all parameters have a subscript i which equals 1 or 2 and refers to each species respectively. H_i represents the number of individuals, r_i the growth rate (birth rate − death rate), K_i the carrying capacity and c_i the competitive effect of species i on the other species. The logistic equation is used to model one species subject to intraspecific competition, while the Lotka-Volterrra equations model the interaction between two species subject to intraspecific and interspecific

competition.

The Lotka-Volterra equations greatly enhanced ecological understanding of predator-prey dynamics, especially the oscillatory population levels observed (Murray, 2002). They also provide theoretical evidence to support the competitive exclusion principal which states that two species that compete for the same resources cannot coexist stably (Begon *et al.*, 1996).

Similar modelling techniques have also been developed to investigate the effect of disease on ecological populations. One of the earliest was proposed by Kermack and McKendrick (1927) to model the Bombay Plague Epidemic in 1905 and 1906. A special case of their model has formed one of the simplest and yet most influential models, in this field (Brauer, 2005). It is aptly named the Kermack-McKendrick epidemic model and consists of three ordinary differential equations as follows

$$\frac{dS}{dt} = -\beta S I \tag{1.3a}$$

$$\frac{dI}{dt} = \beta S I - \gamma I \tag{1.3b}$$

$$\frac{dR}{dt} = \gamma I. \tag{1.3c}$$

The population is split into three classes susceptible (S), infected (I) and removed (R) with β representing the infection rate and γ the removal rate. All the parameters are non-negative and the model maintains a constant population size as $\frac{dS}{dt} + \frac{dI}{dt} + \frac{dR}{dt} = 0$. Although this model is simple, it produces broadly relevant results and introduces us to the basic reproductive number (R_0). R_0 is the expected number of secondary infections caused from one infected individual entering a purely susceptible population ($R_0 = \frac{\beta S_0}{\gamma}$ here, where S_0 is the initial number of susceptibles). If $R_0 > 1$ an epidemic will occur and if $R_0 < 1$ it will not, R_0 is a very powerful threshold value when considering a potential epidemic or the viability of vaccination (Murray, 2002).

The Kermack-McKendrick model formed the basis for many models offering further insight into the effect of disease on a population including Anderson and May (1978) and May and Anderson (1978). Anderson and May (1981) considered a number of different variations, to analyse the different effects of disease including reduction in fecundity, density dependence and the effect of vertical transmission. Their work was further extended

by Holt and Pickering (1985) to consider the effect of two species with a shared disease.

These two areas of similar modelling techniques, the first considering competition and the second disease were first joined to consider the combined effects of intraspecific competition and disease (Begon *et al.*, 1992; Greenman and Hudson, 1997; Hethcote *et al.*, 2005). This work was further extended to include both intraspecific and interspecific competition (Bowers and Turner, 1997; Saenz and Hethcote, 2006). These model frameworks have greatly improved the theoretical understanding of interactions between species.

All the models discussed so far, have considered temporal but not spatial population dynamics. The addition of space into these models is often achieved using a diffusion term (Murray, 2002). Examples of this method of modelling spatial spread (known as reaction-diffusion equations) include the modelling of an advantageous gene through a population by Fisher (1937), the spread of the muskrat (*Ondatra zibethica*) through Europe by Skellam (1951) and the spread of rabies through foxes by Murray *et al.* (1986).

Another possible extension to these continuous-time models is to develop a probabilistic simulation model that takes stochastic effects into consideration. These methods are discussed in detail in Renshaw (1991) and are based on the underlying deterministic frameworks.

One of the aims of this study is to further develop temporal, spatial and probabilistic frameworks to provide a fuller understanding of how competition and a shared disease affect the characteristics of invasion and replacement of native species. We also wish to use insight gained from examining models of competition and disease to allow us to further develop our understanding of the replacement of red squirrels by greys within the UK. Thus, we will outline the background relating the grey squirrel invasion in the UK.

1.3 Squirrels in the UK

The North American grey squirrel was introduced to the UK in 1876, since then it has replaced the native red squirrel throughout much of the UK (Middleton, 1930; Lloyd, 1983; Reynolds, 1985). There are believed to be only 160,000 red squirrels left in the UK, with the majority found in Scotland (Harris *et al.*, 1995; Battersby and Partnership, 2005). It was not initially believed that the decline of red squirrels within the UK was being caused by the introduced grey squirrel (notably Middleton (1932) discounted it).

However, over time as the spread of the greys and associated decline of reds continued, it was accepted that greys were replacing reds and this was initially believed to be as a result of competition for resources (Reynolds, 1985; Gurnell, 1987).

A mathematical model of competition between red and grey squirrels was presented by Okubo *et al.* (1989). They developed a continuous-time deterministic model of a Lotka-Volterra type and considered both competition and diffusion. The model consisted of a set of coupled reaction-diffusion equations (this modelling method is discussed in detail in Chapter 3). They assumed the greys out-competed the reds and "investigated the possibility of travelling waves of invasion of grey squirrels that drive out the reds". They compared their theoretical findings to the field evidence documented by Reynolds (1985) who monitored the spread of grey squirrels through East Anglia from 1961 to 1981. They concluded that competition could account for the replacement of red squirrels by greys.

A different modelling technique was presented by Rushton *et al.* (1997), who used an integrated Geographical Information System (GIS)-spatially explicit population dynamics model. The model simulated mortality, reproduction and dispersal in individual populations of red or grey squirrels within habitat blocks identified using GIS. The squirrels were able to move between the habitat blocks and interspecific competition occurred if both species were present within a block. They also made a comparison with the field data of Reynolds (1985) and modelled the spread of the grey squirrels through East Anglia. They investigated the effect of adult mortality, juvenile mortality, fecundity, carrying capacity and maximum dispersal distance on the spread of grey squirrels. Their results found that fecundity rates had to be raised and the mortality rates lowered from the observed rates to allow a reasonable match with the field data of Reynolds (1985). They conclude in their discussion that competition alone "was sufficient to explain the decline of the red squirrel in Norfolk as the grey expanded its range".

The model presented by Rushton *et al.* (1997) was further extended to include squirrelpox and the results published in 2000 (Rushton *et al.*, 2000). Squirrelpox is a disease shared by red and grey squirrels; it is harmless (at least under laboratory conditions) to greys and lethal to reds (Tompkins *et al.*, 2002). They investigated the effect of different disease parameters including persistence, encounter rate and infection rate. They again compared their findings to those of Reynolds (1985) and concluded that disease could be a potential cause of decline in red squirrels. A deterministic model presented by Tompkins

et al. (2003), further extended our understanding of the role of squirrelpox in the interaction. They showed that competition alone could explain the replacement of red squirrels by greys (again in East Anglia, with Reynolds' (1985) results used for comparison) but at a slower rate than the observed rate. However, the addition of squirrelpox to the model allowed the grey squirrels to replace the reds at a comparable rate to the observed rates. They concluded that squirrelpox was necessary to explain the rapid replacement of red squirrels by grey across the UK.

The importance of squirrelpox in the replacement of red squirrels by greys was further discussed by Rushton *et al.* (2006). They gathered records of red and grey squirrels in Cumbria between 1993 and 2003, and produced comparable maps to those used by Reynolds (1985). Using the models outlined in Rushton *et al.* (1997) and (2000), they investigated the effect of squirrelpox and concluded that the replacement rate of red squirrels by greys is 17–25 times faster if the disease is present. The use of mathematical models in all these studies has greatly improved our understanding of the red and grey squirrel system within the UK.

We hope to use mathematical models to further explore scenarios where a shared disease is influencing an ecological replacement. In the context of squirrels, we hope to build on the work of Tompkins *et al.* (2003), to further develop our understanding of squirrelpox within this system and to investigate current conservation and management strategies employed for the protection of red squirrels within the UK.

1.4 Main objectives

The main objectives of this thesis are as follows:

1. Use mathematical models to help understand the spread of disease in invasive systems. We will concentrate on the effect of disease on the replacement time of a naive native by an alien invader.

2. Analyse the effect of disease on the spatial spread of an alien invader.

3. Develop a red/grey/squirrelpox model to allow modelling of different conservation and management strategies.

4. Evaluate the effectiveness of these conservation and management strategies by modelling a red squirrel refuge (based on the refuge at Formby, Merseyside).

1.5 Outline of thesis

A general outline of the thesis is as follows: in Chapter 2 we consider a two-host shared-parasite framework to examine the effect of disease on the replacement time of ecological invasion. We consider the effect of the relative magnitude of disease-induced fecundity loss, disease-induced mortality and recovery from disease on the replacement time of a native species by an alien invader. In Chapter 3, we extend the temporal findings for the replacement of a native species to a spatial model framework. The spread of the invading species across the landscape is analysed algebraically and critical wave speeds are compared to numerical simulations. An important general phenomenon is highlighted by comparing the wave speed of the disease and the wave speed of replacement in this system.

In both Chapter 2 and Chapter 3, we consider deterministic modelling frameworks for general two-host shared-parasite scenarios. The work in these two chapters provides a good insight into the effect of disease, both temporally and spatially, on the replacement of a native species by an alien invader. We also wish to consider the particular example of the replacement of the UK's native red squirrels by the invading grey squirrel. We begin this examination in Chapter 4 by developing a stochastic individual-based modelling framework for the red/grey/squirrelpox system based on the Tompkins *et al.* (2003) deterministic model framework. In this chapter, we provide an overview of the model studied by Tompkins *et al.* (2003) and detail the method used to build the probabilistic simulation model. This stochastic model is tested and compares favourably with the previous studies on the red/grey/squirrelpox system.

The framework described in Chapter 4 provides a suitable model for the squirrel system and is extended in Chapter 5 to consider a red squirrel refuge model (based on the refuge at Formby, Merseyside). We assess the population dynamics of the red squirrels in the refuge under different conservation and management strategies representing culling of grey squirrels and including a buffer zone around the refuge of unsuitable habitat. The results compare well with observations from the Formby squirrel system.

In the final chapter, we draw together the findings from the previous four chapters: we compare the different modelling techniques considered and their relevance to different ecological examples. We pay particular attention to the red/grey/squirrelpox system and further discuss the current situation within the UK.

I was the primary researcher for all of the work presented in this thesis. The findings described in Chapters 2 and 3 are published in *Theoretical Ecology*, see Bell *et al.* (2009). The work in Chapter 4 is a necessary foundation for the refuge model described in Chapter 5, which is currently being prepared as an article for submission.

Chapter 2

Temporal Modelling of Invasion Dynamics

2.1 Introduction

There is much interest in examining the effect that new or introduced species may have on native ecosystems. The catastrophic damage to native communities of past introductions such as Nile perch, *Lates niloticus*, into Lake Victoria (Kolar and Lodge, 2001) and the rapid spread of the European zebra mussel, *Dreissena polymorpha*, through North America (Lodge, 1993; Vitousek *et al.*, 1996; Pimentel *et al.*, 2001) provides evidence of the role invading species play in reshaping ecosystems. Notwithstanding the documented negative effects on species diversity, the rate at which human activity is introducing species, either accidentally or deliberately, into new habitats is still increasing (Prenter *et al.*, 2004). The large majority of these organisms die-out shortly after introduction, but those invasive species which establish themselves are recognised as a major international threat to native biodiversity (Vitousek *et al.*, 1997; Sala *et al.*, 2000; Kolar and Lodge, 2001). In addition to these human-induced species introductions, current and predicted changes to the climate are likely to lead to significant shifts in species ranges which are also likely to threaten native systems (Dukes and Mooney, 1999; Ims *et al.*, 2008). In general, there are likely to be many factors which affect the success and rate of spread of invasive species, including differences in resource utilisation or life history characteristics between the invasive and native species. More recently a number of studies have highlighted the role of infectious disease as an important determinant in native survival and invasive success (Hudson and Greenman, 1998; Daszak *et al.*, 2000; Prenter *et al.*, 2004).

Commonly, when disease has been considered in the context of invasions, it has been as part of the enemy escape hypothesis. Here the invasive species is thought to gain an advantage in its new environment by virtue of escaping its natural enemies, including virulent parasites as well as predators. For example, Aliabadi and Juliano (2002) found that when the invasive Asian tiger mosquito, *Aedes albopictus*, is released in North America, it initially experiences reduced infection by its gut parasite *Ascogregarina taiwanensis*. This escape gives it a small, but significant, competitive advantage over the native tree-hole mosquito, *Ochlerotatus triseriatus*, allowing it to expand its range more rapidly. It is also increasingly recognised that an invading species can gain an advantage by introducing a novel harmful disease to the native system. This scenario, in which the parasite acts as a "biological weapon", has been an important factor in the replacement of the UK's only native crayfish. The white-clawed crayfish, *Austropotamobius pallipes*, has been replaced throughout much of its range by the introduced North American signal crayfish (*Pascifastacus leniusculus*). The white-clawed crayfish suffers both as a result of competition for resources from the larger and more aggressive signal crayfish, and also the transmission of crayfish plague, *Aphanomyces astaci*, from the invading species. Signal crayfish are resistant to crayfish plague (Cerenius *et al.*, 2003), which is lethal to white-clawed crayfish and has been responsible for mass mortality in many British crayfish populations (Holdich, 2003; Bubb *et al.*, 2004). Other examples include: the replacement of the pedunculate oak, *Quercus robur*, in the UK by the introduced Turkey oak, *Quercus cerris*, due to the impact of the knopper gall wasp, *Andricus quercuscalicis*, which causes huge acorn losses to the native species but has little effect on the introduced species (Hails and Crawley, 1991); monogenean gill fluke, *Nitzschia sturionis*, which was introduced with the Caspian Sea sturgeon, *Huso huso*, in the 1930s and has detrimentally affected the density of the Aral Sea Sturgeon, *Acipenser nudiventris*, (Rohde, 1984); and the expansion of the white-tailed deer, *Odocoileus virginianus*, in North America into territories occupied by moose, *Alces alces*, and caribou, *Rangifer tarandus*, which was aided by the meningeal worm *Parelaphostrongylus tenuis* which is carried by the white-tailed deer but lethal to the other species (Anderson, 1972; Bergerud and Mercer, 1989; Pybus *et al.*, 1990; Oates *et al.*, 2000).

A well known example of invasion and replacement is the decline of the UK's native red squirrels, *Sciurus vulgaris*, over the past 70 years as a result of the introduced North

American grey squirrel, *Sciurus carolinensis*, (Middleton, 1930; Lloyd, 1983; Reynolds, 1985). Red replacement was traditionally believed to result solely from the superior competitive ability of the greys (Okubo *et al.*, 1989). However, recent evidence has revealed the existence of an infectious disease, squirrelpox, which is shared between the two species (Rushton *et al.*, 2000) but is harmless (at least under laboratory conditions) to greys and lethal to reds (Tompkins *et al.*, 2002). In models of the system, the inclusion of the effects of squirrelpox was necessary to explain the rapid replacement of red squirrels by greys in the UK (Tompkins *et al.*, 2003; Rushton *et al.*, 2006).

In all of the above examples the invader gained an advantage through disease. However, there are also examples where disease can be advantageous to the native species. Hoogendoorn and Heimpel (2002) examined ladybird beetles in North America; the native species *Coleomegilla maculata* suffers less from the parasitoid *Dinocampus coccinellae* when the alien species *Harmonia axyridis* is present. This lessens the competitive effects of the alien ladybird beetle and slows the rate of alien invasion. There is also evidence that infectious disease that is endemic in the native population may be highly pathogenic to invading species and therefore prevent the invader from establishing (Hilker *et al.*, 2005; Petrovskii *et al.*, 2005).

An important open question is, how the characteristics of particular parasite interactions affect the likelihood and rate of invasion by different species. In this chapter, a theoretical framework is developed to understand how disease in combination with competition can affect the success of invasion, and the time taken for a native species to be replaced by an invader. Holt and Pickering (1985) studied the effect of an infectious disease attacking two host species. Their model is a two-host version of model B in Anderson and May (1981). It consists of the following four ordinary differential equations with S_i representing the density of individuals susceptible to the disease and I_i the density

of infected individuals in host species i (1 or 2)

$$\frac{dS_1}{dt} = r_1 S_1 - \beta_{11} S_1 I_1 - \beta_{12} S_1 I_2 + a_1(1 - f_1) I_1 + \gamma_1 I_1 \tag{2.1a}$$

$$\frac{dI_1}{dt} = \beta_{11} S_1 I_1 + \beta_{12} S_1 I_2 - d_1 I_1 \tag{2.1b}$$

$$\frac{dS_2}{dt} = r_2 S_2 - \beta_{22} S_2 I_2 - \beta_{21} S_2 I_1 + a_2(1 - f_2) I_2 + \gamma_2 I_2 \tag{2.1c}$$

$$\frac{dI_2}{dt} = \beta_{22} S_2 I_2 + \beta_{21} S_2 I_1 - d_2 I_2. \tag{2.1d}$$

The parameters are all assumed to be non-negative and r_i represents the intrinsic rate of population growth of species i, β_{ij} the disease transmission coefficient from species j to i and $a_i(1 - f_i)$ the per capita birth rate of infected individuals of species i with f_i being the fecundity loss as a result of infection. The per capita net rates of loss of infectives is d_i and comprises natural mortality b_i, pathogen-induced mortality α_i and recovery γ_i. This model assumes no vertical transmission or acquired immunity, and density-dependent (mass action) infection dynamics. There is no interspecific or intraspecific competition, so each host population increases exponentially in the absence of the disease. It is also assumed the disease can regulate each host species in the absence of the other host ($d_i > a_i(1 - f_i) + \gamma_i > 0$).

Their results show that in a two-host model with a shared infectious disease and no interspecific or intraspecific competition, one species excludes the other although if either species was alone with the disease it would coexist with the disease. One species can exclude the other if it has a higher susceptible growth rate, less susceptibility to infection or a higher tolerance to the disease (faster recovery, lower death rates or higher reproductive rates). For more insight into this model and further conclusions drawn from the model see Holt and Pickering (1985). Begon *et al.* (1992) further investigated this model by extending it to include intraspecific competition and investigated the different routes to coexistence of the two species and the disease. They identified five different routes to coexistence with particular discussion of the first case when two hosts, who would be uninfected if alone with the disease, can coexist with the pathogen as a result of disease transmission between the two hosts. In the second case at least one of the species would coexist with the pathogen in the absence of the other species and they both suffer more

within- than between-species infection. This case represents partitioning of predator-free space and is comparable to the coexistence case discussed by Holt and Pickering (1985). The third case describes resource-mediated co-existence where at least one species would coexist with the disease in the absence of the other species but the disease could not regulate either species in the absence of intraspecific competition. In the fourth case, when alone with the disease one species would maintain the disease and the other would exclude it. Furthermore, the excluding species could not be regulated by the disease in the absence of intraspecific competition and/or within-species infection is more prominent than between-species infection. The final case involves two species who when alone coexist with the disease but when both are present the disease is unable to regulate one host in the absence of intraspecific competition. They noted that a combination of "partioning of predator-free space" and "resource-mediated coexistence" allows coexistence and should not be considered as alternative paths to coexistence. For more detail about these cases of coexistence when intraspecific competition is present see Begon *et al.* (1992).

The first model structure to include intraspecific and interspecific competition was developed by Bowers and Turner (1997). They found invasion criteria in a similar host-host-pathogen system with both interspecific and intraspecific host competition. Their model consists of the following four ordinary differential equations with H_i representing the total population density of host species i (1 or 2) while Y_i represents its infected (and infectious) component

$$\frac{dH_1}{dt} = r_1 H_1(1 - c_{11}H_1 - c_{12}H_2) - \alpha_1 Y_1 \tag{2.2a}$$

$$\frac{dY_1}{dt} = \beta_{11}(H_1 - Y_1)Y_1 + \beta_{12}(H_1 - Y_1)Y_2 - \Gamma_1 Y_1 \tag{2.2b}$$

$$\frac{dH_2}{dt} = r_2 H_2(1 - c_{21}H_1 - c_{22}H_2) - \alpha_2 Y_2 \tag{2.2c}$$

$$\frac{dY_2}{dt} = \beta_{21}(H_2 - Y_2)Y_1 + \beta_{22}(H_2 - Y_2)Y_2 - \Gamma_2 Y_2. \tag{2.2d}$$

All parameters are assumed to be non-negative where r_i are the intrinsic per capita rates of population growth, c_{ij} are competitive coefficients, β_{ij} are disease transmission coefficients, α_i are per capita rates of pathogen-induced mortality and Γ_i are per capita net rates of loss of infected individuals (comprising natural mortality b_i, pathogen-induced mortal-

ity α_i and recovery γ_i). This model assumes density-dependent (mass action) infection dynamics. The carrying capacities for each species are represented by K_i and correspond to $K_i = 1/c_{ii}$. Bowers and Turner (1997) investigate the invadability of one species by the other with purely competitive, purely infective and competitive and infective interactions. The criteria required to allow species 2 to invade species 1 for the three different types of interaction are listed in table 2.1.

Interaction	**Criterion for invadability of species 1 by species 2**
Purely competitive	$c_{21}K_1 < c_{22}K_2$
Purely infective	$\beta_{21}\hat{Y}_1 < \beta_{22}\hat{Y}_2$
Competitive and infective	$\frac{c_{21}H_1^*}{c_{22}K_2} + \frac{\beta_{21}Y_1^*}{\beta_{22}Y_2} + \left(\frac{r_2}{\alpha_2 - r_2}\right)\left(\frac{c_{21}H_1^*}{c_{22}K_2}\right)\left(\frac{\beta_{21}Y_1^*}{\beta_{22}Y_2}\right) < 1$

Table 2.1 Invadability criteria for different types of interaction. This table is reproduced from Bowers and Turner (1997). $(\hat{H}_i, \hat{Y}_i)$ is one of the steady states found when only host species i is present; it represents the equilibrium densities when species i is coexisting with the disease. $(H_1^*, Y_1^*, 0, 0)$ is one of the steady states found when both species are present; it represents species 1 coexisting with the disease and excluding species 2.

Bowers and Turner (1997) investigate the effects of the different forces acting on invadability when there are both competitive and infective interactions to examine the possibility of infected coexistence. They show that there are two main routes to infected coexistence. Firstly, infected coexistence occurs if neither species 1 or species 2 support the pathogen alone but coexist in the absence of the pathogen at sufficiently high densities to support the pathogen jointly. Their possible explanation for this is the interspecific infection pathways. Secondly, infected coexistence can occur when either species 1, species 2 or both can support the pathogen alone and both species can invade the other. In summary both species coexist purely competitively and at sufficiently high densities to support the pathogen jointly or if the species would not coexist in the absence of the pathogen but there is strong intraspecific infection (lowering densities) and weak interspecific infection (favouring invadability).

In this chapter we wish to consider a two-host shared-parasite framework. Our work will differ from previous studies (Holt and Pickering, 1985; Begon *et al.*, 1992; Bowers and Turner, 1997) in that our focus will be to understand how the presence of a shared disease affects the replacement time of a native species by an invader. This question has previously been addressed for a specific model set-up and ecological scenario, namely the replacement of red squirrels by greys (Tompkins *et al.*, 2003). In that study it was

shown that the disease enhanced the ability of the greys to invade and greatly reduced the replacement time. We wish to extend this analysis to consider different model frameworks and a wide range of parameters. We aim to determine the scenarios in which the disease will increase or decrease the replacement time of a native species by an invader.

2.2 Model

Below we outline the framework for the full host-host-pathogen system with interspecific and intraspecific competition. The classes of susceptible, S_i, and infected, I_i, individuals are represented by the following system of equations, where $i = 1, 2$ with 1 representing the native species and 2 representing the alien invader

$$\frac{dS_1}{dt} = [a_1 - q_1(H_1 + c_2H_2)](S_1 + f_1I_1) - b_1S_1 - \beta_{11}S_1I_1 - \beta_{12}S_1I_2 + \gamma_1I_1 \tag{2.3a}$$

$$\frac{dI_1}{dt} = \beta_{11}S_1I_1 + \beta_{12}S_1I_2 - b_1I_1 - \alpha_1I_1 - \gamma_1I_1 \tag{2.3b}$$

$$\frac{dS_2}{dt} = [a_2 - q_2(H_2 + c_1H_1)](S_2 + f_2I_2) - b_2S_2 - \beta_{22}S_2I_2 - \beta_{21}S_2I_1 + \gamma_2I_2 \tag{2.3c}$$

$$\frac{dI_2}{dt} = \beta_{22}S_2I_2 + \beta_{21}S_2I_1 - b_2I_2 - \alpha_2I_2 - \gamma_2I_2 \tag{2.3d}$$

where $H_1 = S_1 + I_1$ and $H_2 = S_2 + I_2$. We assume all parameters are non-negative and a_i represents the maximum reproduction rate, b_i the natural mortality rate, c_i the competitive effect of species i on the other species and β_{ij} the disease transmission coefficient from species j to i. In this study we assume that $\beta_{ij} = \beta$ for all i and j, but see Tompkins *et al.* (2003) for an assessment of different within and between species transmission rates. We assume density-dependent (mass action) infection dynamics (Holt and Pickering, 1985; Bowers and Turner, 1997; Tompkins *et al.*, 2003) but see Saenz and Hethcote (2006) for a similar model with frequency-dependent transmission. We assume a positive carrying capacity, K_i, which is related to susceptibility to crowding, q_i, since $K_i = (a_i - b_i)/q_i$. We assume susceptible and infected individuals from the same species are equally competitive. The model assumes infected individuals experience disease induced mortality at rate α_i. Infecteds may recover back to susceptibility at rate γ_i and infecteds experience only a proportion, f_i, of the fecundity of a susceptible host; $f_i \in [0, 1]$ (parameters

Table 2.2 Summary of parameters used in equations (2.3a–d).

Parameter	Symbol
Maximum reproductive rate (species i)	a_i
Natural mortality rate (species i)	b_i
Susceptibility to crowding (species i)	q_i
Carrying capacity (species i); $K_i = (a_i - b_i)/q_i$	K_i
Competitive effect of species i on the other species	c_i
Disease transmission coefficient from species j to i	β_{ij}
Disease induced mortality rate (species i)	α_i
Recovery rate from disease (species i)	γ_i
Proportion of fecundity experienced by infecteds (species i); $f_i \in [0, 1]$	f_i

are summarised in table 2.2). The model framework is similar to that analysed in detail by Bowers and Turner (1997) but we additionally include the possibility of the parasite reducing the fecundity of infected hosts (see also Holt and Pickering (1985); Begon *et al.* (1992); Greenman and Hudson (1997); Saenz and Hethcote (2006); Malchow *et al.* (2008)). The key difference between previous studies that consider ecological interaction and infectious disease and the current study is our focus on determining whether disease increases or decreases the time taken for an invader to replace the native population. By manipulating the infection parameters the model equations (2.3) can represent different classical disease frameworks. If $\gamma_i > 0$ the model represents an SIS framework, whereas if $\gamma_i = 0$ it represents an SI framework. It is also of interest to examine the effects of infection on fecundity in these frameworks. These range from a castrating parasite ($f_i = 0$) to one in which disease has no effect on fecundity ($f_i = 1$). We will investigate the role of disease on invasion under these different scenarios.

2.3 Results

We begin by presenting a summary of the steady states and their stability properties (more detailed analysis is presented in Appendix 2.5). There are seven equilibrium points ob-

tained from setting the right-hand side of equations (2.3a–d) equal to zero.

$$(S_1, I_1, S_2, I_2) = (0, 0, 0, 0), \tag{2.4a}$$

$$(K_1, 0, 0, 0) = \left(\tfrac{a_1 - b_1}{q_1}, 0, 0, 0\right), \tag{2.4b}$$

$$(S_1^*, I_1^*, 0, 0) = \left(\tfrac{b_1 + \alpha_1 + \gamma_1}{\beta_{11}}, \tfrac{\Psi_1 + \sqrt{\Psi_1^2 + \Omega_1}}{2 q_1 f_1 \beta_{11}}, 0, 0\right), \tag{2.4c}$$

$$(0, 0, K_2, 0) = \left(0, 0, \tfrac{a_2 - b_2}{q_2}, 0\right), \tag{2.4d}$$

$$(0, 0, S_2^*, I_2^*) = \left(0, 0, \tfrac{b_2 + \alpha_2 + \gamma_2}{\beta_{22}}, \tfrac{\Psi_2 + \sqrt{\Psi_2^2 + \Omega_2}}{2 q_2 f_2 \beta_{22}}\right), \tag{2.4e}$$

$$(S_1^+, 0, S_2^+, 0) = \left(\tfrac{c_2 K_2 - K_1}{c_1 c_2 - 1}, 0, \tfrac{c_1 K_1 - K_2}{c_1 c_2 - 1}, 0\right), \tag{2.4f}$$

$$(\hat{S_1}, \hat{I_1}, \hat{S_2}, \hat{I_2}) \tag{2.4g}$$

where in the steady state (2.4g) the values are algebraically complicated and therefore omitted for brevity.

If $f_1 > 0$, the steady state defined in equation (2.4c) is expanded with $\Gamma_1 = \alpha_1 + b_1 + \gamma_1$, $\Psi_1 = (a_1 f_1 - b_1 - \alpha_1)\beta_{11} - q_1 f_1 \Gamma_1 - q_1 \Gamma_1$ and $\Omega_1 = 4 f_1 q_1^2 \Gamma_1 (\beta_{11} K_1 - \Gamma_1)$. In the alternative case when $f_1 = 0$, I_1^* in equation (2.4c) becomes $I_1^* = \dfrac{\Gamma_1 (\beta_{11} K_1 - \Gamma_1)(a_1 - b_1)}{\beta_{11} (\Gamma_1 (a_1 - b_1) + K_1 \beta_{11} (\Gamma_1 - \gamma_1))}$. If $f_2 > 0$, the steady state defined by equation (2.4e) is expanded with Γ_2, Ψ_2 and Ω_2; where Γ_2, Ψ_2 and Ω_2 are equivalent to Γ_1, Ψ_1 and Ω_1 respectively with the subscript 1 changed to 2. Alternatively if $f_2 = 0$, I_2^* in equation (2.4e) is equivalent to that for I_1^* with the subscript 1 changed to 2.

The trivial equilibrium is unstable (since we assume $a_1 > b_1$ and $a_2 > b_2$). For the other equilibrium points, we will give a brief description of their stability conditions. These are calculated using standard linear stability analysis (see, for example, Murray (2002)) with the mathematical software package Maple used for algebraic manipulation. At the steady state $(K_1, 0, 0, 0)$, the native is at its carrying capacity and the invader is not present (detailed calculations are presented in Appendix 2.5). This is always feasible

(positive steady state), and is stable if the following two conditions hold

$$c_1K_1 - K_2 > 0 \quad \text{(native has a competitive advantage)}, \tag{2.5a}$$

$$R_0(1) = \frac{K_1\beta_{11}}{\Gamma_1} < 1 \quad \text{(the disease cannot invade the native species)} \tag{2.5b}$$

where $\Gamma_1 = \alpha_1 + b_1 + \gamma_1$ represents the total removal from infection for the native species. $R_0(i)$ represents the basic reproductive number for species i when it is alone with the disease. The basic reproductive number is the expected number of secondary infections caused from one infected individual entering a purely susceptible population. At $(S_1^*, I_1^*, 0, 0)$ the native is at its endemic level and the invader is not present. This is feasible, if $R_0(1) > 1$; when feasible it is stable if the following condition holds

$$(a_2 - b_2 - q_2c_1(S_1^* + I_1^*)) + ((\beta_{21}I_1^*)/\Gamma_2)(f_2a_2 - b_2 - f_2q_2c_1(S_1^* + I_1^*) - \alpha_2) < 0. \tag{2.6}$$

This condition represents the fact that the fitness of the alien species is negative. At $(0, 0, K_2, 0)$ the invader is at its carrying capacity and the native is not present. This is always feasible, and is stable if the following two conditions hold

$$c_2K_2 - K_1 > 0 \quad \text{(invader has a competitive advantage)}, \tag{2.7a}$$

$$R_0(2) = \frac{K_2\beta_{22}}{\Gamma_2} < 1 \quad \text{(the disease cannot invade the alien species)} \tag{2.7b}$$

where $\Gamma_2 = \alpha_2 + b_2 + \gamma_2$ represents the total removal from infection for the alien species. At $(0, 0, S_2^*, I_2^*)$ the invader is at its endemic levels and the native is not present. This is feasible if $R_0(2) > 1$, and when feasible it is stable if the following condition holds

$$(a_1 - b_1 - q_1c_2(S_2^* + I_2^*)) + ((\beta_{12}I_2^*)/\Gamma_1)(f_1a_1 - b_1 - f_1q_1c_2(S_2^* + I_2^*) - \alpha_1) < 0 \tag{2.8}$$

This condition represents the fact that the fitness of the native species is negative.

At $(S_1^+, 0, S_2^+, 0)$ the native and alien species are coexisting with no disease present.

This steady state is feasible and stable if the following five conditions hold

$$c_1 K_1 - K_2 < 0, \tag{2.9a}$$

$$c_2 K_2 - K_1 < 0, \tag{2.9b}$$

$$c_1 c_2 - 1 < 0, \tag{2.9c}$$

$$(\beta_{11} S_1^+ - \Gamma_1) + (\beta_{22} S_2^+ - \Gamma_2) < 0, \tag{2.9d}$$

$$(\beta_{11} S_1^+ - \Gamma_1)(\beta_{22} S_2^+ - \Gamma_2) - \beta_{12}\beta_{21} S_1^+ S_2^+ > 0. \tag{2.9e}$$

The final equilibrium, $(\hat{S}_1, \hat{I}_1, \hat{S}_2, \hat{I}_2)$, represents all the classes having positive densities and both the native and invader coexisting with the parasite. We assume it is stable when all other steady states are unstable (see Bowers and Turner (1997) for a detailed steady state and stability analysis for a similar model). When observed in numerical simulations, it exhibited behaviour of a stable equilibrium point but see Greenman and Hudson (1997) for a discussion of other potential behaviour. The focus of this study is a set-up in which native species is initially at its carrying capacity with no disease $(K_1, 0, 0, 0)$. Parameters are chosen such that when the invader is introduced it has a competitive advantage and replaces the native, with the invader attaining its carrying capacity $(0, 0, K_2, 0)$ in the absence of disease or its endemic steady state $(0, 0, S_2^*, I_2^*)$ when disease is present.

As stated, our focus is to understand how the disease affects the replacement time of the native species by the invader. To achieve this we assume that the non-disease parameters in equations (2.3) are equal for the native and invading species except that the invader has a superior competitive ability, $c_2 > c_1$. In the absence of the disease the native will be replaced and the population will be transformed to the steady state containing a purely susceptible alien species at its carrying capacity $(0, 0, K_2, 0)$ (figure 2.1).

The replacement time is measured as the time taken for the native population to fall below 0.1% of its carrying capacity (which in figure 2.1 is 70.4 time units). To examine how the inclusion of disease alters the replacement time we use the same non-disease parameters as in figure 2.1 and compare the replacement time for competition-mediated replacement to that for competition-and-disease-mediated replacement in which the pop-

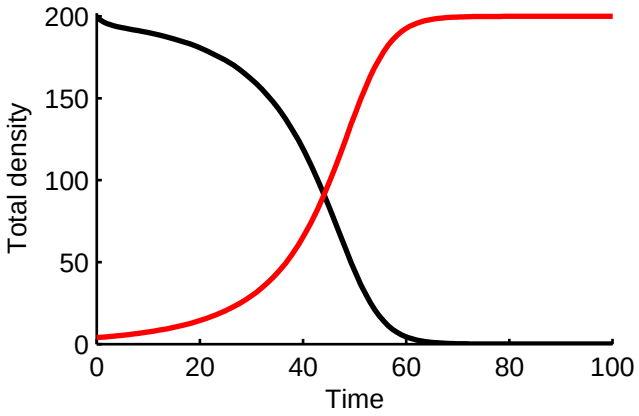

Figure 2.1 Density of the native (black line) and alien (red line) species over time in the absence of disease. Initially the native species is at its carrying capacity and the invader is introduced at low density (neither are infected). The alien species replaces the native species and reaches its carrying capacity. Parameters are: $a_1 = a_2 = 1$, $b_1 = b_2 = 0.4$, $K_1 = K_2 = 200$, $c_1 = 0.9$, $c_2 = 1.5$, and $\beta_{ij} = \alpha_i = \gamma_i = f_i = 0$ for $i = 1, 2$. These results were produced using MATLAB ODE45 which is based on an explicit Runge-Kutta (4,5) formula.

ulation is transformed to the endemic disease equilibrium$(0, 0, S_2^*, I_2^*)$. In this way we examine whether disease increases or decreases the replacement time of the native species for a range of disease parameters.

2.3.1 Disease-induced fecundity loss

The effect on the replacement time when both species suffer equal fecundity loss as a result of the infection for a variety of combinations of the other disease parameters is shown in figure 2.2a. When there is no disease induced mortality and no fecundity loss for infecteds the replacement time is the same as in the absence of disease. As the loss of fecundity due to infection increases (f_i decreases from 1 to 0) the replacement time increases. This trend occurs since fecundity loss leads to a lower overall growth rate for the invader and therefore it takes longer for the invader to increase in number and oust the established native population (figure 2.2a). When there is mortality due to the disease ($\alpha_i > 0$), the replacement time is increased when compared to competition-only for all levels of fecundity loss. When fecundity loss is low, disease induced mortality increases replacement time compared to when it is absent. In contrast when fecundity loss is high, disease induced mortality reduces replacement time (compared to when disease induced mortality is absent) since here infected individuals, which contribute little to the overall growth rate of the invading species, are removed more rapidly. The effect of recovery is to reduce the replacement time at all levels of fecundity when compared to the appropriate

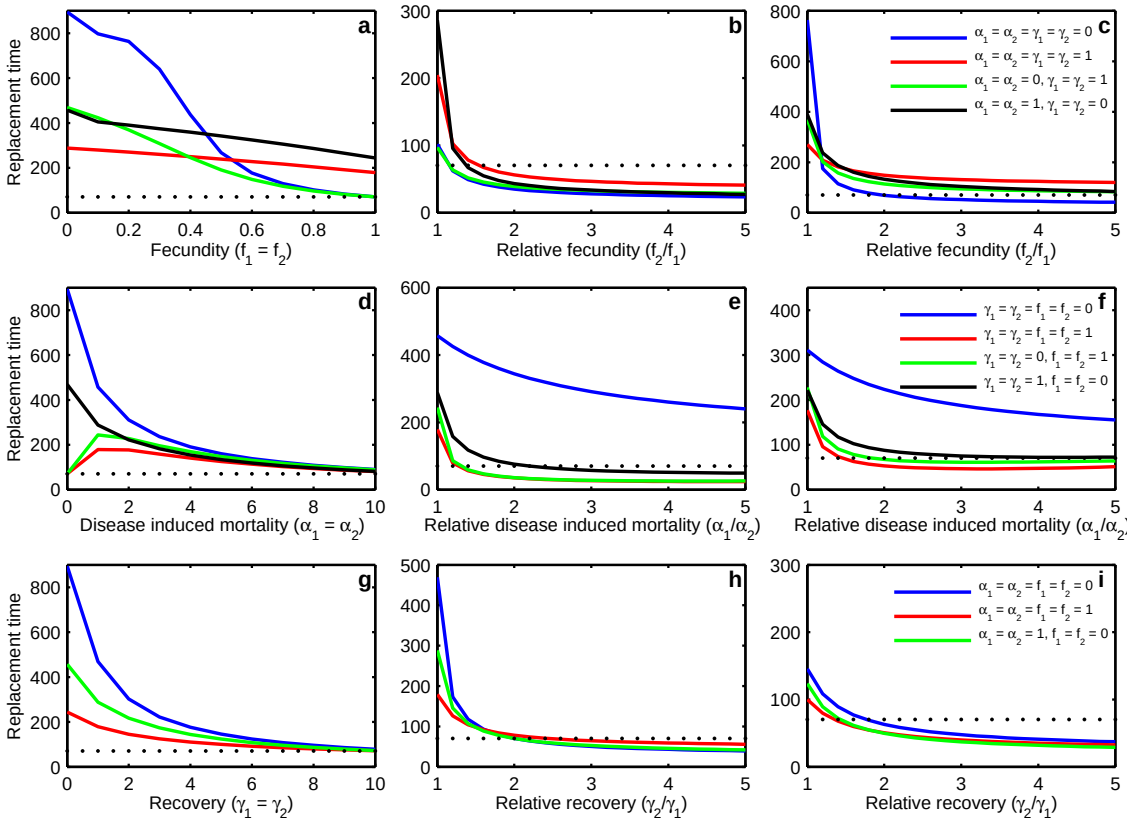

Figure 2.2 The effect of different disease parameters on competition-and-disease-mediated replacement time: panels **a**–**c** disease induced fecundity loss; panels **d**–**f** disease induced mortality; panels **g**–**i** recovery from infection. For each of these parameters, we look at combinations of presence/absence of the other two disease parameters as detailed in the key for each row of plots. In panels **a**, **d** and **g** the native and alien have equal values for the disease parameter, while in the remaining panels the native suffers a relative disadvantage. The dotted line represents the replacement time when disease is absent. Parameters common to every panel are: $a_1 = a_2 = 1$, $b_1 = b_2 = 0.4$, $K_1 = K_2 = 200$, $c_1 = 0.9$, $c_2 = 1.5$ and $\beta_{ij} = 0.06$. In addition we fix the following parameters: in panel **b** $f_2 = 0.8$, panel **c** $f_2 = 0.2$, panel **e** $\alpha_2 = 1$, panel **f** $\alpha_2 = 2$, panel **h** $\gamma_2 = 1$ and panel **i** $\gamma_2 = 5$. The results are qualitatively similar for a wide range of parameters that satisfy the conditions necessary for the invader to have a competitive advantage. All results were produced using MATLAB ODE45 which is based on an explicit Runge-Kutta (4,5) formula.

results for the presence or absence of disease induced mortality (figure 2.2a). The clear general trend is that if disease has the same effect in reducing the native and invading species fecundity the replacement time increases.

We next examine the effect on replacement time when the disease induced reduction in fecundity is more severe for the native than the invading species. If the invading species has a "low" level of fecundity loss then the disease will increase replacement time (compared to in the absence of disease) if the relative fecundity loss of the native is small, but reduce replacement time once the relative fecundity advantage of the invading species exceeds a threshold (figure 2.2b). This threshold increases if individuals can recover to susceptibility (as once recovered the disease induced relative costs are not realised) and if

the disease induces additional mortality (as the death of infected individuals also negates the fecundity advantage of the invading species). The threshold also increases if the invading species has a 'high' level of fecundity loss (figure 2.2c) and here even a high relative fecundity advantage may not be sufficient for the replacement time to be less than in the absence of disease.

2.3.2 Disease-induced mortality

We consider increases in disease induced mortality when it is equal in both species ($\alpha_1 = \alpha_2$) for a variety of combinations of the other disease parameters (figure 2.2d). If the parasite castrates both species ($f_i = 0$), an increase in disease induced mortality reduces replacement time, but it can never be less than that for competition-only replacement (figure 2.2d). Here, the increase in disease induced mortality acts to reduce the prevalence of an infection and so the castrating effect of the parasite becomes less apparent. If the parasite has no effect on fecundity ($f_i = 1$), the replacement time initially increases since disease induced mortality reduces the overall density and therefore lowers total reproduction. As disease induced mortality increases further, replacement time reaches a maximum and then decreases and tends to but is never less than that for competition-only replacement. The approach of the diseased replacement time to the non-diseased time occurs because when disease induced mortality is high, infected individuals are removed so quickly that the model system behaves in a similar manner to the competition-only case. As the fecundity loss increases (f_i changes from 1 to 0) the replacement time at $\alpha_1 = \alpha_2 = 0$ increases and the curves change between the two cases. The effect of recovery is to reduce the replacement time at all levels of disease induced mortality for the all cases (and is similar to the response shown in figure 2.2a).

Next we consider when the native suffers higher disease induced mortality than the invading species. If the parasite is castrating and there is no recovery, the replacement time is always increased even if the native suffers high disease induced mortality compared to the invader (figure 2.2e). With recovery present, if the advantage of the invader (in terms of lower disease induced mortality) is small, the disease will again increase replacement time, but if the relative advantage of the invader exceeds a threshold the replacement time can be reduced compared to competition-only. This threshold is lower if the parasite is non-castrating as this allows higher reproduction into the susceptible class and therefore

faster growth of the invading species. The trend is observed if the underlying level of disease induced mortality of the invading species is increased but the threshold values at which the disease acts to reduce the replacement time are increased and in some circumstance a high relative advantage for the invader may not be sufficient to reduce the replacement time below that of competition-only (figure 2.2f).

2.3.3 Recovery from disease

If both species have an equal recovery rate from the disease ($\gamma_1 = \gamma_2$), the replacement time decreases as the recovery rate increases but replacement is never faster than competition-only (figure 2.2g). If the relative advantage of the invader in terms of recovery exceeds a threshold then the replacement time can be lower than for competition-only (figure 2.2h–i). When the disease is castrating (or leads to a "large" reduction in fecundity) the recovery advantage is particularly important, as recovery acts as a route back to full fecundity.

2.3.4 Generality of results

Above we consider the effects of disease on replacement time when the invader is a superior competitor, but the disease can also have a significant effect when the native species is the superior competitor (and therefore the competition alone would eradicate the invader). The disease can allow a competitively inferior invader to replace a native species (this occurs when criterion (2.8) above is satisfied). When the parasite is castrating the invader requires a high recovery rate to negate its inferior competitive ability (α_i can affect the speed of replacement but cannot alone allow invasion). For a non-castrating parasite, replacement requires the invader to suffer sufficiently lower mortality due to disease (differences in recovery can affect the replacement time but alone cannot allow invasion). In general the qualitative trends in replacement time for changes in disease parameter values are as outlined in figure 2.2. (Although not the focus of this study the invading species could coexist with the native, see Appendix 2.5 for relevant criteria. The disease impacts on the time taken to coexistence in a similar manner to the one outlined above.) It is also possible to have situations where the disease acts to prevent invasion, even if the native is an inferior competitor, providing the native has sufficiently better recovery when $f_i = 0$

or sufficiently lower mortality when $f_i > 0$ (see criterion (2.6) above).

The modelling framework above examined both SI and SIS models, but can be extended to include both SIR and SIRS models where R represents a recovered and immune class. In the SIRS model, immunity can wane and individuals can become susceptible once more. The three classes of susceptible, S_I, infected, I_i, and recovered, R_i, are represented by the following system of equations, with $i = 1, 2$ representing the native and invading species respectively

$$\frac{dS_1}{dt} = [a_1 - q_1(H_1 + c_2H_2)](S_1 + f_1I_1 + R_1) - b_1S_1 - \beta_{11}S_1I_1 - \beta_{12}S_1I_2 + \lambda_1R_1 \tag{2.10a}$$

$$\frac{dI_1}{dt} = \beta_{11}S_1I_1 + \beta_{12}S_1I_2 - b_1I_1 - \alpha_1I_1 - \gamma_1I_1 \tag{2.10b}$$

$$\frac{dR_1}{dt} = \gamma_1I_1 - b_1R_1 - \lambda_1R_1 \tag{2.10c}$$

$$\frac{dS_2}{dt} = [a_2 - q_2(H_2 + c_1H_1)](S_2 + f_2I_2 + R_2) - b_2S_2 - \beta_{22}S_2I_2 - \beta_{21}S_2I_1 + \lambda_2I_2 \tag{2.10d}$$

$$\frac{dI_2}{dt} = \beta_{22}S_2I_2 + \beta_{21}S_2I_1 - b_2I_2 - \alpha_2I_2 - \gamma_2I_2 \tag{2.10e}$$

$$\frac{dR_2}{dt} = \gamma_2I_2 - b_2R_2 - \lambda_2R_2 \tag{2.10f}$$

where $H_1 = S_1 + I_1 + R_1$ and $H_2 = S_2 + I_2 + R_2$. As seen in our earlier model, we assume all parameters are non-negative and a_i represents the maximum reproduction rate, b_i the natural mortality rate, c_i the competitive effect of species i on the other species and β_{ij} the disease transmission coefficient from species j to i. We again assume a positive carrying capacity, K_i, which is related to susceptibility to crowding, q_i, and infected individuals experience disease induced mortality at rate α_i. However, infecteds now recover into the recovered class, R_i at rate γ_i and from the recovered class return to the susceptible class at rate λ_i. The birth rate from the recovered class is the same as the susceptible class and again infecteds experience only a proportion, f_i, of the fecundity of a susceptible host.

Equations (2.10a–f) represent an SIR framework if $\lambda_1 = \lambda_2 = 0$ and an SIRS framework if $\lambda_1 > 0$ and $\lambda_2 > 0$. The results for the SIR and SIRS frameworks are similar to the SIS model results. The effects of mortality from disease on invasion are the same for SIS, SIR and SIRS models. The effects of recovery from disease follow the same patterns for all three models although the effect of recovery is more pronounced with SIRS and SIR

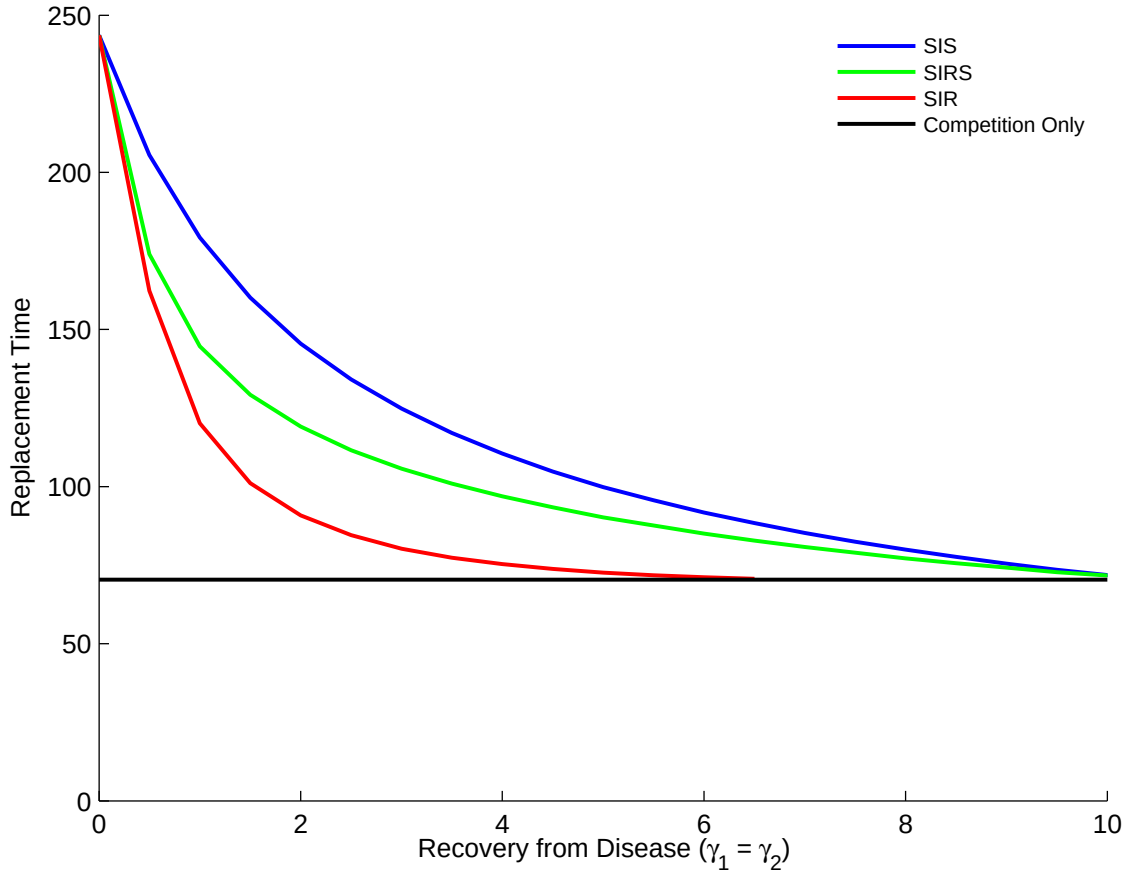

Figure 2.3 The speed of replacement for different model frameworks against recovery from infection. The plot shows an SIS (blue line), SIRS (green line), SIR (red line) and competition-only (black line) frameworks in relation to the effect of recovery. The results for all SIS, SIR and SIRS are qualitively very similar but recovery is having a more pronounced effect in both SIR and SIRS. The parameters used here are: $f_1 = f_2 = 1$, $a_1 = a_2 = 1$, $b_1 = b_2 = 0.4$, $K_1 = K_2 = 200$, $c_1 = 0.9$, $c_2 = 1.5$, $\beta_{ij} = 0.06$, $\alpha_1 = \alpha_2 = 1$ and $\gamma_1 = \gamma_2$.

and increases the replacement speed compared to the SIS framework (figure 2.3).

These temporal results highlight the importance of infection in determining the outcome and time required for an invading species to replace a native species. The replacement time for alien species to invade are shortest when the invader has better recovery than the native species, lower mortality from the disease and a greater reproduction rate when infected. However, a disease introduced by an invading species may not reduce the replacement time. The general message is that a shared disease carried by an invading species may be detrimental to the invaders' attempts to replace the native if the disease has a similar effect on both species, even if it is more "harmful" to the native. Only when the invading species has a sufficient relative advantage does the disease assist in reducing the replacement time.

2.4 Discussion

In this chapter we have considered a strategic theoretical framework to investigate the role of a shared disease, in addition to competition for resources, in the invasion of novel organisms. We have shown that disease can increase or decrease the time taken for an invading species to replace an established native population with the outcome critically dependent on the relative effects that the disease has on the two species and less dependent on the basic epidemiological characteristics of the interaction. Disease may also allow the invasion of a poorer competitor that otherwise would have been excluded by the native species.

Of great conservation concern is the situation where a shared disease can aid the invasion of an exotic species. The extinction of native red squirrel by the introduced grey in much of England and Wales has highlighted the role that disease may play in speeding up the replacement process (Tompkins *et al.*, 2003; Rushton *et al.*, 2006). We have shown that a shared disease is most likely to aid the invasion of a species if the native suffers higher disease-induced mortality, a lower level of fecundity due to infection and a lower rate of recovery compared to the invading species. These characteristics closely match those of the squirrel system in the UK. Squirrelpox virus appears to have little effect on the mortality or fecundity of grey squirrels and greys appear to make a full recovery from infection. Red squirrels however suffer high mortality from the virus, do not reproduce when infected and do not recover from infection (Tompkins *et al.*, 2002). As such the greys benefit from all of the factors that allow disease to increase the speed of invasion.

If an invading species has sufficient advantage due to the disease it can replace a native species even if the invader is an inferior competitor. However, disease does not always benefit invading species. Hoogendoorn and Heimpel (2002) show that for ladybird beetle populations in North America; the native species suffers less from a shared parasitoid when the alien species is present. This reduces the competitive effects of the alien ladybird beetle allowing the native an extra advantage and slowing the alien invasion. If the native suffers less harm from a disease then this can allow the native to repel a potential invasion even if the native is an inferior competitor (Hilker *et al.*, 2005; Petrovskii *et al.*, 2005). A shared disease can increase the replacement time when disease characteristics are similar for the native and invading species even when an invading species has a competitive advantage. This emphasises that detailed epidemiological studies are

needed when we want to predict the impact of disease in natural communities. A virulent disease may increase replacement time as often it is the relative effects of the disease on the native and alien species that are important. Furthermore it is not just the lethal effects that are important. Sub-lethal effects on fecundity can have a pronounced influence on the outcome of the interaction. It is increasingly recognised that sub-lethal fecundity effects, rather than mortality effects, can drive the population dynamics of natural systems (Dobson and Hudson, 1986; Hudson *et al.*, 1998; Boots and Norman, 2000). Our work emphasises that they may also be crucial to invasion dynamics. Therefore disease may be crucial to conservation efforts even if it does not result in large mortality since less obvious and less studied effects on reproduction may be more important.

There are several examples where disease has played an important role in the successful invasion of non-native species. In the UK, the native white-clawed crayfish suffers very high disease induced mortality, with no recovery, while the invasive signal crayfish are resistant (Cerenius *et al.*, 2003; Holdich, 2003; Bubb *et al.*, 2004). If we consider these characteristics under our framework, the relatively higher mortality suffered by the native as a result of the disease decreases replacement time compared to competition-only. More detailed information on the system regarding fecundity, recovery and competition would allow us to gain better insight into this invasion but our framework highlights that the disease should be considered in conservation strategies to save the white-clawed crayfish. In North America, the invasion of white-tailed deer has been aided by the transmission of a meningeal worm which is lethal to caribou (Anderson, 1972; Pybus *et al.*, 1990; Oates *et al.*, 2000). One of the conservation strategies has been to reintroduce caribou; however in regions where infected white-tailed deer are present these reintroductions have been unsuccessful (Bergerud and Mercer, 1989). This emphasises the detrimental effect disease can have on conservation efforts. A further example is the replacement of the native pedunculate oak with Turkey oak in the UK. The Turkey oak is aided in this replacement by the detrimental effects of the knopper gall wasp on the pedunculate oak; the sexual generation of gall wasp develops in Turkey oak but causes little harm. However during the agamic generation, knopper galls develop which distort the growing acorns of pedunculate oak and can greatly reduce fecundity (Hails and Crawley, 1991). The results from our general framework show that replacement time can be lower than competition-only when the native suffers a relative reduction in fecundity compared to the invading

species. This is the case here; with infection giving the Turkey oak an advantage over the native oak species. These effects should be considered in conservation strategies for the pedunculate oak.

In summary, we have used a general model framework to investigate the impact of a shared disease on the replacement time of a native species by an invader. If the characteristics of the disease are similar in both the species the disease acts to increase the time taken for the invading species to replace the native species. The disease can reduce replacement time providing that invading species suffers sufficiently less "harm" from the disease. This may explain the speed of replacement of native species observed in natural systems (Reynolds, 1985; Hails and Crawley, 1991; Holdich, 2003).

The results in this chapter are published in *Theoretical Ecology*, see Bell *et al.* (2009).

2.5 Appendix

In this appendix we provide a detailed analysis of the steady states including their feasibility and stability properties. The dynamics of susceptible (S_i) and infected (I_i) individuals are represented by a system of ordinary differential equations (2.3a–d) , where $i = 1, 2$ with 1 representing the native species and 2 representing the invading species

$$\frac{dS_1}{dt} = [a_1 - q_1(H_1 + c_2H_2)](S_1 + f_1I_1) - b_1S_1 - \beta_{11}S_1I_1 - \beta_{12}S_1I_2 + \gamma_1I_1 \tag{2.11a}$$

$$\frac{dI_1}{dt} = \beta_{11}S_1I_1 + \beta_{12}S_1I_2 - b_1I_1 - \alpha_1I_1 - \gamma_1I_1 \tag{2.11b}$$

$$\frac{dS_2}{dt} = [a_2 - q_2(H_2 + c_1H_1)](S_2 + f_2I_2) - b_2S_2 - \beta_{22}S_2I_2 - \beta_{21}S_2I_1 + \gamma_2I_2 \tag{2.11c}$$

$$\frac{dI_2}{dt} = \beta_{22}S_2I_2 + \beta_{21}S_2I_1 - b_2I_2 - \alpha_2I_2 - \gamma_2I_2 \tag{2.11d}$$

where $H_1 = S_1 + I_1$ and $H_2 = S_2 + I_2$. We assume all parameters are positive and a_i represents the maximum reproduction rate, b_i the natural adult mortality rate, c_i the competitive effect of species i on the other species and β_{ij} the virus transmission rate from species j to i. The carrying capacity is represented by K_i which is related to susceptibility to crowding (q_i) since $K_i = (a_i - b_i)/q_i$. We will always assume a_i is greater than b_i meaning K_i is also always positive. The model assumes infected individuals die at rate α_i, recover back to susceptible at rate γ_i and the reduction in fecundity when infected is represented by f. We will analyse the following three scenarios: both species with no disease present (competition-only), one species with the disease present (disease-only) and both species with the disease present (full-model).

2.5.1 Competition-only model

In this section, we consider the scenario when both species are present but the disease is not. Letting $I_1 = I_2 = 0$, equations (2.11a–d) simplify to the classic Lotka-Volterra equations discussed in Chapter 1 (see Murray (2002) for further discussion), as follows

$$\frac{dS_1}{dt} = [a_1 - q_1(S_1 + c_2S_2)]S_1 - b_1S_1 \tag{2.12a}$$

$$\frac{dS_2}{dt} = [a_2 - q_2(S_2 + c_1S_1)]S_2 - b_2S_2. \tag{2.12b}$$

There are four equilibrium points obtained from setting the right-hand side of equations (2.12a–b) equal to zero,

$$(S_1, S_2) = (0,0), \quad (K_1, 0), \quad (0, K_2) \quad \text{and} \quad (S_1^+, S_2^+), \tag{2.13}$$

where $(S_1^+, S_2^+) = \left(\frac{c_2K_2 - K_1}{c_1c_2 - 1}, \frac{c_1K_1 - K_2}{c_1c_2 - 1}\right)$.

Feasibility and Stability

1. $(\mathbf{0}, \mathbf{0})$

We begin by considering the origin, $(S_1, S_2) = (0,0)$, where both species are extinct. Linearising equations (2.12a–b) about $(0,0)$ gives the following Jacobian matrix

$$\mathbf{J}_{(0,0)} = \begin{pmatrix} a_1 - b_1 & 0 \\ 0 & a_2 - b_2 \end{pmatrix} \tag{2.14}$$

with eigenvalues $\lambda_{11} = a_1 - b_1$ and $\lambda_{12} = a_2 - b_2$. λ_{11} and λ_{12} are always greater than zero, since $a_i - b_i > 0 \quad (i = 1, 2)$. Therefore the origin, where both the resident and invader are extinct, is always unstable.

2. $(\mathbf{K_1}, \mathbf{0})$

At the equilibrium $(K_1, 0)$, the native species is at its carrying capacity and the invader is extinct. This equilibrium is always feasible since $K_1 > 0$. Linearising equations (2.12a–b) about $(K_1, 0)$ gives the following Jacobian matrix

$$\mathbf{J}_{(K_1,0)} = \begin{pmatrix} b_1 - a_1 & c_2(b_1 - a_1) \\ 0 & (a_2 - b_2)\left(1 - \dfrac{c_1K_1}{K_2}\right) \end{pmatrix} \tag{2.15}$$

with the following two eigenvalues

$$\lambda_{21} = b_1 - a_1, \tag{2.16a}$$

$$\lambda_{22} = (a_2 - b_2)\left(1 - \frac{c_1K_1}{K2}\right). \tag{2.16b}$$

The eigenvalue λ_{21} is always less than zero. The other eigenvalue λ_{22} is less than zero if $c_1K_1 - K_2 > 0$. Therefore $(K_1, 0)$ is stable when $c_1K_1 - K_2 > 0$, this represents the native species having a competitive advantage.

3. $(\mathbf{0}, \mathbf{K_2})$

The third equilibrium point $(0, K_2)$, where the native species is excluded and the invader is at its carrying capacity, is always feasible since $K_2 > 0$. Linearising equations (2.12a–b) about $(0, K_2)$ gives the following Jacobian matrix

$$\mathbf{J}_{(0,K_2)} = \begin{pmatrix} (a_1 - b_1)\left(1 - \dfrac{c_2 K_2}{K_1}\right) & 0 \\ c_1(b_2 - a_2) & b_2 - a_2 \end{pmatrix} \tag{2.17}$$

with the following eigenvalues

$$\lambda_{31} = b_2 - a_2, \tag{2.18a}$$

$$\lambda_{32} = (a_1 - b_1)\left(1 - \frac{c_2 K_2}{K_1}\right). \tag{2.18b}$$

The first eigenvalue, λ_{31}, is always less than zero. The second eigenvalue, λ_{32}, is less than zero if $c_2 K_2 - K_1 > 0$. Therefore, this equilibrium is stable when $c_2 K_2 - K_1 > 0$ representing the alien species having a competitive advantage.

4. $(\mathbf{S_1^+}, \mathbf{S_2^+})$

The final equilibrium (S_1^+, S_2^+), where the native and alien coexist, is feasible if $S_1^+ > 0$ and $S_2^+ > 0$ which occurs when $c_2 K_2 - K_1$, $c_1 K_1 - K_2$ and $c_1 c_2 - 1$ are either all positive or all negative. Linearising equations (2.12a–b) about (S_1^+, S_2^+) gives the following Jacobian matrix

$$\mathbf{J}_{(S_1^+, S_2^+)} = \begin{pmatrix} -2q_1 S_1^+ + a_1 - b_1 - q_1 c_2 S_2^+ & -q_1 c_2 S_1^+ \\ -q_2 c_1 S_2^+ & -2q_2 S_2^+ + a_2 - b_2 - q_2 c_1 S_1^+ \end{pmatrix}. \tag{2.19}$$

Since $S_1^+ \neq 0$ and $S_2^+ \neq 0$, equations (2.12a–b) give us $a_1 - b_1 - q_1 S_1^+ - q_1 c_2 S_2^+ = 0$ and $a_2 - b_2 - q_2 S_2^+ - q_2 c_1 S_1^+ = 0$. These two expressions can be used to simplify $\mathbf{J}_{(S_1^+, S_2^+)}$ (2.19) to give

$$\mathbf{J}_{(S_1^+, S_2^+)} = \begin{pmatrix} -q_1 S_1^+ & -q_1 c_2 S_1^+ \\ -q_2 c_1 S_2^+ & -q_2 S_2^+ \end{pmatrix}. \tag{2.20}$$

The equilibrium point (S_1^+, S_2^+) is stable if the following trace and determinant conditions from the Jacobian matrix $\mathbf{J}_{(S_1^+, S_2^+)}$ hold:

$$q_1 S_1^+ + q_2 S_2^+ > 0 \text{ (always holds when feasible)}, \tag{2.21a}$$

$$q_1 q_2 S_1^+ S_2^+ (c_1 c_2 - 1) < 0 \text{ (holds when } c_1 c_2 - 1 < 0). \tag{2.21b}$$

It follows from the feasibility condition that $c_2K_2 - K_1 < 0$, $c_1K_1 - K_2 < 0$ and $c_1c_2 - 1 < 0$ must all hold for stability. Therefore, (S_1^+, S_2^+) is stable when the following three conditions hold:

$$c_1K_1 - K_2 < 0, \tag{2.22a}$$

$$c_2K_2 - K_1 < 0, \tag{2.22b}$$

$$c_1c_2 - 1 < 0. \tag{2.22c}$$

These conditions reflect that neither species can out-compete the other.

2.5.2 Disease-only model

In this section we investigate the scenario where there is only one species and the disease. Letting $S_2 = I_2 = 0$, and dropping subscript 1 as only one species present, equations (2.11a–d) become

$$\frac{dS}{dt} = [a - q(S + I)](S + fI) - bS - \beta SI + \gamma I \tag{2.23a}$$

$$\frac{dI}{dt} = \beta SI - \Gamma I \tag{2.23b}$$

where $\Gamma = \alpha + b + \gamma$. There are three equilibrium points obtained from setting the right-hand side of equations (2.23a–b) equal to zero,

$$(S, I) = (0, 0), \quad (K, 0) \quad \text{and} \quad (S^*, I^*), \tag{2.24}$$

where $(S^*, I^*) = \left(\frac{\Gamma}{\beta}, \frac{\Psi + \sqrt{\Psi^2 + \Omega}}{2qf\beta}\right)$ with $\Psi = (af - \alpha - b)\beta - q\Gamma f - q\Gamma$ and $\Omega = 4f\Gamma q^2(\beta K - \Gamma)$ when $f > 0$. In the case when $f = 0$, the equilibrium point can be rewritten as $(S^*, I^*) = \left(\frac{\Gamma}{\beta}, \frac{\Gamma(\beta K - \Gamma)(a - b)}{\beta(\Gamma(a - b) + K\beta(\Gamma - \gamma))}\right)$.

Feasibility and Stability

1. $(\mathbf{0}, \mathbf{0})$

We begin by considering the origin, $(S, I) = (0, 0)$, where there is no species or disease. Linearising equations (2.23a–b) about $(0, 0)$ gives the following Jacobian matrix

$$\mathbf{J}_{(0,0)} = \begin{pmatrix} a - b & af + \gamma \\ 0 & -\Gamma \end{pmatrix} \tag{2.25}$$

with eigenvalues $\lambda_{41} = a - b$ and $\lambda_{42} = -\Gamma$. λ_{42} is always less than zero but λ_{41} is always greater than zero, since $a - b > 0$. Therefore the origin, where both the species and the disease are excluded, is always unstable.

2. $(\mathbf{K}, \mathbf{0})$

At the equilibrium $(K, 0)$, the native species is at its carrying capacity and the invader is extinct. This equilibrium is always feasible since $K > 0$. Linearising equations (2.23a–b) about $(K, 0)$ gives the following Jacobian matrix

$$\mathbf{J}_{(K,0)} = \begin{pmatrix} b - a & b - a + fb - \beta K + \gamma \\ 0 & \beta K - \Gamma \end{pmatrix} \tag{2.26}$$

with the following eigenvalues

$$\lambda_{51} = b - a, \tag{2.27a}$$

$$\lambda_{52} = \beta K - \Gamma. \tag{2.27b}$$

The eigenvalue λ_{51} is always less than zero. The other eigenvalue λ_{52} is less than zero if $R_0 = \frac{\beta K}{\Gamma} < 1$; R_0 is the basic reproductive number and represents the expected number of secondary infections caused from one infected individual entering a purely susceptible population. Therefore $(K, 0)$ is stable when $R_0 < 1$, this represents that the disease cannot invade the species. When we later consider both species, we will use $R_0(1)$ and $R_0(2)$ to represent the basic reproductive numbers for host species 1 and 2 respectively.

3. $(\mathbf{S}^*, \mathbf{I}^*)$

The third equilibrium point (S^*, I^*) where the native species and the disease are coexisting is feasible if $R_0 > 1$. Linearising equations (2.23a–b) about (S^*, I^*) gives the following Jacobian matrix

$$\mathbf{J}_{(S^*,I^*)} = \begin{pmatrix} a - q(S^* + I^*) - b - q(S^* + fI^*) - \beta I^* & f(a - q(S^* + I^*)) - q(S^* + fI^*) - \beta S^* + \gamma \\ \beta I^* & \beta S^* - \Gamma \end{pmatrix}. \tag{2.28}$$

Since $I^* \neq 0$, equation (2.23b) gives us $\beta S^* - \Gamma = 0$. This expression can be used to simplify $\mathbf{J}_{(S^*,I^*)}$, (2.28), to give

$$\mathbf{J}_{(S^*,I^*)} = \begin{pmatrix} a - q(S^* + I^*) - b - q(S^* + fI^*) - \beta I^* & f(a - q(S^* + I^*)) - q(S^* + fI^*) - \beta S^* + \gamma \\ \beta I^* & 0 \end{pmatrix} \tag{2.29}$$

Since $S^* \neq 0$ and $I^* \neq 0$, equation (2.23a) can be rearranged to give two useful simplifications. Firstly, (2.23a) can be divided by S^* to give

$$\frac{aS^* + afI^* - q(S^* + I^*)S^* - qfI^*S^* - qfI^{*2} - bS^* - \beta S^* I^* + \gamma I^*}{S^*} = 0 \tag{2.30a}$$

$$\Rightarrow \quad a + \frac{afI^*}{S^*} - q(S^* + I^*) - qfI^* - \frac{qfI^{*2}}{S^*} - b - \beta I^* + \frac{\gamma I^*}{S^*} = 0. \tag{2.30b}$$

This can be rearranged to give

$$a - q(S^* + I^*) - b - \beta I^* = -\frac{1}{S^*}\left(afI^* - qfI^*S^* - qfI^{*2} + \gamma I^*\right), \tag{2.30c}$$

and subtracting $q(S^* + fI^*)$ from both sides, we can then rearrange again

$$\begin{aligned} &a - q(S^* + I^*) - b - \beta I^* - q(S^* + fI^*) \\ &\qquad = -\frac{1}{S^*}\left(afI^* - qfI^*S^* - qfI^{*2} + \gamma I^*\right) - q(S^* + fI^*) \end{aligned} \tag{2.30d}$$

$$\Rightarrow \quad a - q(S^* + I^*) - b - \beta I^* - q(S^* + fI^*) = -\frac{1}{S^*}\left(afI^* - qfI^{*2} + \gamma I^* + qS^{*2}\right) \tag{2.30e}$$

$$\Rightarrow \quad a - q(S^* + I^*) - b - \beta I^* - q(S^* + fI^*) = -\frac{1}{S^*}\left((a - qI^*)fI^* + qS^{*2} + \gamma I^*\right). \tag{2.30f}$$

Secondly, equation (2.23a) can be divided by I^* to give

$$\frac{aS^* + afI^* - qS^{*2} - qI^*S^* - qfI^*(S^* + I^*) - bS^* - \beta S^*I^* + \gamma I^*}{I^*} = 0 \tag{2.31a}$$

$$\Rightarrow \quad \frac{aS^*}{I^*} + af - \frac{qS^{*2}}{I^*} - qS^* - qf(S^* + I^*) - \frac{bS^*}{I^*} - \beta S^* + \gamma = 0. \tag{2.31b}$$

This can be rearranged to give

$$f(a - q(S^* + I^*)) - qS^* - \beta S^* + \gamma = -\frac{1}{I^*}\left((a - b - qS^*)S^*\right), \tag{2.31c}$$

and subtracting qfI^* from both sides, we can then rearrange again:

$$f(a - q(S^* + I^*)) - qS^* - \beta S^* + \gamma - qfI^* = -\frac{1}{I^*}\left((a - b - qS^*)S^*\right) - qfI^* \tag{2.31d}$$

$$\Rightarrow \quad f(a - q(S^* + I^*)) - q(S^* + fI^*) - \beta S^* + \gamma = -\frac{1}{I^*}\left((a - b - qS^*)S^* + qfI^{*2}\right). \tag{2.31e}$$

Equations (2.30f) and (2.31e) can then be used to simplify the expression for $\mathbf{J}_{(S^*,I^*)}$, (2.29), to give

$$\mathbf{J}_{(S^*,I^*)} = \begin{pmatrix} -\frac{1}{S^*}\left((a - qI^*)fI^* + qS^{*2} + \gamma I^*\right) & -\frac{1}{I^*}\left((a - b - qS^*)S^* + qfI^{*2}\right) \\ \beta I^* & 0 \end{pmatrix}. \tag{2.32}$$

The equilibrium point (S^*, I^*) is stable if the following trace and determinant conditions from the Jacobian matrix $\mathbf{J}_{(S^*,I^*)}$ (2.32) hold

$$-\frac{1}{S^*}\left((a-qI^*)fI^* + qS^{*2} + \gamma I^*\right) < 0 \quad \text{(holds if } a - qI^* > 0\text{)}, \tag{2.33a}$$

$$\beta\left((a-b-qS^*)S^* + qfI^{*2}\right) > 0 \tag{2.33b}$$

$$\Rightarrow \quad \beta\left(\left(a-b-\frac{q\Gamma}{\beta}\right)\left(\frac{\Gamma}{\beta}\right) + qfI^{*2}\right) > 0 \quad \left(S^* = \frac{\Gamma}{\beta}\right) \tag{2.33c}$$

$$\Rightarrow \quad (\beta(a-b) - q\Gamma)\left(\frac{\Gamma}{\beta}\right) + \beta qfI^{*2} > 0 \quad \text{(holds if } R_0 > 1\text{)}. \tag{2.33d}$$

The trace condition holds if $a - qI^* > 0$, to show this holds we again consider (2.23a)

$$aS^* + afI^* - q(S^* + I^*)S^* - qfI^*S^* - qfI^{*2} - bS^* - \beta S^*I^* + \gamma I^* = 0. \tag{2.34a}$$

This can be rearranged to give

$$a - q(S^* + I^*) = \frac{bS^* + \beta S^*I^* - \gamma I^*}{S^* + fI^*} \tag{2.34b}$$

$$= \frac{bS^* + \Gamma I^* - \gamma I^*}{S^* + fI^*} \qquad [\beta S^* = \Gamma] \tag{2.34c}$$

$$= \frac{bS^* + (\alpha + b + \gamma)I^* - \gamma I^*}{S^* + fI^*} \qquad [\Gamma = \alpha + b + \gamma] \tag{2.34d}$$

$$= \frac{bS^* + (\alpha + b)I^*}{S^* + fI^*} > 0 \qquad [S^* > 0, I^* > 0] \tag{2.34e}$$

$$\text{i.e.} \quad a - q(S^* + I^*) > 0 \tag{2.34f}$$

$$\text{i.e.} \quad a - qI^* > 0 \qquad [a - qI^* > a - q(S^* + I^*)]. \tag{2.34g}$$

Therefore, (S^*, I^*) is feasible and stable if $R_0 > 1$ (this holds for $f \geqslant 0$).

2.5.3 Full model

This section considers both species with the disease present. There are seven equilibrium points, seen earlier in the text (2.4a–g), obtained from setting the right-hand side of equations (2.11a–d) equal to zero,

$$(S_1, I_1, S_2, I_2) = (0, 0, 0, 0), \tag{2.35a}$$

$$(K_1, 0, 0, 0) = \left(\tfrac{a_1 - b_1}{q_1}, 0, 0, 0\right), \tag{2.35b}$$

$$(S_1^*, I_1^*, 0, 0) = \left(\tfrac{\Gamma_1}{\beta_{11}}, \tfrac{\Psi_1 + \sqrt{\Psi_1^2 + \Omega_1}}{2q_1 f_1 \beta_{11}}, 0, 0\right), \tag{2.35c}$$

$$(0, 0, K_2, 0) = \left(0, 0, \tfrac{a_2 - b_2}{q_2}, 0\right), \tag{2.35d}$$

$$(0, 0, S_2^*, I_2^*) = \left(0, 0, \tfrac{\Gamma_2}{\beta_{22}}, \tfrac{\Psi_2 + \sqrt{\Psi_2^2 + \Omega_2}}{2q_2 f_2 \beta_{22}}\right), \tag{2.35e}$$

$$(S_1^+, 0, S_2^+, 0) = \left(\tfrac{c_2 K_2 - K_1}{c_1 c_2 - 1}, 0, \tfrac{c_1 K_1 - K_2}{c_1 c_2 - 1}, 0\right), \tag{2.35f}$$

$$(\hat{S_1}, \hat{I_1}, \hat{S_2}, \hat{I_2}) \tag{2.35g}$$

where in the steady state (2.35g) the values are algebraically complicated and omitted. If $f_1 > 0$, the steady state defined in equation (2.35c) is expanded with $\Gamma_1 = \alpha_1 + b_1 + \gamma_1$, $\Psi_1 = (a_1 f_1 - b_1 - \alpha_1)\beta_{11} - q_1 f_1 \Gamma_1 - q_1 \Gamma_1$ and $\Omega_1 = 4 f_1 q_1^2 \Gamma_1 (\beta_{11} K_1 - \Gamma_1)$. In the alternative case when $f_1 = 0$, I_1^* in equation (2.35c) becomes $I_1^* = \dfrac{\Gamma_1 (\beta_{11} K_1 - \Gamma_1)(a_1 - b_1)}{\beta_{11} (\Gamma_1 (a_1 - b_1) + K_1 \beta_{11} (\Gamma_1 - \gamma_1))}$. If $f_2 > 0$, the steady state defined by equation (2.35e) is expanded with Γ_2, Ψ_2 and Ω_2 ; where Γ_2, Ψ_2 and Ω_2 are equivalent to Γ_1, Ψ_1 and Ω_1 respectively with the subscript 1 changed to 2. Alternatively, if $f_2 = 0$, I_2^* in equation (2.35e) is equivalent to that for I_1^* when $f_1 = 0$ described above, with the subscript 1 changed to 2.

Feasibility and Stability

1. $(\mathbf{0}, \mathbf{0}, \mathbf{0}, \mathbf{0})$

We begin by considering the origin, $(S_1, I_1, S_2, I_2) = (0, 0, 0, 0)$, where there is no species or disease (2.35a). Linearising equations (2.11a–d) about $(0, 0, 0, 0)$ gives the following Jacobian

matrix

$$\mathbf{J}_{(0,0,0,0)} = \begin{pmatrix} a_1 - b_1 & f_1 a_1 + \gamma_1 & 0 & 0 \\ 0 & -\Gamma_1 & 0 & 0 \\ 0 & 0 & a_2 - b_2 & f_2 a_2 + \gamma_2 \\ 0 & 0 & 0 & -\Gamma_2 \end{pmatrix} \tag{2.36}$$

with eigenvalues $\lambda_{61} = a_1 - b_1$, $\lambda_{62} = a_2 - b_2$, $\lambda_{63} = -\Gamma_1$ and $\lambda_{64} = -\Gamma_2$. λ_{63} and λ_{64} are always less than zero but λ_{61} and λ_{62} are always greater than zero, since $a_i - b_i > 0$ (for $i = 1, 2$). Therefore the origin, where both species and the disease are excluded, is always unstable.

2. $(\mathbf{K_1}, \mathbf{0}, \mathbf{0}, \mathbf{0})$

At the equilibrium $(K_1, 0, 0, 0)$, given in (2.35b), the native species is at its carrying capacity and the invader and disease are excluded. This equilibrium is always feasible since $K_1 > 0$. Linearising equations (2.11a–d) about $(K_1, 0, 0, 0)$ gives the following Jacobian matrix

$\mathbf{J}_{(K_1,0,0,0)} =$

$$\begin{pmatrix} b_1 - a_1 & b_1 - a_1 + f_1 b_1 - K_1\beta_{11} + \gamma_1 & c_2(b_1 - a_1) & (b_1 - a_1)c_2 - \beta_{12}K_1 \\ 0 & K_1\beta_{11} - \Gamma_1 & 0 & \beta_{12}K_1 \\ 0 & 0 & (a_2 - b_2)(1 - \frac{c_1 K_1}{K_2}) & f_2 a_2 + \gamma_2 - \frac{f_2(a_2 - b_2)c_1 K_1}{K_2} \\ 0 & 0 & 0 & -\Gamma_2 \end{pmatrix} \tag{2.37}$$

with the following eigenvalues

$$\lambda_{71} = b_1 - a_1, \tag{2.38a}$$

$$\lambda_{72} = -\Gamma_2, \tag{2.38b}$$

$$\lambda_{73} = \beta_{11}K_1 - \Gamma_1, \tag{2.38c}$$

$$\lambda_{74} = \frac{(b_2 - a_2)(c_1 K_1 - K_2)}{K_2}. \tag{2.38d}$$

The eigenvalue λ_{71} is always less than zero, since $a_1 - b_1 > 0$ always holds. λ_{72} is always less than zero since Γ_2 is positive. The eigenvalue λ_{73} is less than zero if $R_0(1) = \frac{\beta_{11}K_1}{\Gamma_1} < 1$. Finally, λ_{74} is less than zero if $c_1 K_1 - K_2 > 0$. Therefore $(K_1, 0, 0, 0)$ is stable when $R_0(1) < 1$ and $c_1 K_1 - K_2 > 0$; these represent that the disease cannot invade the native species but the native species has a competitive advantage over the alien species.

3. $(\mathbf{S_1^*}, \mathbf{I_1^*}, \mathbf{0}, \mathbf{0})$

The third equilibrium point $(S_1^*, I_1^*, 0, 0)$, with the native species and the disease coexisting, is fea-

sible if $R_0(1) > 1$. Linearising equations (2.11a–d) about $(S_1^*, I_1^*, 0, 0)$ gives the following Jacobian matrix

$\mathbf{J}_{(S_1^*,I_1^*,0,0)} =$

$$\begin{pmatrix} a_1 - q_1(S_1^* + I_1^*) - b_1 & f_1(a_1 - q_1(S_1^* + I_1^*)) & -q_1c_2(S_1^* + f_1I_1^*) & -q_1c_2(S_1^* + f_1I_1^*) \\ -q_1(S_1^* + f_1I_1^*) - \beta_{11}I_1^* & -q_1(S_1^* + f_1I_1^*) - \beta_{11}S_1^* + \gamma_1 & & -\beta_{12}S_1^* \\ \beta_{11}I_1^* & \beta_{11}S_1^* - \Gamma_1 & 0 & \beta_{12}S_1^* \\ 0 & 0 & a_2 - b_2 - q_2c_1S_1^* & f_2a_2 - f_2q_2c_1S_1^* \\ & & -q_2c_1I_1^* - \beta_{21}I_1^* & -f_2q_2c_1I_1^* + \gamma_2 \\ 0 & 0 & \beta_{21}I_1^* & -\Gamma_2 \end{pmatrix}. \tag{2.39}$$

To determine the stability, the eigenvalue problem can be factorised into two different quadratic components. These components correspond to two 2x2 submatrices of $\mathbf{J}_{(S_1^*,I_1^*,0,0)}$, (2.39). The first submatrix is the upper left components

$\mathbf{J}_{(S_1^*,I_1^*,0,0)a} =$

$$\begin{pmatrix} a_1 - q_1(S_1^* + I_1^*) - b_1 - q_1(S_1^* + f_1I_1^*) - \beta_{11}I_1^* & f_1(a_1 - q_1(S_1^* + I_1^*)) - q_1(S_1^* + f_1I_1^*) - \beta_{11}S_1^* + \gamma_1 \\ \beta_{11}I_1^* & \beta_{11}S_1^* - \Gamma_1 \end{pmatrix}. \tag{2.40}$$

This is equivalent to the Jacobian matrix $\mathbf{J}_{(S^*,I^*)}$, seen earlier in the disease-only model (2.28). It can be simplified in the same way as used earlier to obtain (2.29)–(2.32) and resulting stability conditions (2.33)–(2.34) found in the same way. Therefore, the first stability condition for $\mathbf{J}_{(S_1^*,I_1^*,0,0)}$ is $R_0(1) > 1$ (holds when $f_1 \geqslant 0$). The second submatrix of $\mathbf{J}_{(S_1^*,I_1^*,0,0)}$, (2.39), is the lower right components

$\mathbf{J}_{(S_1^*,I_1^*,0,0)b} =$

$$\begin{pmatrix} a_2 - b_2 - q_2c_1S_1^* - q_2c_1I_1^* - \beta_{21}I_1^* & f_2a_2 - f_2q_2c_1S_1^* - f_2q_2c_1I_1^* + \gamma_2 \\ \beta_{21}I_1^* & -\Gamma_2 \end{pmatrix} \tag{2.41}$$

with the following trace and determinant conditions

$$a_2 - b_2 - q_2c_1(S_1^* + I_1^*) - \beta_{21}I_1^* - \Gamma_2 < 0, \tag{2.42a}$$

$$-\Gamma_2(a_2 - b_2 - q_2c_1(S_1^* + I_1^*) - \beta_{21}I_1^*) - \beta_{21}I_1^*(f_2(a_2 - q_2c_1(S_1^* + I_1^*)) + \gamma_2) > 0. \tag{2.42b}$$

The determinant condition, (2.42b), can be rearranged as follows

$$a_2 - b_2 - q_2c_1(S_1^* + I_1^*) - \beta_{21}I_1^* + \frac{\beta_{21}I_1^*}{\Gamma_2}\Big(f_2a_2 - f_2q_2c_1(S_1^* + I_1^*) + \gamma_2\Big) < 0 \tag{2.43a}$$

$$\Rightarrow (a_2 - b_2 - q_2c_1(S_1^* + I_1^*)) + \frac{\beta_{21}I_1^*}{\Gamma_2}\Big(f_2a_2 - b_2 - f_2q_2c_1(S_1^* + I_1^*) - \alpha_2\Big) < 0. \tag{2.43b}$$

If we assume the trace condition (2.42a) is equal to zero, we can rearrange it to get the following two equations

$$a_2 - b_2 - q_2 c_1 (S_1^* + I_1^*) - \beta_{21} I_1^* = \Gamma_2, \tag{2.44a}$$

$$a_2 - q_2 c_1 (S_1^* + I_1^*) = \beta_{21} I_1^* + \Gamma_2 + b_2. \tag{2.44b}$$

These two equations (2.44a–b) can then be used to simplify the determinant condition (2.42b) to give

$$-\Gamma_2(\Gamma_2) - \beta_{21} I_1^* (f_2(\beta_{21} I_1^* + \Gamma_2 + b_2)) + \gamma_2) > 0. \tag{2.44c}$$

which never holds as the left hand side is less than zero. When the trace condition (2.42a) is equal to zero, the determinant condition (2.42b) is always less than zero. Therefore, the determinant condition is violated before the trace condition and we only need to consider the determinant condition. Therefore, the simplified determinant condition, (2.43b), is the only stability condition required from submatrix $\mathbf{J}_{(S_1^*, I_1^*, 0, 0)b}$. We can then combine this with the stability condition found from the first submatrix, $\mathbf{J}_{(S_1^*, I_1^*, 0, 0)a}$, to find the stability conditions of the steady state $(S_1^*, I_1^*, 0, 0)$. Hence, the steady state $(S_1^*, I_1^*, 0, 0)$ is feasible and stable when $R_0(1) > 1$ and (2.43b) holds. The condition $R_0(1) > 1$ represents that the disease can invade the native species and (2.43b) represents the fitness of the alien species being negative.

4. $(\mathbf{0}, \mathbf{0}, \mathbf{K_2}, \mathbf{0})$

At the fourth equilibrium $(0, 0, K_2, 0)$, the alien species is at its carrying capacity and the native and disease are excluded (2.35d). This equilibrium is always feasible since $K_2 > 0$. Linearising equations (2.11a–d) about $(0, 0, K_2, 0)$ and reordering to consider (S_2, I_2, S_1, I_1) gives the following Jacobian matrix

$\mathbf{J}_{(0,0,K_2,0)} =$

$$\begin{pmatrix} b_2 - a_2 & b_2 - a_2 + f_2 b_2 - K_2 \beta_{22} + \gamma_2 & c_1(b_2 - a_2) & (b_2 - a_2)c_1 - \beta_{21} K_2 \\ 0 & K_2 \beta_{22} - \Gamma_2 & 0 & \beta_{21} K_2 \\ 0 & 0 & (a_1 - b_1)(1 - \frac{c_2 K_2}{K_1}) & f_1 a_1 + \gamma_1 - \frac{f_1 (a_1 - b_1) c_2 K_2}{K_1} \\ 0 & 0 & 0 & -\Gamma_1 \end{pmatrix} \tag{2.45}$$

with the following eigenvalues

$$\lambda_{81} = b_2 - a_2, \tag{2.46a}$$

$$\lambda_{82} = -\Gamma_1, \tag{2.46b}$$

$$\lambda_{83} = \beta_{22}K_2 - \Gamma_2, \tag{2.46c}$$

$$\lambda_{84} = \frac{(b_1 - a_1)(c_2K_2 - K_1)}{K_1}. \tag{2.46d}$$

The eigenvalue λ_{81} is always less than zero, since $a_2 - b_2 > 0$ always holds. λ_{82} is always less than zero since Γ_1 is positive. The eigenvalue λ_{83} is less than zero if $R_0(2) = \frac{\beta_{22}K_2}{\Gamma_2} < 1$. Finally, λ_{84} is less than zero if $c_2K_2 - K_1 > 0$. Therefore $(0, 0, K_2, 0)$ is stable when $R_0(2) < 1$ and $c_2K_2 - K_1 > 0$; these represent that the disease cannot invade the alien species while the alien species has a competitive advantage over the native species.

5. $(\mathbf{0}, \mathbf{0}, \mathbf{S_2^*}, \mathbf{I_2^*})$

The fifth equilibrium point $(0, 0, S_2^*, I_2^*)$, with the alien species and the disease coexisting is feasible if $R_0(2) > 1$. Linearising equations (2.11a–d) about $(0, 0, S_2^*, I_2^*)$ and reordering to consider (S_2, I_2, S_1, I_1) gives the following Jacobian matrix

$\mathbf{J}_{(0,0,S_2^*,I_2^*)} =$

$$\begin{pmatrix} a_2 - q_2(S_2^* + I_2^*) - b_2 & f_2(a_2 - q_2(S_2^* + I_2^*)) & -q_2c_1(S_2^* + f_2I_2^*) & -q_2c_1(S_2^* + f_2I_2^*) \\ -q_2(S_2^* + f_2I_2^*) - \beta_{22}I_2^* & -q_2(S_2^* + f_2I_2^*) - \beta_{22}S_2^* + \gamma_2 & & -\beta_{21}S_2^* \\ \beta_{22}I_2^* & \beta_{22}S_2^* - \Gamma_2 & 0 & \beta_{21}S_2^* \\ 0 & 0 & a_1 - b_1 - q_1c_2S_2^* & f_1a_1 - f_1q_1c_2S_2^* \\ & & -q_1c_2I_2^* - \beta_{12}I_2^* & -f_1q_1c_2I_2^* + \gamma_1 \\ 0 & 0 & \beta_{12}I_2^* & -\Gamma_1 \end{pmatrix}. \tag{2.47}$$

To determine the stability, the eigenvalue problem can be factorised into two different quadratic components. These components correspond to two 2x2 submatrices of $\mathbf{J}_{(0,0,S_2^*,I_2^*)}$, (2.47). The first submatrix is the upper left components

$\mathbf{J}_{(0,0,S_2^*,I_2^*)a} =$

$$\begin{pmatrix} a_2 - q_2(S_2^* + I_2^*) - b_2 - q_2(S_2^* + f_2I_2^*) - \beta_{22}I_2^* & f_2(a_2 - q_2(S_2^* + I_2^*)) - q_2(S_2^* + f_2I_2^*) - \beta_{22}S_2^* + \gamma_2 \\ \beta_{22}I_2^* & \beta_{22}S_2^* - \Gamma_2 \end{pmatrix}. \tag{2.48}$$

This is equivalent to the Jacobian matrix $\mathbf{J}_{(S^*,I^*)}$, seen earlier in the disease-only model (2.28). It can be simplified in the same way, (2.29)–(2.32) and resulting stability conditions found in the same way, (2.33)–(2.34). Therefore, the first stability condition for $\mathbf{J}_{(0,0,S_2^*,I_2^*)}$ is $R_0(2) > 1$ (holds when $f_2 \geqslant 0$). The second submatrix of $\mathbf{J}_{(0,0,S_2^*,I_2^*)}$,(2.47), is the lower right components

$\mathbf{J}_{(0,0,S_2^*,I_2^*)b} =$

$$\begin{pmatrix} a_1 - b_1 - q_1c_2S_2^* - q_1c_2I_2^* - \beta_{12}I_2^* & f_1a_1 - f_1q_1c_2S_2^* - f_1q_1c_2I_2^* + \gamma_1 \\ \beta_{12}I_2^* & -\Gamma_1 \end{pmatrix} \tag{2.49}$$

with the following trace and determinant conditions

$$a_1 - b_1 - q_1c_2(S_2^* + I_2^*) - \beta_{12}I_2^* - \Gamma_1 < 0, \tag{2.50a}$$

$$-\Gamma_1(a_1 - b_1 - q_1c_2(S_2^* + I_2^*) - \beta_{12}I_2^*) - \beta_{12}I_2^*(f_1a_1 - f_1q_1c_2(S_2^* + I_2^*) + \gamma_1) > 0. \tag{2.50b}$$

The determinant condition, (2.50b), can be rearranged as follows

$$a_1 - b_1 - q_1c_2(S_2^* + I_2^*) - \beta_{12}I_2^* + \frac{\beta_{12}I_2^*}{\Gamma_1}\Big(f_1a_1 - f_1q_1c_2(S_2^* + I_2^*) + \gamma_1\Big) < 0 \tag{2.51a}$$

$$\Rightarrow (a_1 - b_1 - q_1c_2(S_2^* + I_2^*)) + \frac{\beta_{12}I_2^*}{\Gamma_1}\Big(f_1a_1 - b_1 - f_1q_1c_2(S_2^* + I_2^*) - \alpha_1\Big) < 0. \tag{2.51b}$$

If we assume the trace condition (2.50a) is equal to zero, we can rearrange it to get the following two equations

$$a_1 - b_1 - q_1c_2(S_2^* + I_2^*) - \beta_{12}I_2^* = \Gamma_1, \tag{2.52a}$$

$$a_1 - q_1c_2(S_2^* + I_2^*) = \beta_{12}I_2^* + \Gamma_1 + b_1. \tag{2.52b}$$

These two equations (2.52a–b) can then be used to simplify the determinant condition (2.50b) to give

$$-\Gamma_1(\Gamma_1) - \beta_{12}I_2^*(f_1(\beta_{12}I_2^* + \Gamma_1 + b_1)) + \gamma_1) > 0. \tag{2.52c}$$

which never holds as the left hand side is less than zero. When the trace condition (2.50a) is equal to zero, the determinant condition (2.50b) is always less than zero. Therefore, the determinant condition is violated before the trace condition and we only need to consider the determinant condition. Therefore, the simplified determinant condition, (2.51b), is the only stability condition required from submatrix $\mathbf{J}_{(0,0,S_2^*,I_2^*)b}$. We can then combine this with the stability condition found from the first submatrix, $\mathbf{J}_{(0,0,S_2^*,I_2^*)a}$, to find the stability conditions of the steady state $(0, 0, S_2^*, I_2^*)$. Hence, the steady state $(0, 0, S_2^*, I_2^*)$ is feasible and stable when $R_0(2) > 1$ and (2.51b) holds. The condition $R_0(2) > 1$ represents that the disease can invade the alien species and (2.51b) represents the fitness of the native species being negative.

6. $(\mathbf{S_1^+}, \mathbf{0}, \mathbf{S_2^+}, \mathbf{0})$

The sixth equilibrium $(S_1^+, 0, S_2^+, 0)$, (2.35f), with the native and alien coexisting and no disease present is feasible if $S_1^+ > 0$ and $S_2^+ > 0$ which occurs when $c_2K_2 - K_1$, $c_1K_1 - K_2$ and $c_1c_2 - 1$ are either all positive or all negative. Linearising equations (2.11a–d) about $(S_1^+, 0, S_2^+, 0)$ and re-

ordering to consider (S_1, S_2, I_1, I_2) gives the following Jacobian matrix
$\mathbf{J}_{(S_1^+,0,S_2^+,0)} =$

$$\begin{pmatrix} -2q_1S_1^+ + a_1 - b_1 & -q_1c_2S_1^+ & f_1(a_1 - q_1(S_1^+ + c_2S_2^+)) & -q_1c_2S_1^+ - \beta_{12}S_1^+ \\ -q_1c_2S_2^+ & & -q_1S_1^+ - \beta_{11}S_1^+ + \gamma_1 & \\ -q_2c_1S_2^+ & -2q_2S_2^+ + a_2 - b_2 - q_2c_1S_1^+ & -q_2c_1S_2^+ - \beta_{21}S_2^+ & f_2(a_2 - q_2(S_2^+ + c_1S_1^+)) \\ & & & -q_2S_2^+ - \beta_{22}S_2^+ + \gamma_2 \\ 0 & 0 & \beta_{11}S_1^+ - \Gamma_1 & \beta_{12}S_1^+ \\ 0 & 0 & \beta_{21}S_2^+ & \beta_{22}S_2^+ - \Gamma_2 \end{pmatrix}. \tag{2.53}$$

To determine the stability, the eigenvalue problem can be factorised into two different quadratic components. These components correspond to two 2x2 submatrices of $\mathbf{J}_{(S_1^+,0,S_2^+,0)}$, (2.53). The first submatrix,$\mathbf{J}_{(S_1^+,0,S_2^+,0)a}$, is the upper left components

$$\mathbf{J}_{(S_1^+,0,S_2^+,0)a} = \begin{pmatrix} -2q_1S_1^+ + a_1 - b_1 - q_1c_2S_2^+ & -q_1c_2S_1^+ \\ -q_2c_1S_2^+ & -2q_2S_2^+ + a_2 - b_2 - q_2c_1S_1^+ \end{pmatrix}. \tag{2.54}$$

This is equivalent to the Jacobian matrix $\mathbf{J}_{(S_1^+,S_2^+)}$, (2.19), seen earlier in the competition-only model. It can be simplified in the same way, (2.20), and resulting stability conditions found in the same way, (2.21a–b). Therefore, the first three stability conditions for $\mathbf{J}_{(S_1^+,0,S_2^+,0)}$ are

$$c_1K_1 - K_2 < 0, \tag{2.55a}$$

$$c_2K_2 - K_1 < 0, \tag{2.55b}$$

$$c_1c_2 - 1 < 0. \tag{2.55c}$$

The second submatrix of $\mathbf{J}_{(S_1^+,0,S_2^+,0)}$, (2.53), is the lower right components

$$\mathbf{J}_{(S_1^+,0,S_2^+,0)b} = \begin{pmatrix} \beta_{11}S_1^+ - \Gamma_1 & \beta_{12}S_1^+ \\ \beta_{21}S_2^+ & \beta_{22}S_2^+ - \Gamma_2 \end{pmatrix} \tag{2.56}$$

with the following trace and determinant conditions

$$\beta_{11}S_1^+ - \Gamma_1 + \beta_{22}S_2^+ - \Gamma_2 < 0, \tag{2.57a}$$

$$(\beta_{11}S_1^+ - \Gamma_1)(\beta_{22}S_2^+ - \Gamma_2) - \beta_{12}\beta_{21}S_1^+S_2^+ > 0. \tag{2.57b}$$

We can combine these with the stability conditions found from the first submatrix, $\mathbf{J}_{(S_1^+,0,S_2^+,0)a}$, to find the stability conditions of the steady state $((S_1^+,0,S_2^+,0)$. Hence, the steady state $(S_1^+,0,S_2^+,0)$ is feasible and stable when the following five conditions hold

$$c_1K_1 - K_2 < 0, \tag{2.58a}$$

$$c_2K_2 - K_1 < 0, \tag{2.58b}$$

$$c_1c_2 - 1 < 0, \tag{2.58c}$$

$$\beta_{11}S_1^+ - \Gamma_1 + \beta_{22}S_2^+ - \Gamma_2 < 0, \tag{2.58d}$$

$$(\beta_{11}S_1^+ - \Gamma_1)(\beta_{22}S_2^+ - \Gamma_2) - \beta_{12}\beta_{21}S_1^+S_2^+ > 0. \tag{2.58e}$$

This reflects the fact that neither species can out-compete the other and that the disease cannot invade either single population or the joint population.

7. $(\hat{\mathbf{S_1}}, \hat{\mathbf{I_1}}, \hat{\mathbf{S_2}}, \hat{\mathbf{I_2}})$

The final equilibrium $(\hat{S_1}, \hat{I_1}, \hat{S_2}, \hat{I_2})$, (2.35g), represents all the classes having positive densities and both the native and invader coexisting with the parasite. We do not discuss the stability of this steady state here as the algebra is intractable. Bowers and Turner (1997) and Greenman and Hudson (1997) both give a detailed steady state and stability analysis for a similar model.

Chapter 3

Spatial Modelling of Invasion Dynamics

3.1 Introduction

We now extend our analysis to investigate how the temporal findings for the replacement of a native species extend to a spatial model framework by developing a system of reaction-diffusion equations. This is a classical modelling approach, that assumes random movement, and involves adding a diffusion term to a set of spatially homogeneous population differential equations (Murray, 2002; Cantrell and Cosner, 2003; De Vries *et al.*, 2006). Reaction-diffusion equations were used by Fisher (1937) to model the spread of an advantageous gene through a population and by Skellam (1951) to investigate the spread of the muskrat, *Ondatra zibethica*, in central Europe following its introduction in 1905. This approach has been used in single species epidemiological models. An example of particular relevance to our study is Murray *et al.* (1986) extension of Anderson *et al.* (1981) model to include a diffusion term for the random wanderings of rabid foxes. This modelling allowed Murray *et al.* to investigate the effect of a rabies introduction to the UK and potential strategies for stopping an epidemic. Another particularly relevant example is White *et al.* (1999) who extended the Anderson and May (1981) model G using this approach to model the effects of movement on an insect host-pathogen model with a free-living stage. Diffusion terms can also be added when more than one species is involved. In particular Okubo *et al.* (1989) used coupled reaction-diffusion equations to model the competition-mediated replacement of red squirrels by greys in the UK.

To understand some of the key features of the reaction-diffusion system we will begin by examining a variation of the Fisher-Kolmogorov equation (Fisher, 1937; Kolmogorov *et al.*, 1937) that considers a single-species competition-only version of the model seen in chapter two

$$\frac{dS}{dt} = rS - qS^2 + D\frac{\partial^2 S}{\partial x^2}. \tag{3.1}$$

Here, S represents the population density, r the growth rate (birth − death), t time, x spatial position and D is the diffusion coefficient. We assume positive carrying capacity, K, which is related to susceptibility to crowding, q, since $K = r/q$. We will consider a situation where the species is introduced to a homogeneous landscape and investigate travelling wave solutions (figure 3.1). To investigate travelling wave solutions we consider $S(x,t) = S(x-\theta t)$ where $\theta > 0$ is the wave speed. By using $Z = x - \theta t$ we can examine equation (3.1) in a coordinate system that moves at the same speed as the travelling wave. Substituting these solution forms into equation (3.1) and denoting differentiation with respect to Z by prime gives

$$-\theta S' = rS - qS^2 + DS'' \tag{3.2}$$

Using $\dot{S} = S'$, equation (3.2) can be written as the following system of first-order ordinary differential equations

$$S' = \dot{S} \tag{3.3a}$$

$$\dot{S}' = (-1/D)(rS - qS^2 + \theta\dot{S}) \tag{3.3b}$$

There are two equilibrium points obtained from setting the right-hand side of equations (3.3a) and (3.3b) equal to zero, $(S, \dot{S}) = (0,0)$ and $(K,0)$. To investigate possible wave speeds, we linearise at the steady state ahead of the wave. Linearising equations (3.3a) and (3.3b) at $(0,0)$, gives the following Jacobian matrix

$$\mathbf{J}_{(0,0)} = \begin{pmatrix} 0 & 1 \\ -\frac{r}{D} & -\frac{\theta}{D} \end{pmatrix}. \tag{3.4}$$

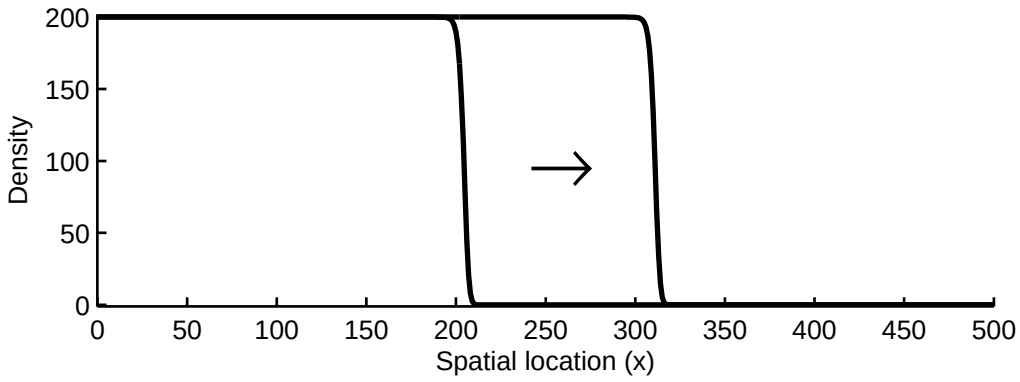

Figure 3.1 Spread across a spatial landscape from Fisher-type equation. The density is recorded at time points 300 and 500. The parameters are: $r = 0.4$, $K = 200$, $q = 0.002$ and $D = 0.18$. We assumed zero flux boundary conditions and the initial conditions are $S = K$ for $x < 50$ and $S = 0$ otherwise. These observed values were produced using a semi-implicit Crank-Nicolson method with a grid spacing of 10^{-2} and a time step of 10^{-2}.

It follows that $(0, 0)$ is a stable node or focus with the following eigenvalues

$$\lambda_{1,2} = \frac{1}{2}\left(\frac{-\theta}{D} \pm \sqrt{\left(\frac{\theta}{D}\right)^2 - 4\left(\frac{r}{D}\right)}\right). \tag{3.5}$$

λ_1 and λ_2 are either real and negative (stable node), or a complex conjugate pair with a negative real part (stable focus). To ensure we do not have negative population densities $(0, 0)$ must not be a focus (the eigenvalues must be real). We therefore impose the following condition

$$\left(\frac{\theta}{D}\right)^2 - 4\left(\frac{r}{D}\right) \geqslant 0 \tag{3.6a}$$

$$\Rightarrow \theta^2 \geqslant 4rD \tag{3.6b}$$

$$\Rightarrow \theta \geqslant 2\sqrt{rD} = \theta_f. \tag{3.6c}$$

Kolmogorov *et al.* (1937) showed that, providing local dynamics satisfy some simple conditions, there are wave front solutions for any value of the wave speed above the critical minimum value. Moreover, for biologically sensible initial conditions, the travelling wave will typically move at the minimum speed. For instance, if

$$S(x, 0) = S_0(x) \geqslant 0, \quad S_0(x) = \begin{cases} K & \text{if} \quad x < x_1, \\ 0 & \text{if} \quad x > x_2, \end{cases} \tag{3.7}$$

where $x_1 < x_2$ and $S_0(x)$ is continuous in $x_1 < x < x_2$, then the solution $S(x, t)$ of equation (3.1) evolves to the the travelling wave solution $S(Z)$ with the minimum wave speed θ_f, given by:

$$\theta_f = 2\sqrt{rD}. \tag{3.8}$$

For the parameters used in figure 3.1 the minimum wave speed is calculated as $\theta_f = 0.54$. This matches very closely with the wave speed that can be calculated from simulations (figure 3.1). An overview of the methods used above can be found in Shigesada and Kawasaki (1997), Kot (2001), Okubo *et al.* (2001) and Murray (2002). We will now extend these methods to investigate the spatial model framework for the model seen in chapter two.

3.2 Model

We extend our system of ordinary differential equations (2.3a–d) by adding diffusion terms, to give the following reaction-diffusion equations. The classes of susceptible, S_i, and infected, I_i individuals are represented by the following system of equations, where $i = 1, 2$ with 1 representing the native species and 2 the alien invader.

$$\frac{\partial S_1}{\partial t} = [a_1 - q_1(H_1 + c_2H_2)](S_1 + f_1I_1) - b_1S_1 - \beta_{11}S_1I_1 - \beta_{12}S_1I_2 + \gamma_1I_1 + D_1\frac{\partial^2 S_1}{\partial x^2} \tag{3.9a}$$

$$\frac{\partial I_1}{\partial t} = \beta_{11}S_1I_1 + \beta_{12}S_1I_2 - b_1I_1 - \alpha_1I_1 - \gamma_1I_1 + D_1\frac{\partial^2 I_1}{\partial x^2} \tag{3.9b}$$

$$\frac{\partial S_2}{\partial t} = [a_2 - q_2(H_2 + c_1H_1)](S_2 + f_2I_2) - b_2S_2 - \beta_{22}S_2I_2 - \beta_{21}S_2I_1 + \gamma_2I_2 + D_2\frac{\partial^2 S_2}{\partial x^2} \tag{3.9c}$$

$$\frac{\partial I_2}{\partial t} = \beta_{22}S_2I_2 + \beta_{21}S_2I_1 - b_2I_2 - \alpha_2I_2 - \gamma_2I_2 + D_2\frac{\partial^2 I_2}{\partial x^2} \tag{3.9d}$$

where $H_1 = S_1 + I_1$ and $H_2 = S_2 + I_2$. We assume all parameters are non-negative and a_i represents the maximum reproduction rate, b_i the natural mortality rate, c_i the competitive effect of species i on the other species and β_{ij} the disease transmission coefficient from species j to i. We assume a positive carrying capacity, K_i, which is related to susceptibility to crowding, q_i, since $K_i = (a_i - b_i)/q_i$. The model assumes that infected individuals experience disease-induced mortality at rate α_i. Infecteds may recover back to susceptibility at rate γ_i and experience only a proportion, f_i of the fecundity of a susceptible host; $f_i \in [0, 1]$. The diffusion coefficients, D_1 and D_2, approximate random movement for each of the species; we assume the same dispersal rate for susceptible and infected individuals.

3.3 Results

Our aim is to investigate the spatial spread and replacement when an invading species is introduced at one location into a disease-free native population. Again we compare results for competition-mediated and competition-and-disease-mediated replacement. We consider a situation in which the alien species has a competitive advantage in the absence of disease.

In competition-only replacement a travelling wave sweeps across the landscape, transforming the population from the native carrying capacity in front of the wave to a population of invaders only, at their carrying capacity, behind the wave. This is shown in figure 3.2(a) and these numerical solutions can be used to determine that this competition-only wave has speed 0.2. The spatial results for competition-and-disease-mediated replacement are shown in figure 3.2(b).

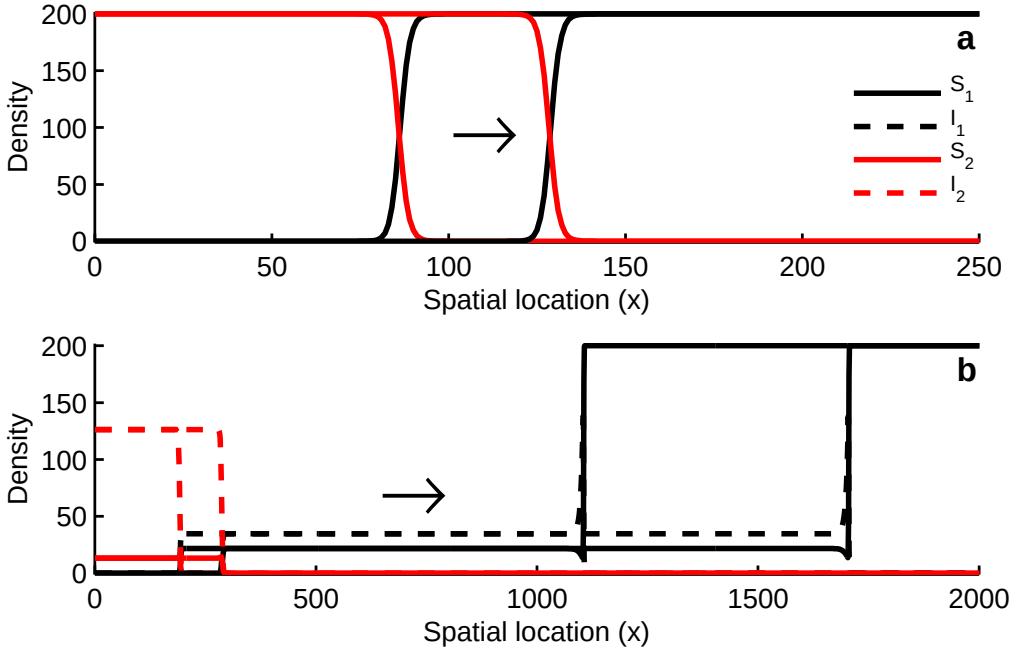

Figure 3.2 Density of the native (S_1, I_1) and alien (S_2, I_2) species across the spatial landscape. In panel **a** competition-mediated and in panel **b** competition-and-disease-mediated spatial replacement is shown at time points 400 and 600 respectively (note the difference in spatial scale in panels **a** and **b**). The parameters are: $f_1 = f_2 = 1$, $a_1 = a_2 = 1$, $b_1 = b_2 = 0.4$, $K_1 = K_2 = 200$, $c_1 = 0.9$, $c_2 = 1.5$, $\alpha_1 = 0.7$, $\alpha_2 = 0.2$, $\gamma_1 = \gamma_2 = 0.2$, $\beta_{ij} = 0.06$ and $D_1 = D_2 = 0.18$. The initial conditions in **a** are $S_1 = K_1$, $I_1 = I_2 = 0$ for all x and $S_2 = 4$ for $x \leqslant 10$, $S_2 = 0$ otherwise. The initial conditions in **b** are $S_1 = K_1$ for all x, $I_1 = 0$ for all x, $S_2 = I_2 = 2$ for $x \leqslant 10$, $S_2 = I_2 = 0$ otherwise. In a temporal model, these parameters result in a decrease in replacement time when disease is present. Similarly, in the spatial model we see the invading species spreading further across the landscape when disease is present (panel **b**) compared to when absent (panel **a**). Note in panel **b** the wave of replacement occurs behind the wave of disease. These observed values were produced using a semi-implicit Crank-Nicolson method with zero flux boundary conditions, a grid spacing of 10^{-2} and a time step of 10^{-2}.

In an extensive program of numerical simulations, we have found that when disease is present, a rapid "wave of disease" spreads across the landscape, followed by a slower "wave of replacement". The wave of disease spreads through the native population (in the absence of the invading species) and transforms the native population from its disease-free state to its endemic population level. For the results shown in figure 3.2(b) the wave of disease has speed 3.0. Behind the wave of disease is a wave of replacement in which the invading species replaces the native species, leaving the invading species at its endemic population level. In figure 3.2(b) the wave of replacement has speed 0.5. For the parameter values used in figure 3.2 the temporal model predicts that the replacement of the native species will be faster when the disease is included. In line with this, the invading wave moves faster when the disease is present. For parameter values for which the disease would slow the replacement of the native species in the temporal system, our results indicate that the spatial replacement is also slower than in the absence of disease. Thus, the spatial results parallel the temporal findings in terms of the effect disease will have on the replacement of

a native species. We will begin by calculating the wave speed for the three types of waves.

3.3.1 Critical wave speed

Competition-only

The "competition-only" PDEs are given by setting $I_1 = I_2 = 0$ in the full model (3.9a–d), giving

$$\frac{\partial S_1}{\partial t} = [a_1 - b_1 - q_1(S_1 + c_2 S_2)]S_1 + D_1 \frac{\partial^2 S_1}{\partial x^2} \tag{3.10a}$$

$$\frac{\partial S_2}{\partial t} = [a_2 - b_2 - q_2(S_2 + c_1 S_1)]S_2 + D_2 \frac{\partial^2 S_2}{\partial x^2}. \tag{3.10b}$$

To investigate travelling wave solutions we consider $S_i(x,t) = S_i(x - \theta t)$ where $\theta > 0$ is the wave speed. We use $Z = x - \theta t$ to denote the travelling wave variable. Substituting these solution forms into equations (3.10a) and (3.10b) and denoting differentiation with respect to Z by prime gives

$$-\theta S_1' = [a_1 - b_1 - q_1(S_1 + c_2 S_2)]S_1 + D_1 S_1'' \tag{3.11a}$$

$$-\theta S_2' = [a_2 - b_2 - q_2(S_2 + c_1 S_1)]S_2 + D_2 S_2''. \tag{3.11b}$$

Using $\dot{S_1} = S_1'$ and $\dot{S_2} = S_2'$, equations (3.11a) and (3.11b) can be written as the following four first-order ordinary differential equations

$$S_1' = \dot{S_1} \tag{3.12a}$$

$$\dot{S_1}' = (-1/D_1)([a_1 - b_1 - q_1(S_1 + c_2 S_2)]S_1 + \theta \dot{S_1}) \tag{3.12b}$$

$$S_2' = \dot{S_2} \tag{3.12c}$$

$$\dot{S_2}' = (-1/D_2)([a_2 - b_2 - q_2(S_2 + c_1 S_1)]S_2 + \theta \dot{S_2}). \tag{3.12d}$$

There are four equilibrium points obtained from setting the right-hand side of equations (3.12a) to (3.12d) equal to zero,

$$(S_1, \dot{S_1}, S_2, \dot{S_2}) = (0,0,0,0), \quad (K_1,0,0,0), \quad (0,0,K_2,0) \text{ and } (S_1^+,0,S_2^+,0),$$

where $S_1^+ = (c_2K_2 - K_1)/(c_1c_2 - 1)$ and $S_2^+ = (c_1K_1 - K_2)/(c_1c_2 - 1)$.

In this case the native species is at its carrying capacity until the alien species invades so the equilibrium in front of the wave will be $(K_1, 0, 0, 0)$ (see figure 3.3a). Linearising equations (3.12a)

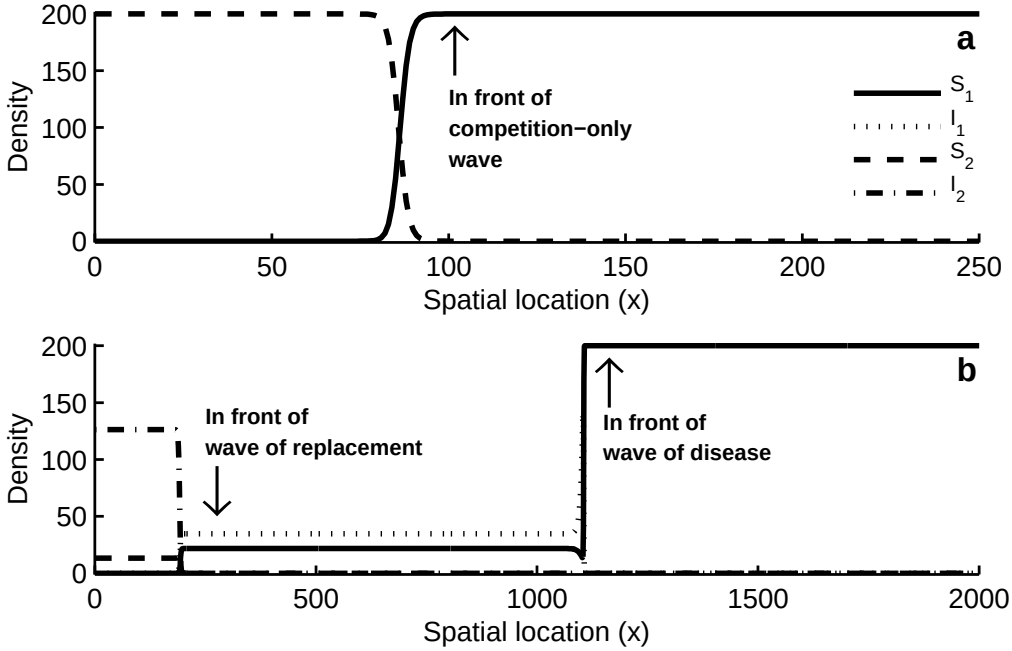

Figure 3.3 Spatial replacement across landscape highlighting competition-only wave, wave of replacement and wave of disease. In panel **a** competition-mediated and in panel **b** competition-and-disease-mediated spatial replacement is shown at time point 400. The parameters are: $f_1 = f_2 = 1$, $a_1 = a_2 = 1$, $b_1 = b_2 = 0.4$, $K_1 = K_2 = 200$, $c_1 = 0.9$, $c_2 = 1.5$, $\alpha_1 = 0.7$, $\alpha_2 = 0.2$, $\gamma_1 = \gamma_2 = 0.2$, $\beta_{ij} = 0.06$ and $D_1 = D_2 = 0.18$. The initial conditions in **a** are $S_1 = K_1$, $I_1 = I_2 = 0$ for all x and $S_2 = 4$ for $x \leqslant 10$, $S_2 = 0$ otherwise. The initial conditions in **b** are $S_1 = K_1$ for all x, $I_1 = 0$ for all x, $S_2 = I_2 = 2$ for $x \leqslant 10$, $S_2 = I_2 = 0$ otherwise. These observed values were produced using a semi-implicit Crank-Nicolson method with zero flux boundary conditions, a grid spacing of 10^{-2} and a time step of 10^{-2}.

to (3.12d) at $(K_1, 0, 0, 0)$ gives the following Jacobian matrix

$$\mathbf{J}_{(K_1,0,0,0)} = \begin{pmatrix} 0 & 1 & 0 & 0 \\ \frac{a_1-b_1}{D_1} & -\frac{\theta}{D_1} & \frac{(a_1-b_1)c_2}{D_1} & 0 \\ 0 & 0 & 0 & 1 \\ 0 & 0 & \frac{(a_2-b_2)(c_1K_1-K_2)}{D_2K_2} & -\frac{\theta}{D_2} \end{pmatrix} \tag{3.13}$$

with the following four eigenvalues

$$\lambda_{1,2} = \frac{-\theta \pm \sqrt{\theta^2 + 4D_2(a_2 - b_2)(\frac{c_1K_1}{K_2} - 1)}}{2D_2}, \tag{3.14a}$$

$$\lambda_{3,4} = \frac{-\theta \pm \sqrt{\theta^2 + 4D_1(a_1 - b_1)}}{2D_1}. \tag{3.14b}$$

λ_3 and λ_4 are always real since $\theta^2 + 4D_1(a_1 - b_1) > 0$; one is positive and the other is negative. λ_1 and λ_2 are either both real and negative, or a complex conjugate pair with negative real part; the

condition for them being real is

$$\theta^2 + 4D_2(a_2 - b_2)\left(\frac{c_1K_1}{K_2} - 1\right) \geqslant 0 \tag{3.15a}$$

$$\Leftrightarrow \theta^2 \geqslant 4D_2(a_2 - b_2)\left(1 - \frac{c_1K_1}{K_2}\right) \tag{3.15b}$$

$$\Leftrightarrow \theta \geqslant 2\sqrt{D_2(a_2 - b_2)\left(1 - \frac{c_1K_1}{K_2}\right)} \tag{3.15c}$$

(since $\theta > 0$). This suggests that the competition-only wave will move with speed θ_C, given by:

$$\theta_C = 2\sqrt{D_2(a_2 - b_2)\left(1 - \frac{c_1K_1}{K_2}\right)}. \tag{3.16}$$

Wave of disease

The "wave of disease" is the wave seen ahead of the wave of replacement, in which the native species is reduced from its carrying capacity to its endemic state (see figure 3.3b). This transition occurs without direct involvement from the alien species, so that the relevant equations are given by setting $S_2 = I_2 = 0$ in the full model, giving

$$\frac{\partial S_1}{\partial t} = (a_1 - q_1(S_1 + I_1))(S_1 + f_1I_1) - b_1S_1 - \beta_{11}S_1I_1 + \gamma_1I_1 + D_1\frac{\partial^2 S_1}{\partial x^2} \tag{3.17a}$$

$$\frac{\partial I_1}{\partial t} = \beta_{11}S_1I_1 - b_1I_1 - \alpha_1I_1 - \gamma_1I_1 + D_1\frac{\partial^2 I_1}{\partial x^2}. \tag{3.17b}$$

To investigate travelling waves, we look for a solution of the form $S_1(x,t) = S_1(x - \theta t)$ and $I_1(x,t) = I_1(x - \theta t)$ where $\theta > 0$ is the wave speed. As before, we define the wave variable $Z = x - \theta t$ and denote differentiation with respect to Z by prime. Therefore, equations (3.17a) and (3.17b) become

$$-\theta S_1' = (a_1 - q_1(S_1 + I_1))(S_1 + f_1I_1) - b_1S_1 - \beta_{11}S_1I_1 + \gamma_1I_1 + D_1S_1'' \tag{3.18a}$$

$$-\theta I_1' = \beta_{11}S_1I_1 - b_1I_1 - \alpha_1I_1 - \gamma_1I_1 + D_1I_1''. \tag{3.18b}$$

Using $\dot{S}_1 = S_1'$ and $\dot{I}_1 = I_1'$, equations (3.18a) to (3.18b) can be written as the following four

first-order ordinary differential equations

$$S_1' = \dot{S}_1 \tag{3.19a}$$

$$\dot{S}_1' = (-1/D_1)((a_1 - q_1(S_1 + I_1))(S_1 + f_1 I_1) - b_1 S_1 - \beta_{11} S_1 I_1 + \gamma_1 I_1 + \theta \dot{S}_1) \tag{3.19b}$$

$$I_1' = \dot{I}_1 \tag{3.19c}$$

$$\dot{I}_1' = (-1/D_1)(\beta_{11} S_1 I_1 - b_1 I_1 - \alpha_1 I_1 - \gamma_1 I_1 + \theta \dot{I}_1). \tag{3.19d}$$

We are considering a situation in which the native species is at its carrying capacity ahead of the wave, with no disease and no invader present; so we linearise equations (3.18a) to (3.19d) about the steady state $(S_1, \dot{S}_1, I_1, \dot{I}_1) = (K_1, 0, 0, 0)$ (see figure 3.3b). The Jacobian matrix is

$$\mathbf{J}_{(K_1,0,0,0)} = \begin{pmatrix} 0 & 1 & 0 & 0 \\ \frac{a_1 - b_1}{D_1} & \frac{-\theta}{D_1} & \frac{a_1 - b_1 - f_1 b_1 + \beta_{11} K_1 - \gamma_1}{D_1} & 0 \\ 0 & 0 & 0 & 1 \\ 0 & 0 & \frac{-\beta_{11} K_1 + b_1 + \alpha_1 + \gamma_1}{D_1} & \frac{-\theta}{D_1} \end{pmatrix} \tag{3.20}$$

with the following four eigenvalues

$$\lambda_{1,2} = \frac{-\theta \pm \sqrt{\theta^2 - 4D_1(\beta_{11} K_1 - b_1 - \alpha_1 - \gamma_1)}}{2D_1}, \tag{3.21a}$$

$$\lambda_{3,4} = \frac{-\theta \pm \sqrt{\theta^2 + 4D_1(a_1 - b_1)}}{2D_1}. \tag{3.21b}$$

λ_3 and λ_4 are real since $\theta^2 + 4D_1(a_1 - b_1) > 0$; one is positive and the other is negative. λ_1 and λ_2 are either both real and negative, or a complex conjugate pair with negative real part; the condition for them being real is

$$\theta^2 - 4D_1(\beta_{11} K_1 - \alpha_1 - b_1 - \gamma_1) \geqslant 0 \tag{3.22a}$$

$$\Leftrightarrow \theta^2 \geqslant 4D_1(\beta_{11} K_1 - \alpha_1 - b_1 - \gamma_1) \tag{3.22b}$$

$$\Leftrightarrow \theta \geqslant \sqrt{4D_1(\beta_{11} K_1 - \alpha_1 - b_1 - \gamma_1)}. \tag{3.22c}$$

This suggests that the wave of disease will move with speed θ_D, given by:

$$\theta_D = 2\sqrt{D_1(\beta_{11}K_1 - \alpha_1 - b_1 - \gamma_1)}. \tag{3.23}$$

Wave of replacement

The "wave of replacement" is the wave seen behind the wave of disease, in which the invading species is replacing the native species (see figure 3.3b). This transition involves both species so we must consider the full model equations as follows

$$\frac{\partial S_1}{\partial t} = [a_1 - q_1(H_1 + c_2H_2)](S_1 + f_1I_1) - b_1S_1 - \beta_{11}S_1I_1 - \beta_{12}S_1I_2 + \gamma_1I_1 + D_1\frac{\partial^2 S_1}{\partial x^2} \tag{3.24a}$$

$$\frac{\partial I_1}{\partial t} = \beta_{11}S_1I_1 + \beta_{12}S_1I_2 - b_1I_1 - \alpha_1I_1 - \gamma_1I_1 + D_1\frac{\partial^2 I_1}{\partial x^2} \tag{3.24b}$$

$$\frac{\partial S_2}{\partial t} = [a_2 - q_2(H_2 + c_1H_1)](S_2 + f_2I_2) - b_2S_2 - \beta_{22}S_2I_2 - \beta_{21}S_2I_1 + \gamma_2I_2 + D_2\frac{\partial^2 S_2}{\partial x^2} \tag{3.24c}$$

$$\frac{\partial I_2}{\partial t} = \beta_{22}S_2I_2 + \beta_{21}S_2I_1 - b_2I_2 - \alpha_2I_2 - \gamma_2I_2 + D_2\frac{\partial^2 I_2}{\partial x^2}. \tag{3.24d}$$

To investigate travelling waves, we look for a solution of the form $S_1(x,t) = S_1(x - \theta t)$, $I_1(x,t) = I_1(x - \theta t)$, $S_2(x,t) = S_2(x - \theta t)$ and $I_2(x,t) = I_2(x - \theta t)$ where $\theta > 0$ is the wave speed. As before, we define the wave variable $Z = x - \theta t$ and denote differentiation with respect to Z by prime. Therefore, equations (3.24a) to (3.24d) become

$$-\theta S_1' = [a_1 - q_1(H_1 + c_2H_2)](S_1 + f_1I_1) - b_1S_1 - \beta_{11}S_1I_1 - \beta_{12}S_1I_2 + \gamma_1I_1 + D_1S_1'' \tag{3.25a}$$

$$-\theta I_1' = \beta_{11}S_1I_1 + \beta_{12}S_1I_2 - b_1I_1 - \alpha_1I_1 - \gamma_1I_1 + D_1I_1'' \tag{3.25b}$$

$$-\theta S_2' = [a_2 - q_2(H_2 + c_1H_1)](S_2 + f_2I_2) - b_2S_2 - \beta_{22}S_2I_2 - \beta_{21}S_2I_1 + \gamma_2I_2 + D_2S_2'' \tag{3.25c}$$

$$-\theta I_2' = \beta_{22}S_2I_2 + \beta_{21}S_2I_1 - b_2I_2 - \alpha_2I_2 - \gamma_2I_2 + D_2I_2''. \tag{3.25d}$$

Using $\dot{S}_i = S_i'$ and $\dot{I}_i = I_i'$, equations (3.25a) to (3.25d) can be rewritten as the following eight

first-order equations

$$S_1' = \dot{S}_1 \tag{3.26a}$$

$$\dot{S}_1' = (-1/D_1)([a_1 - q_1(H_1 + c_2H_2)](S_1 + f_1I_1) - b_1S_1 - \beta_{11}S_1I_1 - \beta_{12}S_1I_2 + \gamma_1I_1 + \theta\dot{S}_1) \tag{3.26b}$$

$$I_1' = \dot{I}_1 \tag{3.26c}$$

$$\dot{I}_1' = (-1/D_1)(\beta_{11}S_1I_1 + \beta_{12}S_1I_2 - b_1I_1 - \alpha_1I_1 - \gamma_1I_1 + \theta\dot{I}_1) \tag{3.26d}$$

$$S_2' = \dot{S}_2 \tag{3.26e}$$

$$\dot{S}_2' = (-1/D_2)([a_2 - q_2(H_2 + c_1H_1)](S_2 + f_2I_2) - b_2S_2 - \beta_{22}S_2I_2 - \beta_{21}S_2I_1 + \gamma_2I_2 + \theta\dot{S}_2) \tag{3.26f}$$

$$I_2' = \dot{I}_2 \tag{3.26g}$$

$$\dot{I}_2' = (-1/D_2)(\beta_{22}S_2I_2 + \beta_{21}S_2I_1 - b_2I_2 - \alpha_2I_2 - \gamma_2I_2 + \theta\dot{I}_2). \tag{3.26h}$$

As before, we will examine the stability of the equilibrium point in front of the wave. We are considering a situation where the native species has already been reduced to its endemic state by the disease (via the "wave of disease") and there is no invader present, so we linearise about $(S_1, \dot{S}_1, I_1, \dot{I}_1, S_2, \dot{S}_2, I_2, \dot{I}_2) = (S_1^*, 0, I_1^*, 0, 0, 0, 0, 0)$ (see figure 3.3b). Equations (3.26e) to (3.26h) decouple from equations (3.26a) to (3.26d). For realistic travelling wave solutions we require the four eigenvalues obtained from these decoupled equations (3.26e) to (3.26h) to be non-oscillatory (if they have negative real part). The other four eigenvalues have zero components for S_2 and I_2 and therefore do not impose any restrictions on population densities being positive in the travelling wave. For notational simplicity we define

$$A = a_2 - q_2c_1H_1^* - b_2 - \beta_{21}I_1^*, \tag{3.27}$$

$$B = (a_2 - q_2c_1H_1^*)f_2 + \gamma_2, \tag{3.28}$$

$$E = \beta_{21}I_1^*, \tag{3.29}$$

$$\Delta = -b_2 - \alpha_2 - \gamma_2. \tag{3.30}$$

The relevant part of the Jacobian is then

$$\mathbf{J}_{(0,0,0,0)} = \begin{pmatrix} 0 & 1 & 0 & 0 \\ \frac{-A}{D3} & \frac{-\theta}{D_2} & \frac{-B}{D3} & 0 \\ 0 & 0 & 0 & 1 \\ \frac{-E}{D_2} & 0 & \frac{-\Delta}{D_2} & \frac{-\theta}{D_2} \end{pmatrix} \tag{3.31}$$

with four eigenvalues ($i = 1, \ldots, 4$)

$$\lambda_{1,2} = \frac{-\theta \pm \sqrt{\theta^2 - 2D_2\left(A + \Delta + \sqrt{(A+\Delta)^2 - 4A\Delta + 4EB}\right)}}{2D_2}, \tag{3.32}$$

$$\lambda_{3,4} = \frac{-\theta \pm \sqrt{\theta^2 - 2D_2\left(A + \Delta - \sqrt{(A+\Delta)^2 - 4A\Delta + 4EB}\right)}}{2D_2}. \tag{3.33}$$

We are concerned with parameter values in which the native species, in its endemic state, is unstable to the introduction of the alien species. The condition for this is $(a_2 - b_2 - q_2c_1(S_1^* + I_1^*)) + (\beta_{21}I_1^*)/(\alpha_2 + b_2 + \gamma_2)(f_2a_2 - b_2 - f_2q_2c_1(S_1^* + I_1^*) - \alpha_2) > 0$ (2.6 from chapter two), which is equivalent to $EB - A\Delta > 0$. As a result of this the eigenvalues λ_3 and λ_4 are real with one positive and the other negative. λ_1 and λ_2 are either both real and negative, or a complex conjugate pair with negative real part; the condition for them being real is

$$\theta^2 - 2D_2\left(A + \Delta + \sqrt{(A+\Delta)^2 - 4A\Delta + 4EB}\right) \geqslant 0 \tag{3.34}$$

$$\Leftrightarrow \theta^2 \geqslant 2D_2\left(A + \Delta + \sqrt{(A+\Delta)^2 - 4A\Delta + 4EB}\right) \tag{3.35}$$

$$\Leftrightarrow \theta \geqslant \sqrt{2D_2\left(A + \Delta + \sqrt{(A+\Delta)^2 - 4A\Delta + 4EB}\right)}. \tag{3.36}$$

This suggests that the wave of replacement will move with speed θ_R, given by

$$\theta_R = \sqrt{2D_2\left(A + \Delta + \sqrt{(A+\Delta)^2 - 4A\Delta + 4EB}\right)}. \tag{3.37}$$

Single wave

If the speed of the wave of replacement is faster than the wave of disease, we may no longer expect to see two separate waves. Instead, we may expect to see one combined disease and competition wave referred to here as the "single wave". To understand the properties of the single wave we must again consider the full model equations. This requires us to follow the previous procedure to examine travelling waves and we will need to re-examine the system of equations (3.26a–h). However, the situation ahead of the single wave is different when compared to the wave of replacement. For the single wave the native species is at its carrying capacity ahead of the wave with no disease and no invader present. Behind the wave the system is at the alien species endemic

equilibrium. We consider the full model, equations (3.26a–h), and linearise about the steady state $(S_1, \dot{S}_1, I_1, \dot{I}_1, S_2, \dot{S}_2, I_2, \dot{I}_2) = (K_1, 0, 0, 0, 0, 0, 0, 0)$. The resulting Jacobian is

$$\mathbf{J}_{(K_1,0,0,0,0,0,0,0)} =$$

$$\begin{pmatrix}
0 & 1 & 0 & 0 & 0 & 0 & 0 & 0 \\
(a_1 - b_1) & -\theta & (a_1 - b_1 - f_1 b_1 & 0 & ((a_1 - b_1)c_2) & 0 & (\beta_{12}K_1 & 0 \\
/D_1 & /D_1 & +\beta_{11}K_1 - \gamma_1)/D_1 & & /D_1 & & +c_2(a_1 - b_1))/D_1 & \\
0 & 0 & 0 & 1 & 0 & 0 & 0 & 0 \\
0 & 0 & (-\beta_{11}K_1 + b_1 & -\theta & 0 & 0 & -\beta_{12}K_1 & 0 \\
 & & +\alpha_1 + \gamma_1)/D_1 & /D_1 & & & /D_1 & \\
0 & 0 & 0 & 0 & 0 & 1 & 0 & 0 \\
0 & 0 & 0 & 0 & (a_2 - b_2)(c_1K_1 & -\theta & (f_2(c_1K_1(a_2 - b_2)- & 0 \\
 & & & & -K_2)/D_2K_2 & /D_2 & a_2K_2) - \gamma_2K_2)/D_2K_2 & \\
0 & 0 & 0 & 0 & 0 & 0 & 0 & 1 \\
0 & 0 & 0 & 0 & 0 & 0 & (b_2 + \alpha_2 + \gamma_2) & -\theta \\
 & & & & & & /D_2 & /D_2
\end{pmatrix} \tag{3.38}$$

with the following eight eigenvalues

$$\lambda_{(1,2)} = \frac{-\theta \pm \sqrt{\theta^2 + 4D_1(a_1 - b_1)}}{2D_1}, \tag{3.39a}$$

$$\lambda_{(3,4)} = \frac{-\theta \pm \sqrt{\theta^2 + 4D_2(b_2 + \alpha_2 + \gamma_2)}}{2D_2}, \tag{3.39b}$$

$$\lambda_{(5,6)} = \frac{-\theta \pm \sqrt{\theta^2 + 4D_2(a_2 - b_2)(\frac{c_1K_1}{K_2} - 1)}}{2D_2}, \tag{3.39c}$$

$$\lambda_{(7,8)} = \frac{-\theta \pm \sqrt{\theta^2 - 4D_1(\beta_{11}K_1 - b_1 - \alpha_1 - \gamma_1)}}{2D_1}. \tag{3.39d}$$

Eigenvalues λ_1 and λ_2 are always real since $\theta^2 + 4D_1(a_1 - b_1) > 0$; one is positive and the other is negative. λ_3 and λ_4 are always real since $\theta^2 + 4D_2(b_2 + \alpha_2 + \gamma_2) > 0$; again one is positive and one is negative. λ_5 and λ_6 are either both real and negative, or a complex conjugate pair with negative

real part; the condition for them being real is

$$\theta^2 + 4D_2(a_2 - b_2)\left(\frac{c_1K_1}{K_2} - 1\right) \geqslant 0 \tag{3.40a}$$

$$\Leftrightarrow \theta^2 \geqslant 4D_2(a_2 - b_2)\left(1 - \frac{c_1K_1}{K_2}\right) \tag{3.40b}$$

$$\Leftrightarrow \theta \geqslant 2\sqrt{D_2(a_2 - b_2)\left(1 - \frac{c_1K_1}{K_2}\right)} = \theta_C. \tag{3.40c}$$

Recall that θ_C is our predicted speed of the competition-only wave. λ_7 and λ_8 are either both real and negative, or a complex conjugate pair with negative real part; the condition for them being real is

$$\theta^2 - 4D_1(\beta_{11}K_1 - \alpha_1 - b_1 - \gamma_1) \geqslant 0 \tag{3.41a}$$

$$\Leftrightarrow \theta^2 \geqslant 4D_1(\beta_{11}K_1 - \alpha_1 - b_1 - \gamma_1) \tag{3.41b}$$

$$\Leftrightarrow \theta \geqslant \sqrt{4D_1(\beta_{11}K_1 - \alpha_1 - b_1 - \gamma_1)} = \theta_D \tag{3.41c}$$

Recall that θ_D is our predicted speed of the wave of disease. To ensure positive population densities the speed of the single wave must satisfy both $\theta \geqslant \theta_C$ and $\theta \geqslant \theta_D$. This suggests that the single wave will move with speed θ_S, given by

$$\theta_S = \max\{\theta_C, \theta_D\}. \tag{3.42}$$

Comparison with numerical wave speeds

For the parameters used in figure 3.2, the values of these speeds are $\theta_C = 0.2$, $\theta_R = 0.5$ and $\theta_D = 2.8$. These match very closely with the numerical simulations plotted in figure 3.2, and this is true for a wide range of other parameters for which $\theta_D > \theta_R$. When $\theta_D < \theta_R$, one might expect that the wave of replacement would "catch up with" the wave of disease, leading to the formation of a single, combined wave front. However, in numerical simulations we observe different behaviour, namely that while the wave of replacement still travels at speed θ_R, the wave of disease travels at a speed faster than θ_D, and indeed faster than θ_R (illustrated in figure 3.4). This is reminiscent of the behaviour observed by Hosono (1998) in competition-only models; a detailed understanding of what determines the actual wave speed is lacking even in that much simpler case. The only exception that we found to this behaviour was in the case $D_1 = 0$; then a wave of disease is not possible, and the invasion occurs via a single travelling wave, moving at speed θ_C. Apart from in

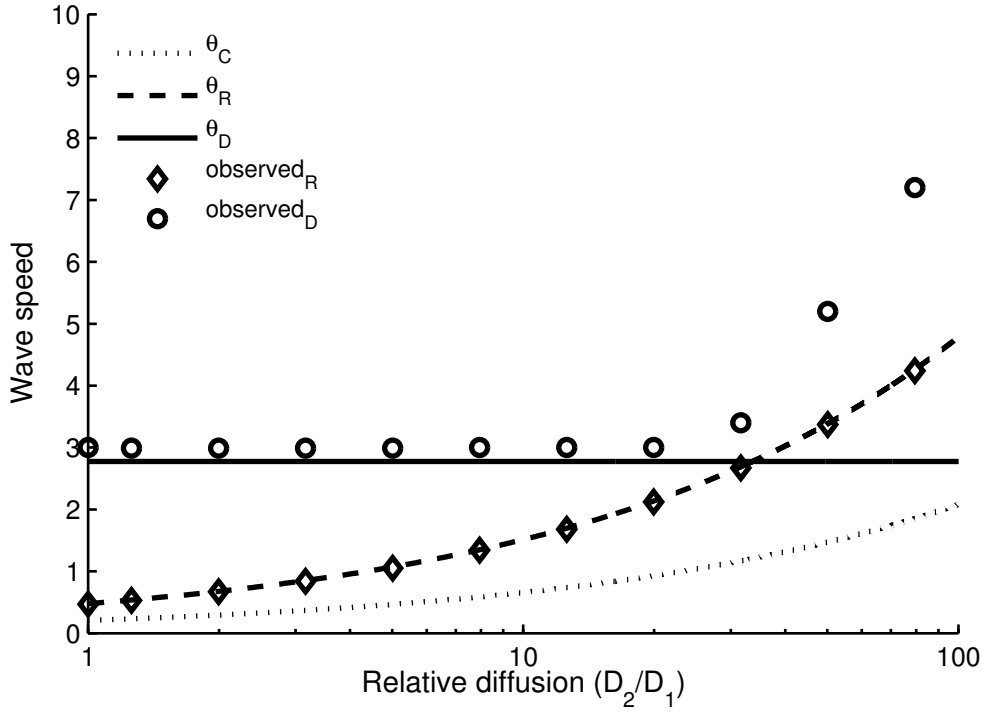

Figure 3.4 Effect of relative diffusion on observed and critical wave speeds. Critical minimum wave speeds are calculated for the three types of waves seen in our solutions (competition-only wave (θ_C), wave of disease (θ_D) and wave of replacement (θ_R)) for a range of relative diffusion rates (D_2/D_1). In this scenario, the alien species invades and replaces the native species with disease present. This results in two waves, a wave of disease followed by a wave of replacement. When $\theta_D > \theta_R$, the observed wave speeds seen in numerical simulations match very closely with the critical wave speeds. If $\theta_D < \theta_R$, the observed wave of replacement ($observed_R$) still travels at speed θ_R however the observed wave of disease ($observed_D$) travels at a speed faster than θ_D. The parameters used are: $f_1 = f_2 = 1$, $a_1 = a_2 = 1$, $b_1 = b_2 = 0.4$, $K_1 = K_2 = 200$, $c_1 = 0.9$, $c_2 = 1.5$, $\alpha_1 = 0.7$, $\alpha_2 = 0.2$, $\gamma_1 = \gamma_2 = 0.2$, $\beta_{ij} = 0.06$ and $D_1 = 0.18$. The "observed" results come from numerical solutions of the equations using a semi-implicit Crank-Nicolson method with zero flux boundary conditions, grid spacings of 10^{-2} and time steps of 10^{-2}. For larger ratios of the diffusion coefficients, the numerical simulations are relatively time consuming as they require a large spatial domain.

this very special case, our results always show that a rapid wave of disease spreads through the native population, with the actual invasion of the alien population occurring more slowly. This occurs regardless of whether disease acts to increase or decrease the replacement time.

3.3.2 Range of spatial spread

The spatial investigation has shown that when the disease decreases the temporal replacement time, it also results in a faster spatial wave of replacement. We also investigated whether disease can change the spatial range over which the alien species can invade. To examine this we considered a heterogeneous spatial landscape in which the carrying capacity of the invader decreases across the spatial landscape while the carrying capacity of the native species increases. In the absence of the disease, the wave of invasion causes replacement of the native population. However, as this wave

spreads across the landscape it begins to slow and eventually stops (figure 3.5a). The wave halts as the competitive advantage of the invader is countered by its inferior carrying capacity. When the disease is included, the wave of replacement is again observed, with the wave speed slowing as the invader progresses across the landscape, but the disease allows the wave to progress further (figure 3.5b). Thus, not only can disease speed up the replacement of a native species, it can also extend the spatial range over which replacement can occur.

3.4 Discussion

The results for the temporal replacement of a native species can be extended to understand the spatial spread of invasion. When a disease reduces the temporal replacement time (compared to the absence of disease) this translates into a faster wave of replacement in the spatial framework (and increased temporal replacement time relates to a slower wave of replacement). This correla-

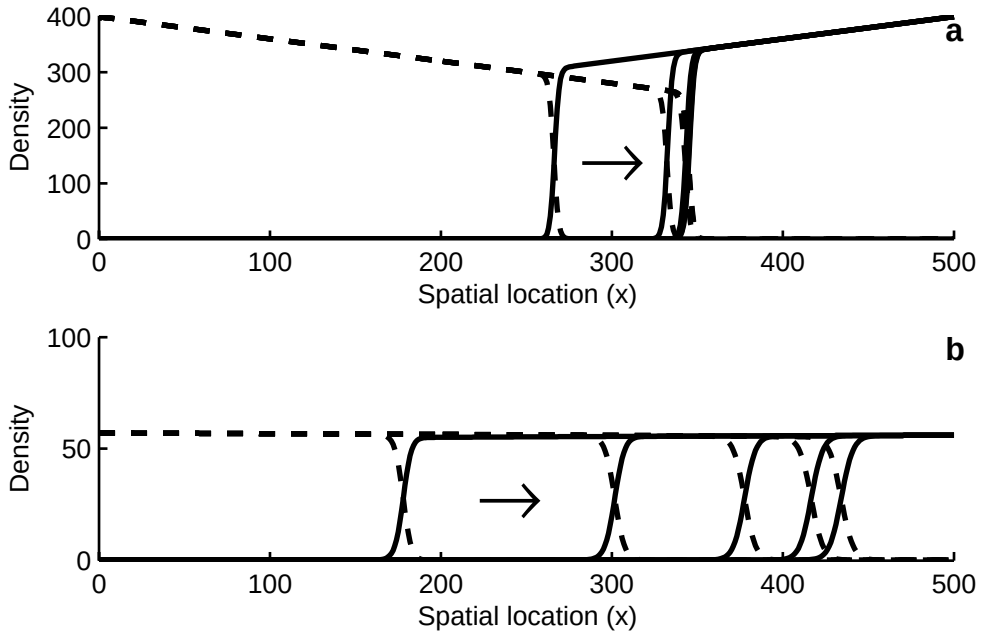

Figure 3.5 Total density of the native (solid line) and alien (dashed line) species across a heterogeneous landscape. The heterogeneity is created by altering their carrying capacities; the invader's is 400 at $x = 0$ and decreases linearly to 200 at $x = 500$ while the native's is 200 at $x = 0$ and increases linearly to 400 at $x = 500$. In panel **a** the disease is absent and the competitive advantage, which is modified by the difference in carrying capacity, allows the native to halt the spread of the invader at approximately $x = 350$. In panel **b** the disease is present and the invading species can spread further across the landscape and is halted at approximately $x = 450$ (note the change in scale on the y-axis). The time points of each wave are 800, 1600, 2400, 3200 and 4000 in both plots (although in panel **a** the final three time plots are effectively superimposed). The parameters used are $f_1 = f_2 = 0$, $a_1 = a_2 = 1$, $b_1 = b_2 = 0.4$, $c_1 = 0.9$, $c_2 = 1.5$, $\alpha_1 = 1.1$, $\alpha_2 = 1.0$, $\gamma_1 = 1.0$, $\gamma_2 = 1.1$, $\beta_{ij} = 0.06$ and $D_1 = D_2 = 0.18$. These results were produced using a semi-implicit Crank-Nicolson method with zero flux boundary conditions, a grid spacing of 10^{-2} and a time step of 10^{-2}.

tion emphasises how informative relatively straightforward temporal models can be in informing spatial behaviour. The spatial model framework was also analysed and it was possible to determine algebraic expressions for the minimum wave speed at the possible wave front transitions exhibited by our model. In the absence of disease a competition-only wave occurs with the native species at its carrying capacity ahead of the wave and with the alien species at its carrying capacity behind the wave front. These results are in accordance with the study of Okubo *et al.* (1989), who examined the interaction of red and grey squirrels within the UK. Okubo *et al.* (1989) modelled the effect of competition and diffusion on this interaction using a set of coupled reaction-diffusion equations similar to our competition-only framework. The wave front seen in Okubo *et al.* (1989) and our competition-only wave front exhibit similar behaviour (see figure 3.2a).

When disease is included in the spatial model we find that the initial response is for a wave of disease to spread across the landscape transforming the native species from its carrying capacity to its endemic level. The alien species is not involved in the transition. The system is therefore similar to that of Murray *et al.* (1986) who modelled the spread of rabies among foxes. Murray *et al.* (1986) extended a susceptible-infected-recovered model framework (Anderson *et al.*, 1981) to include a diffusion term for the random wanderings of rabid foxes. They examined the situation where a few rabid foxes were introduced into a stable disease free population. Their results show a wave-front transforming the population from an uninfected zone with the susceptible population at its carrying capacity to a infected population at its endemic level. The wave front has a very similar shape as the wave of disease seen in our simulations, however we do not see a similar pattern of repeated outbreaks. Murray *et al.* (1986) further investigated these repeated outbreaks and also possibilities for stopping the spread of rabies. We have calculated the critical wave speed of the wave of disease and represent it by θ_D. In our numerical simulations the wave of disease travelled at a speed very close to θ_D when $\theta_R < \theta_D$. However, when $\theta_D < \theta_R$ the wave of disease travelled at a speed greater than θ_D (see figure 3.4 for further details).

The wave of replacement which occurs behind the wave of disease and the possibility of a single wave are findings that have not been reported in previous studies. The wave of replacement describes the replacement of the native species by the alien invading species. It occurs after the wave of disease has swept through the landscape and transformed the native species to its endemic level. The wave of replacement then sweeps across, replacing the native at its endemic level with the alien species at its endemic level. We have calculated the critical wave speed of the wave of replacement and denote it by θ_R (see 3.37). For a wide range of parameter values, our numerical simulations show the wave of replacement moving at a speed very similar to θ_R. The single wave occurs when the wave of replacement catches up with the wave of disease resulting in a single

combined wave. We expected to see the single wave when $\theta_D < \theta_R$, however in our wide ranging numerical simulations we only found the single wave occurring in one special case ($D_1 = 0$). In this special case, we observed the single wave travelling at its critical wave speed $\theta_S = \max\{\theta_C, \theta_D\}$ (3.42).

The spatial results highlight an important, general, phenomenon. When a diseased population invades a landscape composed of a disease-free native population the initial response is for a wave of disease to sweep through the native population, reducing the population to its endemic level. The wave of replacement of the invading species travels well behind the wave of infection. Importantly this phenomenon is observed even when the wave of replacement is slowed down by the presence of disease. There is some evidence that this may occur in natural systems. Reynolds (1985) catalogued the replacement of red squirrels by greys in East Anglia between 1960 and 1981. He reported that diseased red squirrels where found well in advance of grey squirrels being reported at a particular spatial location. At the time this was used as evidence to dismiss disease being linked to the subsequent replacement of red squirrels. Our study suggests that such observations may be a direct result of the invasion of a disease-carrying species. From a conservation point of view, the emergence of the disease in a protected native population before the invader has reached the area may indicate the imminent replacement of the protected species. This could be used as an early warning system to implement emergency conservation efforts.

Disease can also allow an invading species to change the spatial range of replacement. The results shown in figure 3.5 indicate that disease can increase the range of replacement. This happens when the disease allows the alien to spread further through the landscape by reducing the native population to its endemic level, thereby giving the alien species a relative advantage. Disease can also reduce the range over which a species is replaced or even prevent replacement entirely. This happens when a competitively inferior native suffers relatively less "harm" from the disease than the alien species. The native would need relatively better recovery than the alien species if fecundity was unaffected by the disease and lower mortality from the disease if fecundity was affected. Hilker *et al.* (2005) studied the possibility of a disease slowing down or preventing an invasion in a frequency-dependent model. Their results show that an infectious disease is capable of slowing or stopping an invasion. This depends on the virulence of the disease: if the extra mortality through infection is high enough to over-balance the growth at the head of the population front, the invasion will be reversed. For further details of this, see Hilker *et al.* (2005).

The results indicating that disease can change the range of replacement of a native species has important biological implications. The boundary between species often arises due to niche separation whereby in its own niche a species can out-compete another species. However the

shared disease can act to remove the competitive advantage of a species within its niche resulting in its replacement. Grey squirrels have still to invade some regions of Scotland and this is believed to be partly due to habitat characteristics that favour reds over greys. Conservation efforts are also being used to provide red squirrel refuges in such suitable habitat. Our study indicates that such conservation efforts should also consider the role of squirrelpox virus as this may spread beyond grey squirrel occupied areas and allow greys to invade regions which would otherwise be unsuitable. From a conservation point of view, the manipulation of habitat may not be enough to prevent the spread of the invasive species since the prevention of the disease is also crucial. The results in this chapter are published in *Theoretical Ecology*, see Bell *et al.* (2009).

Chapter 4

A Stochastic Framework for Modelling Competition and Disease

4.1 Introduction

In previous chapters we investigated the population dynamics and spread of disease-carrying invading species using deterministic modelling frameworks. These frameworks treat the population density as a continuous variable, whereas in reality populations are composed of distinct individuals. Notwithstanding, deterministic frameworks have been fundamental in advancing our understanding of infectious disease. They highlight key phenomena such as threshold levels of susceptible hosts below which the disease cannot persist (Anderson and May (1991), and see Chapter 2) and travelling wave of disease spread (Murray (2002), and see Chapter 3).

Deterministic systems can also produce unrealistic results when population classes can recover from very small densities, referred to as "atto-foxes" and "nano-hawks" (Mollison, 1991; Grenfell and Dobson, 1995). The systems examined in Chapters 2 and 3, considering the invasion of a new species into an established native population, assume the invader is initially at a low density. Also, the infected classes in these systems often reach a low density endemic level. When a population falls to very small numbers there is a greater probability of population extinction or the disease dying out. Therefore, it is important to investigate the impact of such low densities on our findings.

The main motivation, for this investigation, is to develop a realistic model of the red/grey/squirrelpox system. Such a model can be used to assess conservation strategies for maintaining red squirrel populations, but will require that we consider individual-based modelling frameworks. To achieve this we will consider a stochastic individual-based model framework based on the Tompkins *et al.* (2003) squirrel model. This will allow a comparison between stochastic and deterministic frameworks in a system with a disease-carrying invasive species. The stochas-

tic framework developed can then be used to consider conservation strategies to protect the red population (see later, Chapter 5, where we will focus on a system that provides a refuge for red squirrels similar to the refuge in Formby, Merseyside).

4.2 Model

We begin by giving a brief overview of the deterministic model and results of Tompkins *et al.* (2003) (see Chapter 1 for a description of the red/grey/squirrelpox system). The Tompkins *et al.* (2003) model uses five ordinary differential equations (4.1a–e) to represent the system. Since the reds cannot recover from the disease there are only two classes of reds: susceptible (S_R) and infected (I_R). The greys can recover from the disease so are represented by three classes: susceptible (S_G), infected (I_G) and recovered (R_G). H_R represents the total red population ($S_R + I_R$) and H_G represents the total grey population ($S_G + I_G + R_G$). The equations are:

$$\frac{\partial S_R}{\partial t} = (a_R - q_R(H_R + c_G H_G))H_R - bS_R - \beta S_R(I_R + I_G) \tag{4.1a}$$

$$\frac{\partial I_R}{\partial t} = \beta S_R(I_R + I_G) - I_R(b + \alpha) \tag{4.1b}$$

$$\frac{\partial S_G}{\partial t} = (a_G - q_G(H_G + c_R H_R))H_G - bS_G - \beta S_G(I_R + I_G) \tag{4.1c}$$

$$\frac{\partial I_G}{\partial t} = \beta S_G(I_R + I_G) - I_G(b + \gamma) \tag{4.1d}$$

$$\frac{\partial R_G}{\partial t} = \gamma I_G - bR_G. \tag{4.1e}$$

All parameters are assumed to be non-negative and a_i represents the maximum reproduction rate (where $i = R$ for reds and $i = G$ for greys), b the natural adult mortality rate for both species, c_i the competitive effect of species i on the other species and β the virus transmission rate between species. We assume a positive carrying capacity, K_i, which is related to susceptibility to crowding (q_i) since $K_i = (a_i - b_i)/q_i$. Red squirrels experience an additional mortality due to the disease, at rate α, while the grey squirrels recover, to R_G, at rate γ. Tompkins *et al.* (2003) investigated the time taken to transform the disease-free red squirrel population equilibrium ($(S_R, I_R, S_G, I_G, R_G) = (K_R, 0, 0, 0, 0)$) to either the disease-free grey squirrel population equilibrium, $(0, 0, K_G, 0, 0)$, when considering competition-mediated replacement or the grey squirrel population equilibrium with endemic infection, $(0, 0, S_G^*, I_G^*, R_G^*)$, when considering competition and infection-mediated replacement.

Table 4.1 Parameters used in Tompkins *et al.* (2003).

Parameter	Symbol	Value	Original Reference
Maximum reproductive rate (red)	a_R	1.0 $(year^{-1})$	Okubo *et al.* (1989)
Maximum reproductive rate (grey)	a_G	1.2 $(year^{-1})$	Okubo *et al.* (1989)
Natural mortality rate	b	0.4 $(year^{-1})$	Gurnell (1987), Wauters *et al.* (2000)
Carrying capacity (red)	K_R	60 $(5km^{-2})$	Rushton *et al.* (1997)
Carrying capacity (grey)	K_G	80 $(5km^{-2})$	Rushton *et al.* (1997)
Competitive effect on grey	c_R	0.61	Bryce *et al.* (2001)
Competitive effect on red	c_G	1.65	Bryce *et al.* (2001)
Virus transmission coefficient	β	0.75 $(km^2 year^{-1})$	Tompkins *et al.* (2003)
Mortality rate due to virus	α	26 $(year^{-1})$	Tompkins *et al.* (2002)
Recovery rate from virus per	γ	13 $(year^{-1})$	Tompkins *et al.* (2002)

Tompkins *et al.* (2003) estimated parameters from experimental and field data (table 4.1), and with these parameters reds were always replaced if greys were introduced. The addition of squirrelpox enabled grey squirrels to replace reds more quickly. Figure 4.1a shows the replacement of reds with competition-only replacement while figure 4.1b shows the replacement when competition and infection are mediating replacement. The reds are initially at their carrying capacity ($K_R = 60$) and the greys invade at a low density. The greys replace the reds and reach their carrying capacity, while the red population dies out. The greys replace the reds faster when the disease is also introduced (replacement took approximately 15 years in figure 4.1a but only 6 years in figure 4.1b). This is caused by an initial epidemic in the reds, reducing the density of red squirrels, which lessens the competition for resources and allows the greys to replace the reds more easily.

Tompkins *et al.* (2003) also shows that the endemic levels of infection in a red-only or grey-only system are at low density. When a small number of infected reds are introduced into a

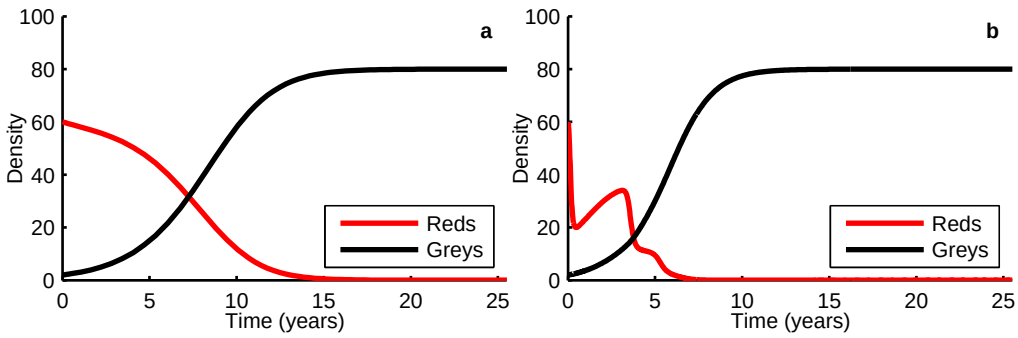

Figure 4.1 Results from Tompkins *et al.* (2003) deterministic model (4.1a–e). Panel **a** shows the results from competition-only mediated replacement and panel **b** the results from competition and disease mediated replacement. The parameters are the same as those used by Tompkins *et al.* (2003) and can be found in table 4.1. The initial conditions are the red squirrels at their carrying capacity ($K_R = 60$) and 2 susceptible greys (per 5km square) introduced in panel **a** and 2 infected greys (per 5km square) introduced in panel **b**.

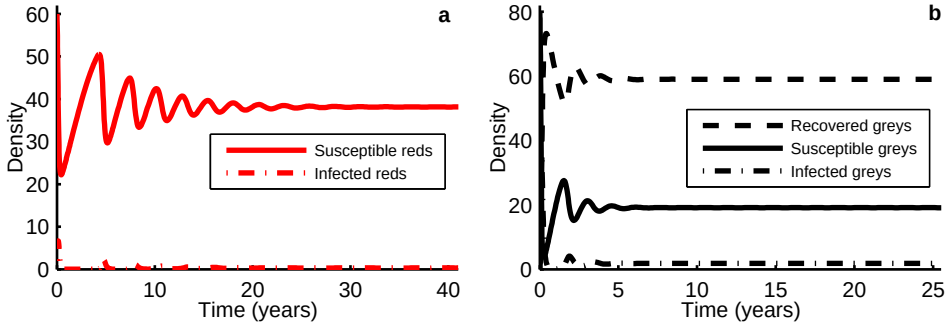

Figure 4.2 Results from Tompkins *et al.* (2003) deterministic model (4.1a–e). In panel **a**, the susceptible reds at their carrying capacity ($K_R = 60$) and 2 infected reds are introduced. In panel **b**, the susceptible greys at their carrying capacity ($K_G = 80$) and 2 infected greys introduced.

disease-free red population the disease persists in the population at its endemic level $(S_R^*, I_R^*, 0, 0, 0)$ (figure 4.2a). Similarly, when a small number of infected greys are introduced, into a disease-free grey population, the disease persists in the population at its endemic level $(0, 0, S_G^*, I_G^*, R_G^*)$ (figure 4.2b). This persistence of the disease in low levels was highlighted by Tompkins *et al.* (2003) as a potential reason why the disease was overlooked as a factor in the replacement of red squirrels by greys. However, in a stochastic model framework the low level of disease may lead to disease extinction.

Stochastic Model

We develop a probabilistic simulation model of Tompkins *et al.* (2003) system by following the methods outlined in Renshaw (1991). These methods convert the rates in the Tompkins *et al.* (2003) framework, such as the birth rate of a susceptible red squirrel, into probabilities that an event will happen, such as the probability of a birth of a susceptible red squirrel. All the birth, death, infection and recovery rates in the Tompkins framework are converted to an event, with an associated probability of the event occurring. When an event occurs it changes the number of individuals in any particular class and hence the probabilities of an event occurring are updated. There are 10 possible events that can occur in this model (see table 4.2) with a Probability Calculation Value ($PCV(i)$, i=1:10) connected to each one calculated from ((4.1a)–(4.1e)). The probability of each event($p(i)$, i=1:10) can then be calculated using:

$$p(i) = \frac{PCV(i)}{PCV_{sum}} \quad \text{where} \quad PCV_{sum} = \sum_{i=1}^{10} PCV(i) \tag{4.2}$$

The strategy to determine which event happens is as follows. A random-number (Y_1) between 0 and 1 is calculated using a random number generator: if $Y_1 \in [0 : p(1))$ then event 1 occurs

Table 4.2 Events in the stochastic Tompkins *et al.* (2003) model.

i	**Description**	**Outcome**	**PCV**
1	Red birth	$S_R \to S_R + 1$	$(a_R - q_R(H_R + c_G H_G))H_R$
2	Susceptible red death	$S_R \to S_R - 1$	bS_R
3	Infected red death	$I_R \to I_R - 1$	$(\alpha + b)I_R$
4	Infection of red	$S_R \to S_R - 1$ & $I_R \to I_R + 1$	$\beta S_R(I_R + I_G)$
5	Grey birth	$S_G \to S_G + 1$	$(a_G - q_G(H_G + c_R H_R))H_G$
6	Susceptible grey death	$S_G \to S_G - 1$	bS_G
7	Infection of grey	$S_G \to S_G - 1$ & $I_G \to I_G + 1$	$\beta S_G(I_G + I_R)$
8	Death of infected grey	$I_G \to I_G - 1$	bI_G
9	Recovery of infected grey	$I_G \to I_G - 1$ & $R_G \to R_G + 1$	γI_G
10	Death of recovered grey	$R_G \to R_G - 1$	bR_G

and S_R becomes $S_R + 1$, if $Y_1 \in [p(1) : p(1) + p(2))$ event 2 occurs and S_R becomes $S_R - 1$, if $Y_1 \in [p(2) : p(1) + p(2) + p(3))$ event 3 occurs and I_R becomes $I_R - 1$ and so on for all 10 possibilities. This method determines the event and updates the density of each population class. We also need to determine when each event occurs, we again follow a method from Renshaw (1991). The time between each event is called the inter-event time and denoted Te. From Renshaw (1991), the time T from the current event to the next is assumed to be an exponentially distributed random variable with

$$\Pr(T \geqslant Te) = \exp\{-PCV_{sum}Te\}. \tag{4.3a}$$

To simulate the inter-event time $T = Te$ we generate a second random number, $Y_2 \in (0, 1)$, and set

$$\exp\{-PCV_{sum}Te\} = Y_2. \tag{4.3b}$$

Taking logarithms of both sides of 4.3b we get

$$-PCV_{sum}Te = log_e(Y_2) \tag{4.3c}$$

$$\Leftrightarrow Te = -\frac{log_e(Y_2)}{PCV_{sum}}. \tag{4.3d}$$

This process can be repeated for any number of events or length of time. The stochastic nature of the simulations means that each simulation will produce different results. We will therefore repeat each simulation many times to provide a clear reflection of the trends and variability of our results.

4.3 Results

To reproduce comparable scenarios to those investigated by Tompkins *et al.* (2003), the initial conditions are set as the red squirrels at their carrying capacity with no disease present $(K_R, 0, 0, 0, 0)$. A small number of greys are introduced (to analyse competition-mediated replacement) and a small number of infected greys are introduced (to analyse competition and infection-mediated replacement). The default number of runs for the stochastic model was 10,000 and, to allow a direct comparison with Tompkins *et al.* (2003), the same parameters were used (see table 4.1).

4.3.1 Competition-only scenario

To consider the system with no squirrelpox present, a small number of uninfected greys were introduced. There are two possible outcomes in this stochastic competition-only model. The greys can invade and replace the red squirrels $(0, 0, K_G, 0, 0)$ or the greys fail to invade and the reds stabilise at their carrying capacity $(K_R, 0, 0, 0, 0)$ (figure 4.3). Figure 4.3a shows the percentage of different outcomes recorded, just over half the time the greys manage to invade and replace the reds. Figures 4.3b–c show the density of reds and greys over time in two typical simulations; the greys die out in 4.3b while in 4.3c the greys manage to invade and replace the reds.

The number of greys, initially introduced, was altered to see the effect this had on the percentage of different outcomes. In figure 4.3a one grey has been introduced, in figure 4.4a two greys have been introduced, in figure 4.4b five greys have been introduced and in figure 4.4c ten greys have been introduced. We have not considered male and female squirrels separately as this would greatly complicate the model. We have calculated the probability of a grey birth taking the number of greys present, annual birth rates and competitive effects into account, therefore one squirrel may reproduce alone without the presence of another squirrel. It can be seen that as

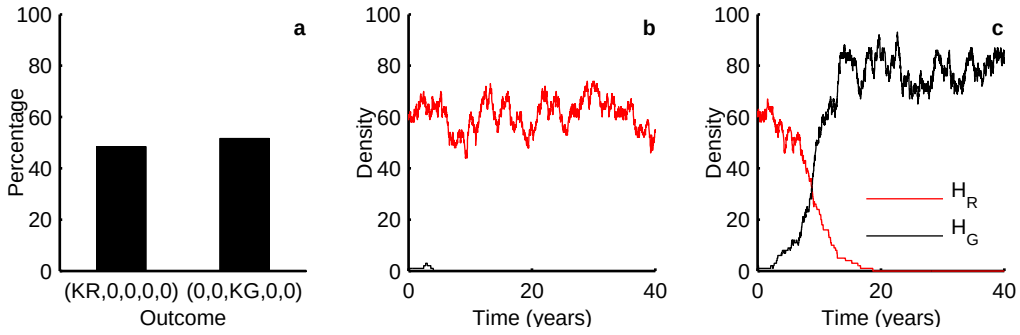

Figure 4.3 Results from competition-mediated stochastic model with 1 grey invading. Panel **a** shows the percentage of the two possible outcomes after 10,000 runs . Panels **b** and **c** show the density of red and grey squirrels over time in two typical simulations. The parameters are the same as those used by Tompkins *et al.* (2003) and can be found in table 4.1. The initial conditions are the red squirrels at their carrying capacity ($K_R = 60$) and one grey introduced.

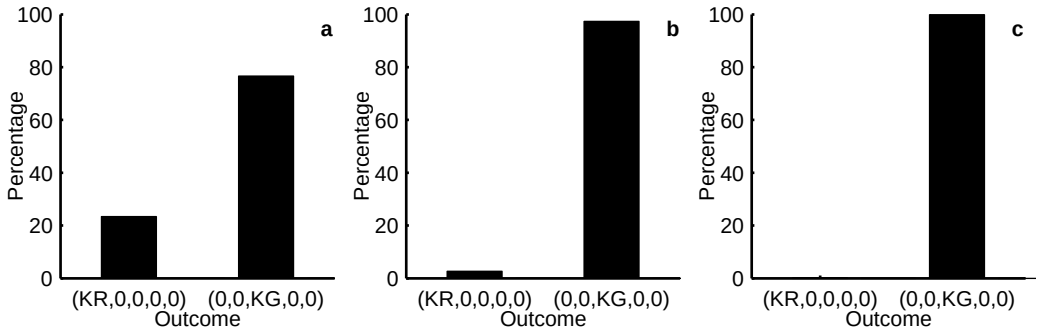

Figure 4.4 Percentage of the two possible outcomes from competition-mediated stochastic model with different numbers of greys invading. There are 2 greys introduced in panel **a**, 5 in panel **b** and 10 in panel **c**. All other parameters and initial conditions are the same as figure 4.3.

the number of greys increases, the proportion of simulations resulting in the greys excluding the reds increases until the greys manage to invade and replace the reds in all of the simulations. In Tompkins *et al.* (2003) the greys always successfully invade and replace the reds, regardless of the number of greys introduced. The two outcomes seen here are a result of either the greys dying out from small numbers or the greys establishing themselves and replacing the reds. If the greys manage to establish themselves they always replace the reds.

These results highlight the differences between the deterministic and stochastic frameworks. For a single realisation of the stochastic framework, there is a chance that a population at low density will become extinct. However, if the introduction of greys is not at a low density or there are repeated introductions of greys into the red populations over time, then at some point the grey population will become established and replace the reds. The results would then mirror the results found by Tompkins *et al.* (2003).

4.3.2 Competition-and-infection scenario

We next examine the effect on the replacement when there is disease present in the system, by introducing a small number of infected greys. In Tompkins *et al.* (2003) model this resulted in the greys replacing the reds and the disease persisting in the population at its endemic state $(0, 0, S_R^*, I_R^*, R_G^*)$.

Figure 4.5 shows the effect when one infected grey is introduced into a red population at its carrying capacity. Figure 4.5a shows the percentage of different outcomes recorded, just over half the time the greys manage to invade and replace the reds. This result is almost identical to the result seen for the competition-only stochastic framework (figure 4.3a). Figures 4.5b–c show the density of reds and greys over time in two typical simulations; as seen previously, the greys die out in 4.5b and replace the reds in 4.5c. The success rate of the greys replacing the reds is not affected by the

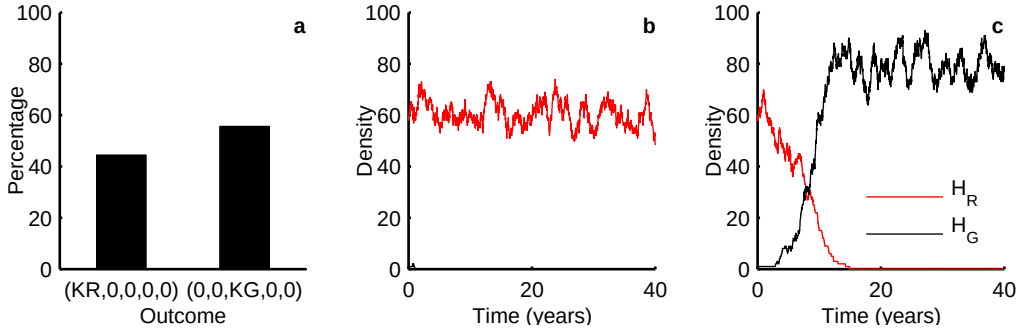

Figure 4.5 Results from competition-and-infection-mediated stochastic model with one grey invading. Panel **a** shows the percentage of the two recorded outcomes after 10,000 simulations. Panels **b** and **c** show the density of red and grey squirrels over time in two individual simulations. The parameters are the same as those used by Tompkins *et al.* (2003) and can be found in table 4.1. The initial conditions are the red squirrels at their carrying capacity ($K_R = 60$) and one infected grey introduced.

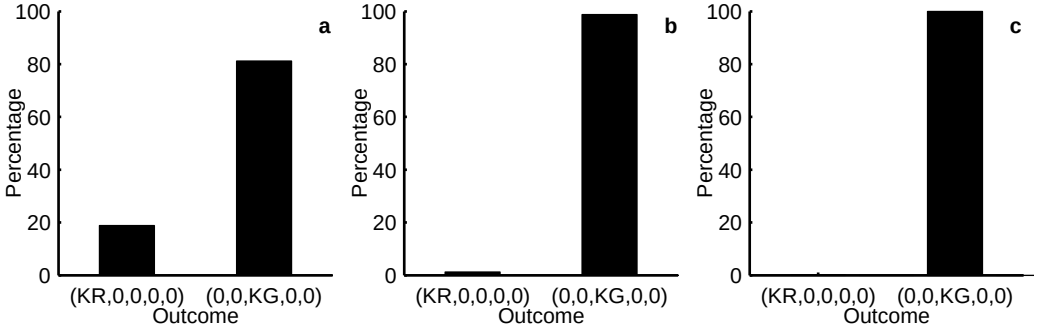

Figure 4.6 Percentage of the two possible outcomes from competition-and-infection-mediated stochastic model with different numbers of greys invading. There are 2 infected greys introduced in panel **a**, 5 in panel **b** and 10 in panel **c**. All other parameters and initial conditions are the same as figure 4.5.

disease. However, the replacement when successful is faster with disease present (see figures 4.3c and 4.5c for a comparison). When we compare the average replacement time with and without disease, in the simulations where replacement occurs, it can be shown that disease speeds up the replacement.

If the numbers of introduced infected greys are increased, the proportion of successful invasions increases (see figure 4.6). Only two outcomes are seen, the reds only with no disease $(K_R, 0, 0, 0, 0)$ and the greys only with no disease $(0, 0, K_G, 0, 0)$. Regardless of the proportion of simulations resulting in invasion and replacement of the reds, the disease does not persist in any of the simulations (figure 4.6). The disease can cause an epidemic in the reds, however it always dies out when the reds reach a low density and before the greys reach a high density (see figure 4.7). The disease does allow the greys to replace reds more quickly, due to the initial epidemic in reds rapidly reducing red numbers but the disease does not remain at endemic levels in the grey population (figure 4.7). Thus, the outcome for the stochastic model is similar under competition-only

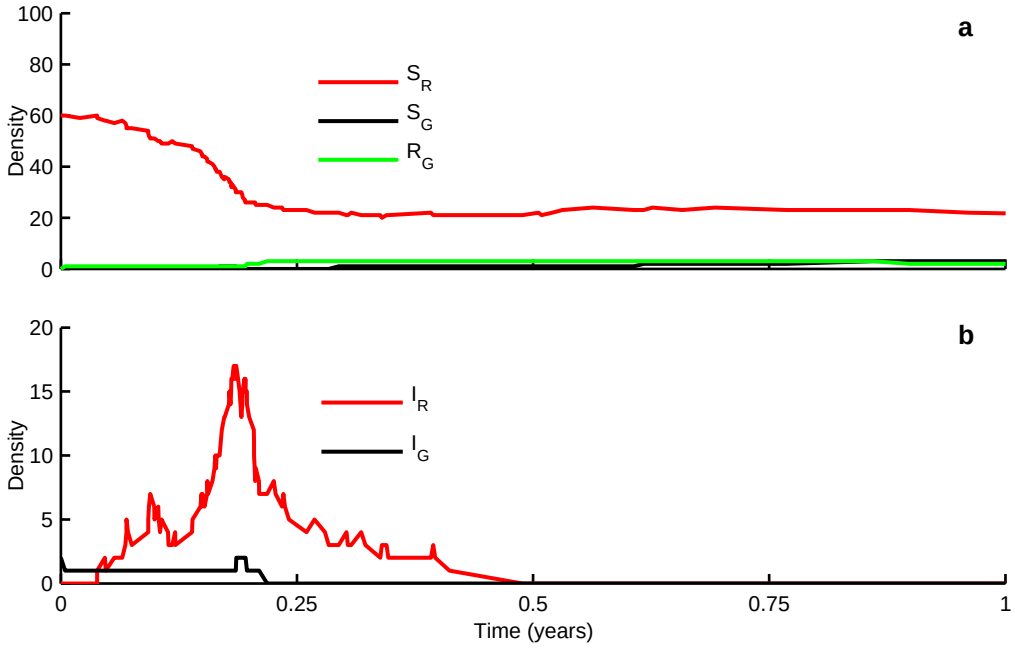

Figure 4.7 Density of red and grey squirrels over time in one run (two infected greys introduced). The time scale on the x-axis has been chosen to highlight the disease epidemic phase. Panel **a** shows the density of susceptible reds (S_R) and susceptible greys (S_G) over time, the greys are invading and replacing the reds. Panel **b** provides the densities of infected reds (I_R) and infected greys (I_G) over time. Note that the infection dies out in both the red and grey populations. All other parameters and initial conditions are the same as figure 4.5.

and competition and disease scenarios.

A motivation for producing this stochastic model is to develop a framework that can be compared to "realistic" red squirrel refuge sites in the field. As the disease is endemic in grey populations in the field, it is important that our model can also capture this behaviour. Therefore, the following sections explore possible modifications to the stochastic model framework to allow disease persistence in the grey population.

4.3.3 Grey-only scenario

We consider a model framework for the grey squirrels only and investigate a range of model modifications that may allow the disease to persist within the the grey population. If one infected grey is introduced to a grey-only population $(0, 0, K_G, 0, 0)$, in our stochastic model framework, the disease does not persist in any of the simulations (figure 4.8a). Although the outcome is always the same, there are two different paths to this outcome. Firstly, the disease does not manage to invade and the population of susceptible population remains at the carrying capacity (see figure 4.8b). Secondly, the disease manages to invade the susceptible population, there is an initial epidemic causing the population to crash but the disease always dies out and the population recovers (see figure 4.8c).

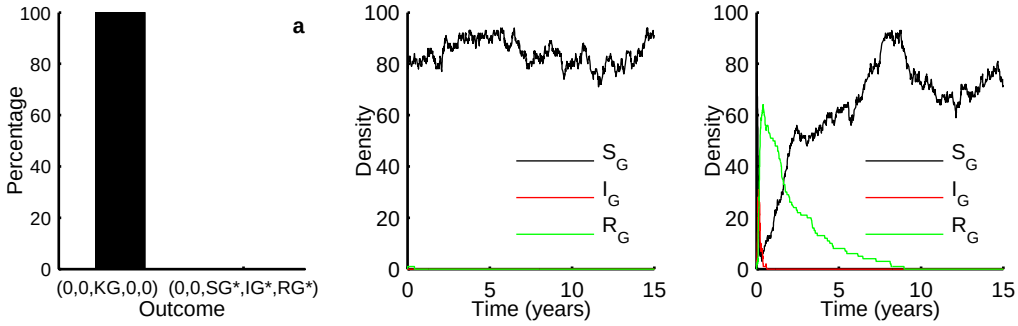

Figure 4.8 Results from grey-only stochastic model with only one infected grey introduced. Panel **a** shows the percentage of recorded outcomes after 10,000 runs. Panels **b** and **c** show the density of susceptible (S_G), infected (I_G) and recovered (R_G) grey squirrels over time in two typical simulations. The parameters are the same as those used by Tompkins *et al.* (2003) and can be found in table 4.1. The initial conditions are the susceptible greys at their carrying capacity ($K_G = 80$), no reds and one infected grey introduced.

The disease does not persist if the number of introduced infected greys is increased. If the number of introduced infected greys is increased, the proportion of simulations involving a disease epidemic followed by the disease dying out increases. If enough infected greys are introduced (ten is sufficient), the disease will always invade the susceptible population, cause an epidemic and then die out. Therefore, either the model assumptions or chosen parameters are inappropriate for the stochastic model. Hence, we will investigate the following modifications to the model framework and assess their effect on disease persistence:

- Carrying capacity

  The carrying capacity currently considered is 80, this may be too small to sustain the infection. We are going to investigate the potential for improving disease persistence by increasing the carrying capacity.

- Seroprevalence

  The seroprevalence is currently set at 74%, and defined to be the percentage of the recovered class in the total population. The remaining 26% of the population encompasses the susceptible and infected population. There is some uncertainty about the level and definition of the seroprevalence, we will investigate the effects of changing its level and its definition (by assuming the seroprevalence includes the recovered and infected classes).

- Recovery time

  There is a wide range of different values used, in the literature, for the recovery period. These range from four weeks (Tompkins *et al.*, 2003) to the lifetime of an infected grey (Rushton *et al.*, 2000). The current version of the model assumes a recovery period of four weeks; hence we will investigate the effect, on disease persistence, of increasing this period

of recovery.

- Spatial structure

  Spatial structure, in particular metapopulations in which collections of subpopulations are linked by dispersal, have been shown to allow populations to persist "globally" although they may go extinct "locally" (Levins, 1969; Begon *et al.*, 1996; Hanski and Gilpin, 1997; Hanski, 1998). To assess whether spatial structure allows disease persistence, we will develop a metapopulation representation of our system by linking a grid of subpopulations that contain the temporal stochastic framework.

Carrying capacity

The value for the carrying capacity of the greys (K_G), comes from Tompkins *et al.* (2003) (table 4.1). To test the effect of this parameter on persistence of the disease within a grey-only scenario, the carrying capacity is altered within the stochastic model. All other parameters remain as in table 4.1 except the rate of virus transmission, β, which alters as the carrying capacity alters. Tompkins *et al.* (2003) calculated β using the value for average seroprevalence against squirrelpox seen in grey squirrel populations in England and Wales (74%) (Sainsbury *et al.*, 2000). This can be interpreted as 74% of the total population, at equilibrium, in a grey-only model is found in the recovered class (R_G^*)

$$\frac{R_G^*}{S_G^* + I_G^* + R_G^*} = 0.74. \tag{4.4}$$

Since, $S_G^* = \dfrac{b+\gamma}{\beta}$, $I_G^* = \dfrac{b(\beta K_G - b - \gamma)}{\beta(b+\gamma)}$ and $R_G^* = \dfrac{\gamma(\beta K_G - b - \gamma)}{\beta(b+\gamma)}$ we get

$$\frac{R_G^*}{S_G^* + I_G^* + R_G^*} = \frac{\gamma(\beta K_G - b - \gamma)}{\beta K_G(b+\gamma)} = 0.74 \tag{4.5}$$

$$\therefore \quad \beta = \frac{\gamma(b+\gamma)}{K_G(\gamma - 0.74(b+\gamma))} \tag{4.6}$$

$$\therefore \quad \beta = \frac{56.485}{K_G} \quad (\ \gamma = 13 \text{ and } b = 0.4 \ (\text{ from table 4.1}))\,. \tag{4.7}$$

As our estimate of the carrying capacity increases, we must decrease our estimate of the disease transmission rate, β, to maintain the correct seroprevalence level. Figure 4.9 shows that as the carrying capacity increases, the disease is more likely to persist. Although the rate of transmission is lower, the higher density of the grey population allows the disease to be maintained within the population. However, the carrying capacity has to be increased considerably to allow the disease to persist and this means we are considering a large, well-mixed population and, therefore, ap-

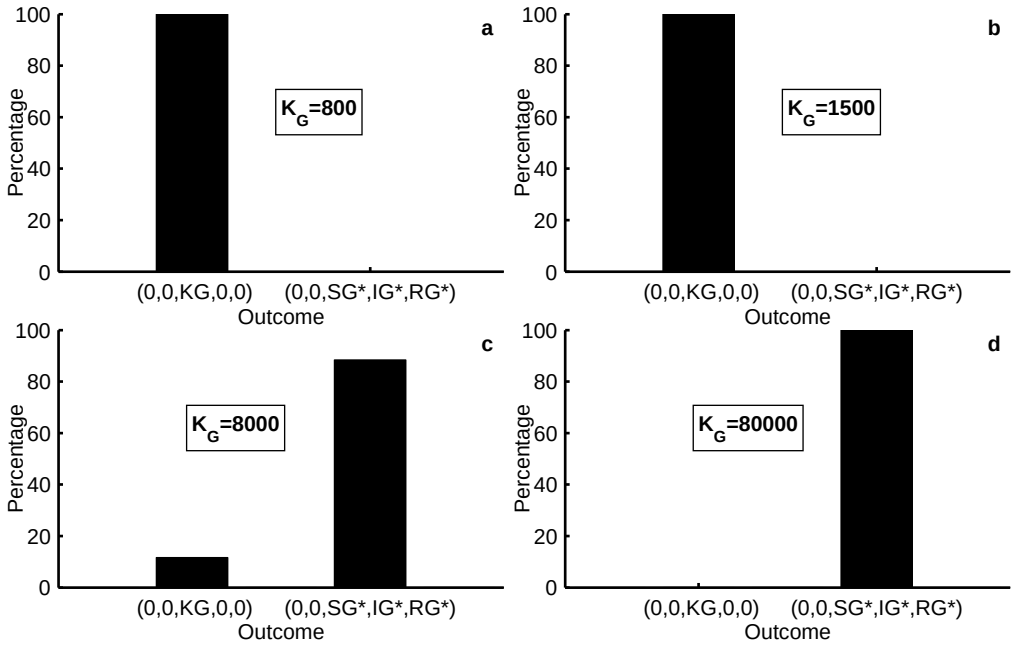

Figure 4.9 Effect of varying carrying capacity (K_G) on grey-only stochastic model with ten infected greys introduced. In panel **a** $K_G = 800$, in panel **b** $K_G = 1500$, in panel **c** $K_G = 8000$ and in panel **d** $K_G = 80000$. All other parameters are the same as those used by Tompkins *et al.* (2003) and can be found in table 4.1.

proximating the mean-field system. We want to consider a stochastic model in which low density is important, and increasing the carrying capacity to large levels will not allow us to consider this effect. In further model formulations we will consider the grey carrying capacity to be 80 or 1500, and examine other modifications that will allow disease persistence. (Here we choose 1500 as it represents the size of the squirrel population in the Formby refuge, hence it will be important in Chapter 5.)

Seroprevalence

To allow investigation into the effect of seroprevalence on disease persistence, we apply two different modifications to the model. Firstly, we will lower the seroprevalence to allow the susceptible and infected class to represent a larger proportion of the population. Secondly, we modify the seroprevalence definition to include both the recovered and infected classes, which may boost infected numbers.

Although seroprevalence is not a parameter, it is used to calculate the rate of virus transmission (β). If the seroprevalence is varied, the rate of virus transmission will subsequently change (see equations 4.4–4.7). The virus transmission rate β is calculated for each of the different values of seroprevalence and carrying capacity (see table 4.3).

At the original carrying capacity of 80 used by Tompkins *et al.* (2003) altering seroprevalence,

Table 4.3 Virus transmission rate (β)

Seroprevalence	β **when** $K_G = 80$	β **when** $K_G = 1500$
0.1	0.187	0.01
0.25	0.226	0.012
0.5	0.346	0.018
0.74	0.706	0.038

and consequently virus transmission rate, has no effect on the outcome of the invasion (figure 4.10). Identical results, to those seen in figure 4.10, are obtained if the carrying capacity is increased to 1500. The value of seroprevalence does not affect the persistence of the disease at either of the carrying capacities.

Tompkins *et al.* (2003) defined seroprevalence, s, to be the proportion of the whole population in the recovered class. It could, conceivably, be defined as the proportion of the whole population who are infected, that is

$$\frac{I_G^* + R_G^*}{S_G^* + I_G^* + R_G^*} = s. \tag{4.8}$$

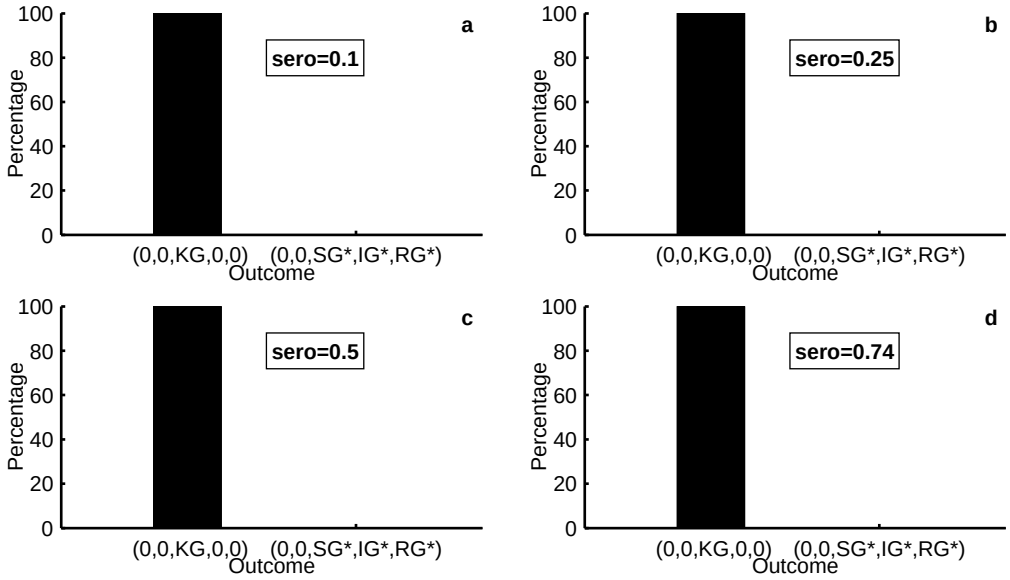

Figure 4.10 Effect of varying seroprevalence in the grey-only stochastic model. In panel **a** the seroprevalence is set to 0.1, in panel **b** 0.25, in panel **c** 0.5 and in panel **d** 0.74. All other parameters are the same as those used by Tompkins *et al.* (2003) and can be found in table 4.1. The initial conditions are the susceptible greys at their carrying capacity ($K_G = 80$), no reds and ten infected greys introduced.

Table 4.4 Virus transmission rate (β) with seroprevalence defined as $\frac{I_G^*+R_G^*}{S_G^*+I_G^*+R_G^*}$.

Seroprevalence	β **when** $K_G = 80$	β **when** $K_G = 1500$
0.1	0.186	0.01
0.25	0.223	0.012
0.5	0.335	0.018
0.74	0.644	0.035

This can be used to calculate a new value for β as follows

$$\frac{I_G^* + R_G^*}{S_G^* + I_G^* + R_G^*} = \frac{\beta K_G - b - \gamma}{\beta K_G} = s \tag{4.9}$$

$$\therefore \quad \beta = \frac{b + \gamma}{(1 - s)K_G} \tag{4.10}$$

$$\beta = \frac{13.4}{(1 - s)K_G} \quad (\gamma = 13 \text{ and } b = 0.4 \text{ (from table 4.1)}). \tag{4.11}$$

We again consider the values 0.1, 0.25, 0.5 and 0.74 for seroprevalence and both 80 and 1500 for carrying capacity. The resulting virus transmission rates (β) are very similar to those seen earlier (see table 4.4).

The disease did not manage to persist within the population in any of the simulations, all results were identical to those seen in figure 4.10. Therefore, redefining seroprevalence did not allow the disease to persist within the population. We conclude that seroprevalence has no notable effect on the persistence of disease within the grey-only population.

Recovery time

There is uncertainty, within the literature, regarding the length of time grey squirrels remain infected. Tompkins *et al.* (2003) used a recovery time (defined as the average length of time for an infected grey to recover) of 4 weeks while Rushton *et al.* (2000) assume a grey remains infected for the rest of its life. We wish to investigate the effect of altering the recovery time, on disease persistence, in our stochastic model. The recovery time is calculated as the inverse of the recovery rate $\left(\frac{1}{\gamma}\right)$.

We fix the seroprevalence as $\frac{R_G^*}{S_G^* + I_G^* + R_G^*} = 0.74$ and examine grey carrying capacities of 80 and 1500; resulting in a possible range of γ from 13 to 2 (with consequential recovery times of 4 to 26 weeks). If the carrying capacity is 80, the length of the recovery period has no effect on disease persistence. When the carrying capacity is 1500, the disease persists within the population

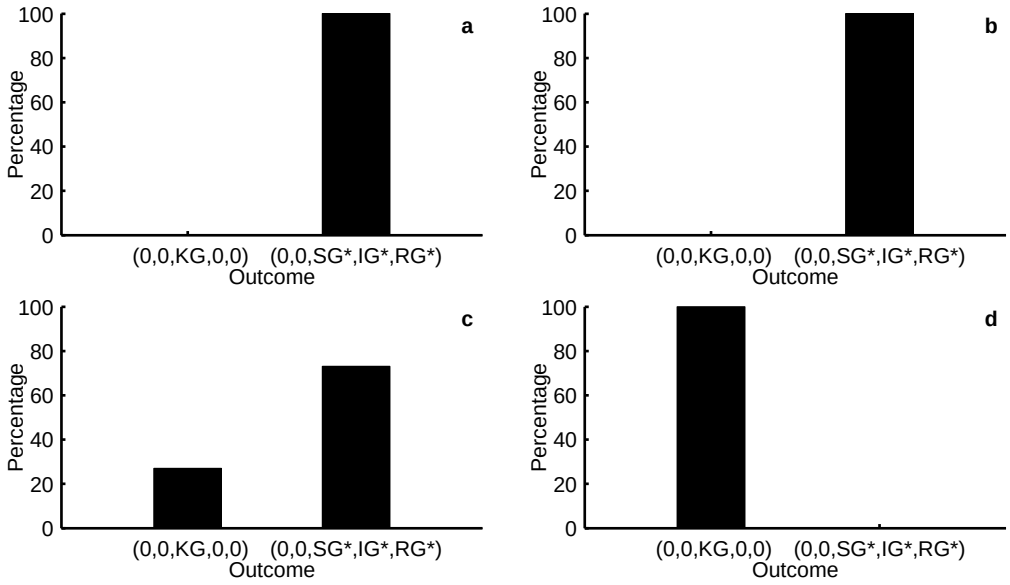

Figure 4.11 Effect of varying recovery (γ) in the grey-only stochastic model with a carrying capacity of 1500. The recovery time in panel **a** is 26 weeks, panel **b** is 10.4 weeks, panel **c** is 6.5 weeks and panel **d** is 4.7 weeks. All other parameters and initial conditions are identical to figure 4.9.

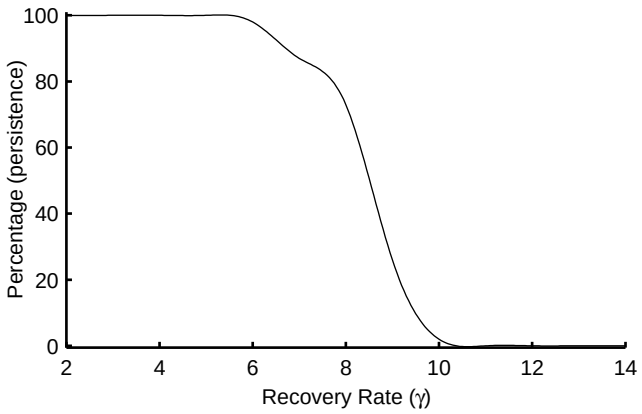

Figure 4.12 Effect of varying recovery (γ) on infection-only stochastic model with a carrying capacity of 1500. All other parameters and initial conditions are identical to figure 4.9.

provided the recovery time is long enough (see figure 4.11). This can be seen clearly by plotting the percentage of disease persistence against the recovery rate (figure 4.12). At low recovery rates (longer recovery times) the disease always persists. For intermediate levels of recovery (γ between 6 and 11) there is a gradual decrease in the proportion of simulations resulting in disease persistence and at high recovery rate the disease is excluded.

Similar results are also found for the alternative definition of seroprevalence, $\frac{I_G^* + R_G^*}{S_G^* + I_G^* + R_G^*}$, see figure 4.13 where γ is varied from 0 to 14 (here, $\gamma = 0$ implies that we are representing the grey population by an SI disease framework and equates to the assumption of lifetime infection used by Rushton *et al.* (2000)).

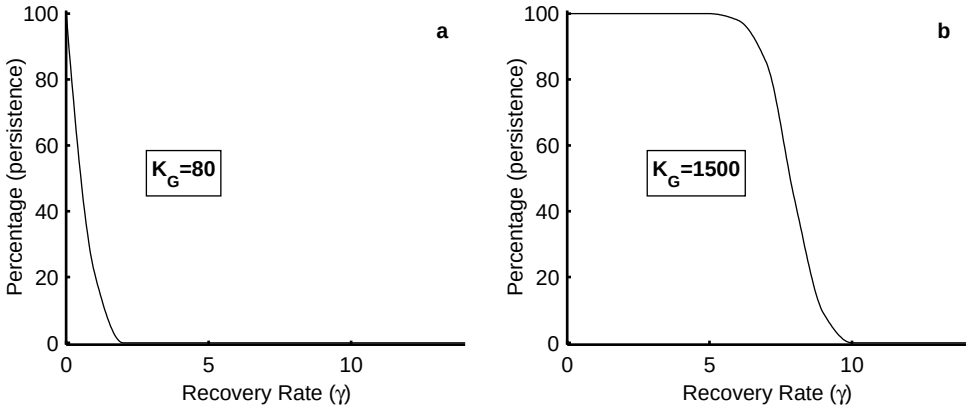

Figure 4.13 Effect of varying recovery (γ) in the grey-only stochastic model with a carrying capacity of 80 in panel **a** and 1500 in panel **b**. Seroprevalence is now defined as $\frac{I_G^*+R_G^*}{S_G^*+I_G^*+R_G^*}$. All other parameters and initial conditions are identical to figure 4.9.

Therefore, extending the recovery time is a modification that can be employed to allow the disease to persist. Later in this chapter, we will consider the implications of this modification in the "full" red/grey/squirrelpox stochastic model.

Spatial structure

Spatial structure has been shown to allow metapopulation persistence, even when local populations can temporarily become extinct (Begon *et al.*, 1996; Hanski and Gilpin, 1997). To generate a spatial stochastic version of our model we let the current model (as described in section 4.2) represent one patch, and consider an array of connected patches. The disease may manage to persist if it can spread to another patch before it dies out in its current patch. Our spatial model will extend our earlier stochastic model; therefore in each patch there is the possibility of the previous birth, death, infection or recovery event (table 4.2) but in addition there is the possibility of dispersal to a neighbouring patch.

We consider a one-dimensional row of eleven identical patches that link in a circular manner (figure 4.14). Individuals can move to an adjacent patch on either side, with patches 1 and 11

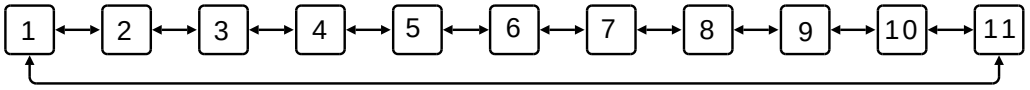

Figure 4.14 One-dimension grid for spatial stochastic model.

linked. All individuals are assumed to move at a rate, m, proportional to squirrel density; this is used to calculate the probability of movement with an equal chance of the squirrels moving in both directions. Our model assumes a healthy population of susceptible greys in every patch and introduce a small number of infected grey squirrels into patch 6. The spatial model is implemented

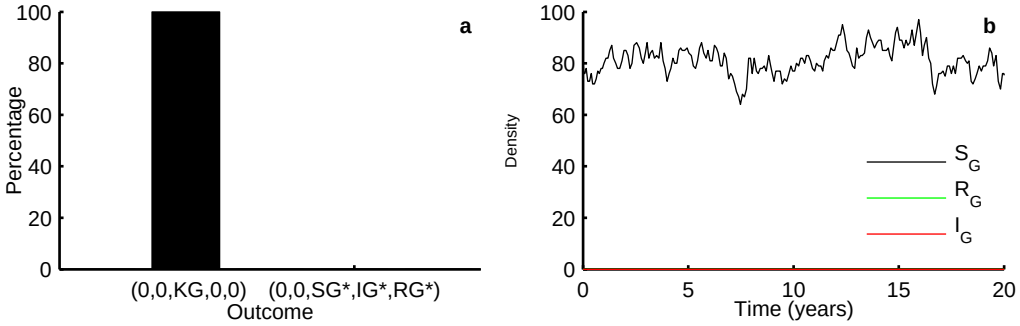

Figure 4.15 Outcomes from one-dimensional spatial stochastic model with 11 patches, carrying capacity of 80 and a spatial parameter $m = 0.4$. Panel **a** shows the percentage of simulations resulting in each outcome. Panel **b** plots the density of each class over time in patch 1.

by firstly calculating a PCV for each possible event, including all those in table 4.2 and movement to adjacent patches, in each patch. Therefore, the model considers each event in each patch with its own PCV and the probability of each event is then calculated using equation 4.2. The same strategy as earlier, involving a random number, is implemented to determine which of all the events in all the patches happens.

The disease does not persist when the carrying capacity is 80 and the dispersal rate is small (figure 4.15a). The low dispersal rate results in the disease failing to spread across the landscape (it fails to reach patch 1, following its introduction into patch 6 and there are no infected individuals at any time point in figure 4.15b). This is shown clearly by plotting the populations density against space at different times (figure 4.16). The disease is introduced into patch 6, causing an initial wave of infected greys (see figure 4.16b). The infected greys do not spread further than patches 4 and 8 (figure 4.16b,e,h, and k), before dying out or recovering (figure 4.16n). The populations is behaving like a single patch, with the disease dying out due to small numbers of infected individuals.

When the dispersal rate is increased, for patches with a carrying capacity of 80, the disease does spread across the whole landscape; however, it does not persist (see figure 4.17a). There is one outbreak of the disease in patch 1, resulting in an epidemic followed by the population recovering and the disease dying out (figure 4.17b). By examining the spatial dynamics over time it can be seen that the disease spreads across the landscape in two waves (figure 4.18). However, these two waves eventually collide and behind the wave there is no susceptible population to infect, meaning the infection dies out. We have carried out further investigation in which the one-dimensional spatial array is extended or a two-dimensional array patches is considered, but in all cases the disease dies out when the patch carrying capacity is 80.

If the carrying capacity is increased to 1500, the disease persists in all simulations (see figure 4.19a). It again spreads out with two waves of infection (figure 4.20) causing an initial epi-

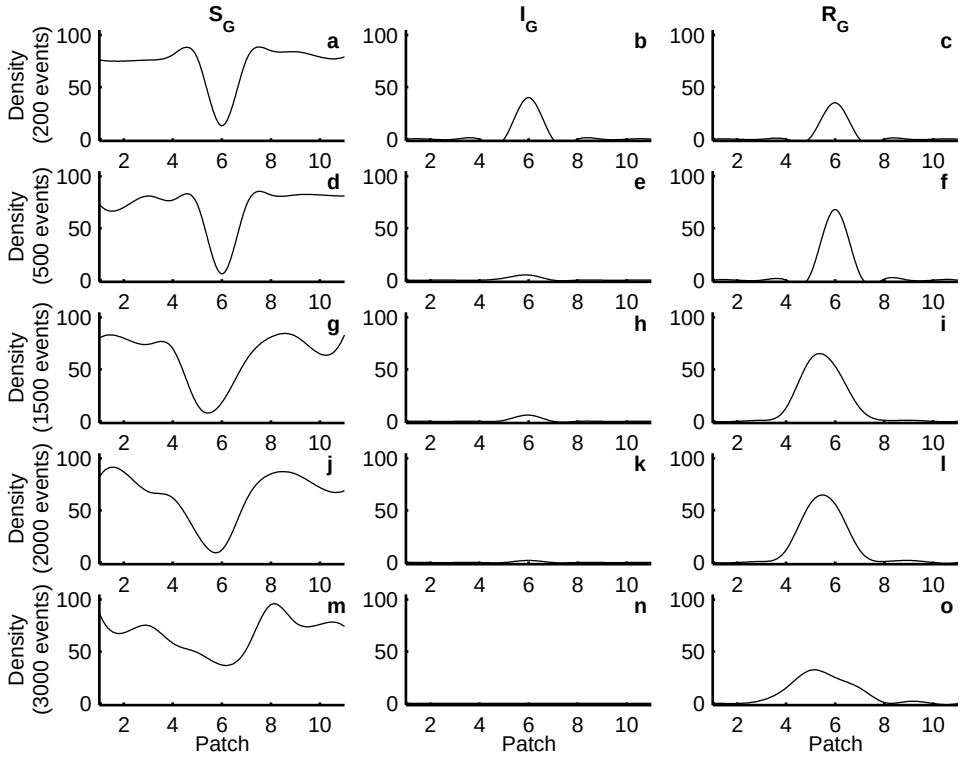

Figure 4.16 Effect on different classes in one-dimensional spatial stochastic model with carrying capacity of 80 and a spatial parameter $m = 0.4$. Density of susceptible greys (panels **a**, **d**, **g**, **j** and **m**), infected greys (panels **b**, **e**, **h**, **i** and **j**) and recovered greys (panels **c**, **f**, **i**, **l** and **o**) in all 11 patches. These results have been smoothed using a spline function to allow representation of the spatial waves.

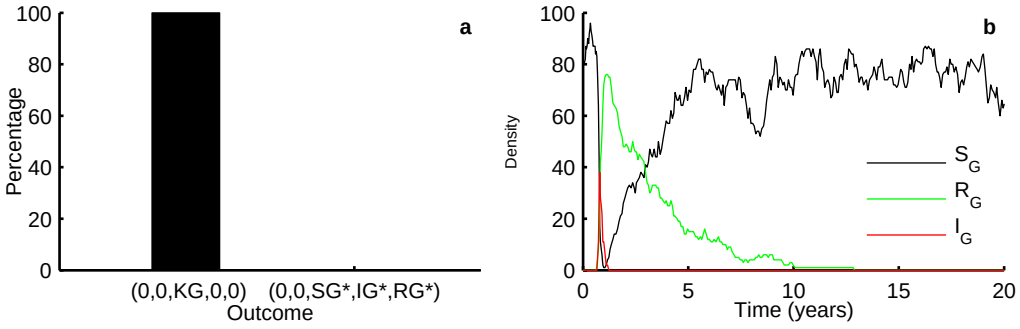

Figure 4.17 Outcomes from one-dimensional spatial stochastic model with 11 patches, carrying capacity of 80 and a spatial parameter $m = 0.8$. Panel **a** shows the percentage of simulations resulting in each outcome. Panel **b** plots the density of each class over time in patch 1.

demic in each patch (see patch 1 in figure 4.19b). However when these waves meet, unlike earlier, there are enough susceptibles behind the wavefront to allow the disease to persist within the landscape (figure 4.20). The disease is sustained in each patch with small oscillations close to zero.

Therefore, spatial structure allows the disease to persist, provided the carrying capacity in each patch is sufficiently large. However it is important to note, in the absence of space, the disease did not persist with a carrying capacity of 1500 (see figure 4.9). The spatial structure is

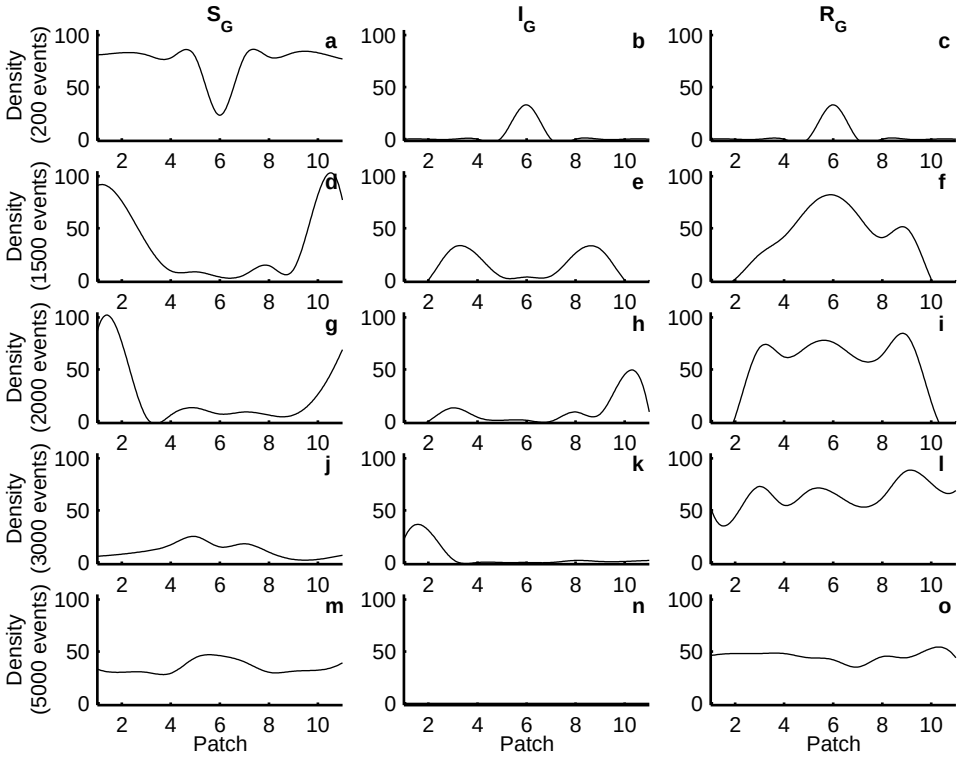

Figure 4.18 Effect on different classes in one-dimensional spatial stochastic model with carrying capacity of 80 and a spatial parameter of m=0.8. Density of susceptible greys (panels **a**, **d**, **g**, **j** and **m**), infected greys (panels **b**, **e**, **h**, **i** and **j**) and recovered greys (panels **c**, **f**, **i**, **l** and **o**) in all 11 patches. These results have been smoothed using a spline function to allow representation of the spatial waves.

not equivalent to increasing the overall carrying capacity, it allows the disease to persist at lower total population numbers than would be possible in a single site. The results, here, hold for a large range of dispersal rates (above a minimum value).

The one-dimensional spatial structure applied to the stochastic model allows the disease to persist in the grey-only population. Other forms of spatial structure could be included and we have examined a range of two-dimensional spatial arrangements including a 11x11 patch grid and

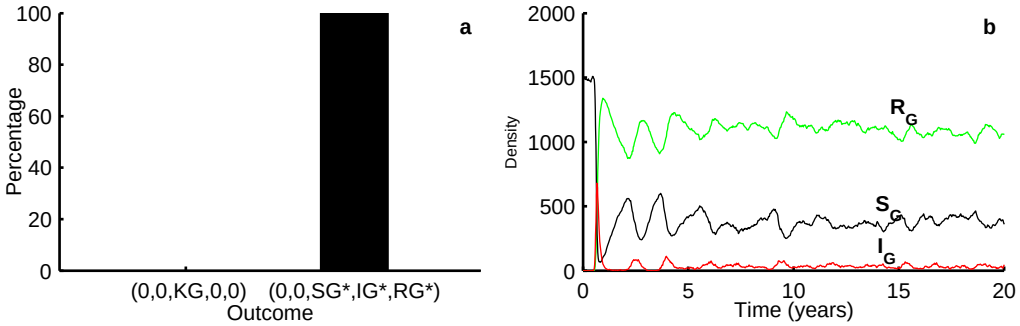

Figure 4.19 Outcomes from one-dimensional spatial stochastic model with 11 patches, carrying capacity of 1500 and a spatial parameter of $m = 0.4$. Panel **a** shows the percentage of simulations resulting in each outcome. Panel **b** plots the density of each class over time in patch 1.

a 51x51 patch grid. This also allows the disease to persist, at carrying capacities lower than 1500, but the results are qualitatively similar (persistence over all patches with small oscillations, near zero, in infected numbers in an individual patch). The two-dimensional spatial arrangement is more complicated to model and implement, due to movement in four directions rather than two, resulting in longer computational time. Therefore, as the results are qualitatively similar we chose to use a one-dimensional grid.

Summary

The following four modifications were examined to investigate their effect on disease persistence in a grey-only stochastic model.

- Carrying capacity

  The disease can persist if the carrying capacity is increased considerably. However, this does not reflect the importance of small population numbers on the outcome, so will only consider carrying capacities of 80 and 1500 for grey squirrels.

- Seroprevalence

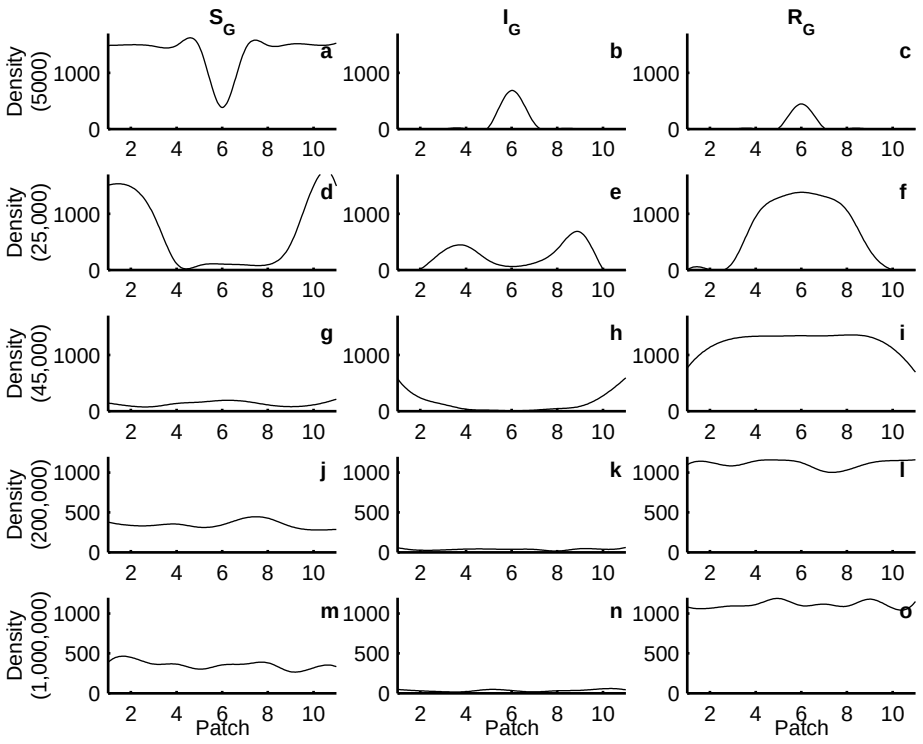

Figure 4.20 Effect on different classes in one-dimensional spatial stochastic model with carrying capacity of 1500 and a spatial parameter of $m = 0.4$. Density of susceptible greys (panels **a**, **d**, **g**, **j** and **m**), infected greys (panels **b**, **e**, **h**, **i** and **j**) and recovered greys (panels **c**, **f**, **i**, **l** and **o**) in all 11 patches. These results have been smoothed using a spline function to allow representation of the spatial waves.

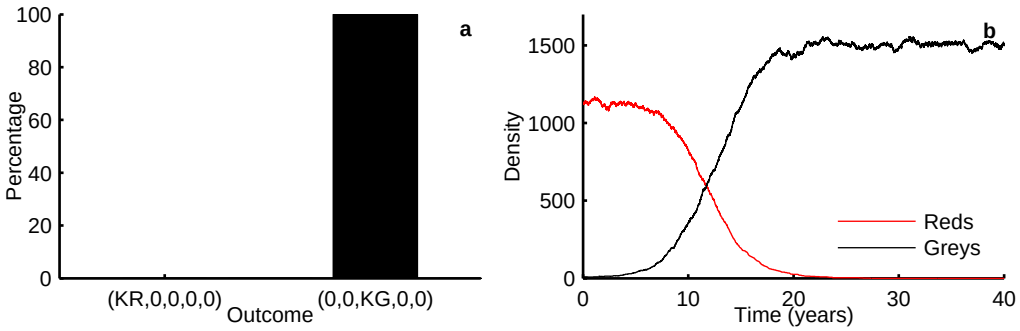

Figure 4.21 Results from competition-mediated stochastic model with carrying capacities $K_G = 1500$ and $K_R = 1125$. Panel **a** shows the percentage of possible outcomes and panel **b** shows the density of red and grey squirrels over time in an individual run. All other parameters are the same as those used by Tompkins *et al.* (2003) and can be found in table 4.1. The initial conditions are the red squirrels at their carrying capacity ($K_R = 1125$) with ten greys introduced.

Altering the seroprevalence has no notable effect on the persistence of disease within the grey-only population.

- Recovery time

  The disease persists, with a carrying capacity of 1500, if the recovery time is greater than 8.7 weeks (recovery rate is less than 6).

- Spatial structure

  If the carrying capacity is 1500, a one-dimensional spatial structure allows the disease to persist.

We did not find any "realistic" modifications, that allowed the disease to persist with a carrying capacity of 80, the baseline carrying capacity value used in Tompkins *et al.* (2003). If the carrying capacity is 1500, realistic changes in the recovery time or a simple spatial structure allow the disease to persist. We now wish to investigate the effect of these modifications on the full red/grey/squirrelpox model framework and examine their effect on competition-only and competition-and-infection mediated replacement of red squirrels by greys.

4.3.4 Model modifications

The modifications we wish to consider, all assume the carrying capacity of the greys is 1500. To maintain the same relationship between the carrying capacities as Tompkins *et al.* (2003), we set the red carrying capacity as 1125. In a competition-only scenario, the greys always replace the reds (see figure 4.21a). This replacement takes approximately 21 years as shown in figure 4.21b.

Recovery time

If we examine the effect of increasing the recovery time (from 8.7 weeks up to the lifetime of the infected grey) on competition-and-infection replacement we find that the disease dies out; the results are analogous to those of competition-only replacement (figure 4.21). Here, the disease does not manage to persist, in the red population, and dies out before there are sufficient greys to sustain it. Therefore, although disease can be sustained in a grey-only population it does not play a significant role in the invasion and replacement dynamics of red squirrels by greys.

Spatial Structure

We consider a one-dimensional spatial framework as displayed in figure 4.14. We consider the red squirrels at their carrying capacity in every patch except one patch with greys present. The greys will either be at their carrying capacity, when considering competition-only, or at endemic levels when considering disease. The grey squirrels invade and replace the reds across the landscape (in every patch), regardless of the presence of disease (see figure 4.22). If the disease is present, it persists across the landscape in the grey population (figure 4.22b). The disease enables the greys to replace the reds more quickly; it takes approximately 15 years without disease and 8 years with the disease (figure 4.22). This agrees with the earlier findings from the deterministic model (Tompkins *et al.* (2003)).

The disease is spreading in two waves, from it's introduction in patch 6, across the landscape. In a similar manner to the models discussed in chapter 3, the disease spreads across the landscape in advance of the greys (figure 4.23b highlights this phenomenon).

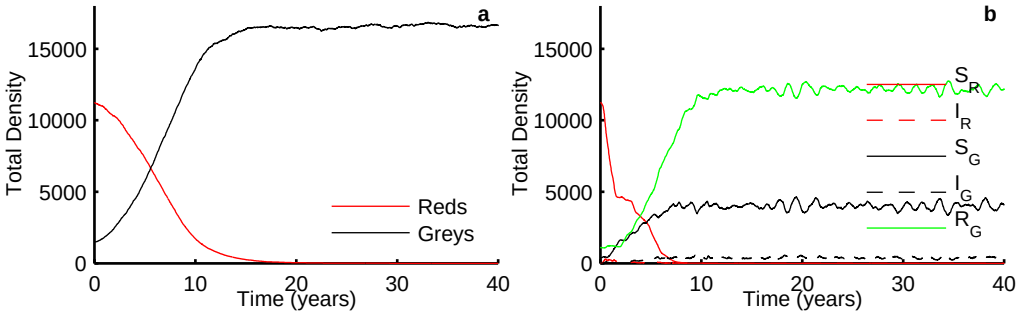

Figure 4.22 Total densities, across landscape, in competition-only (panel **a**) and competition-and-infection (panel **b**) spatial stochastic frameworks. The spatial framework is a one-dimensional loop of 11 patches; the densities, of each class, have been summed over all patches. The carrying capacities are $K_G = 1500$ and $K_R = 1125$ and all other parameters are the same as those used by Tompkins *et al.* (2003) and can be found in table 4.1.

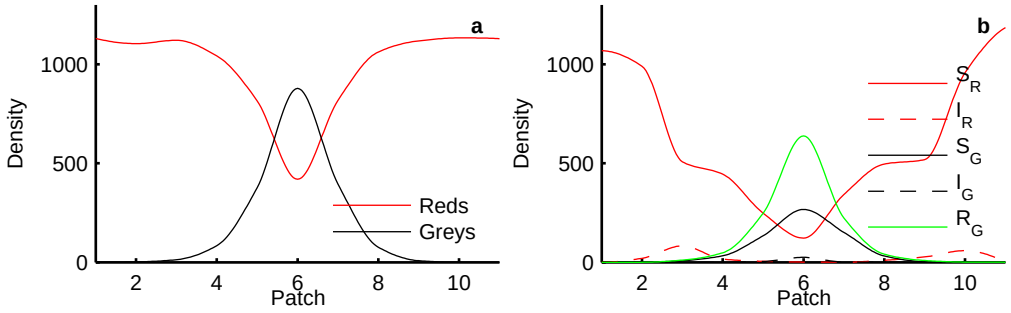

Figure 4.23 Effect on different classes in competition-only (panel **a**) and competition-and-infection (panel **b**) spatial stochastic model (time = 1 year). The parameters are the same as those used in figure 4.22.

4.4 Discussion

In this chapter, we developed a stochastic model of the red/grey/squirrelpox system, to examine the effects of small numbers on this system. A further motivation, for considering this model, is to develop a "realistic" framework to model red squirrel refuge sites in the field. The model was based on, and allowed comparison with, the deterministic model framework proposed by Tompkins *et al.* (2003) for the squirrel system.

Our initial comparisons between competition-only and competition-and-infection scenarios, showed that the disease did not persist within the grey population. An assessment of the grey-only model framework, concluded that either the model assumptions or chosen parameters were inappropriate. Therefore, we investigated the following modifications to the stochastic model framework to assess their effect on disease persistence:

- Carrying capacity

  The baseline carrying capacity of 80, used by Tompkins *et al.* (2003), was increased to investigate its effect on disease persistence. Although significantly larger carrying capacities would allow the disease to persist, we would no longer be modelling the importance of small population numbers on the outcome. Therefore, we chose to only consider carrying capacities of 80 and 1500 for grey squirrels.

- Seroprevalence

  Tompkins *et al.* (2003) used a seroprevalence value of 74% and defined this as the percentage of the recovered class in the total population. We assessed the effect of lowering seroprevalence, and also the effect of changing the definition to include both the recovered and infected classes. Neither of these modifications allowed the disease to persist resulting in a conclusion that seroprevalence has no notable effect on the persistence of disease in a grey-only population.

- Recovery time

  The recovery time, calculated as the inverse of the recovery rate $\left(\frac{1}{\gamma}\right)$, was modified to assess its effect on disease persistence. It was considered for both carrying capacities (80 and 1500) and over a wide range of values (from 4 weeks (the value used by Tompkins *et al.* (2003)) to the lifetime of an infected grey squirrel (as considered by Rushton *et al.* (2000))). Our investigation showed that the disease did not persist with a carrying capacity of 80. However, we concluded that with a carrying capacity of 1500, the disease persists if the recovery time is greater than 8.7 weeks (a recovery rate of less than 6).

- Spatial structure

  We applied a one-dimensional spatial grid to our stochastic model to assess its potential for allowing disease persistence. Our spatial structure consisted of eleven linked patches and each patch was modelled using the temporal stochastic model. This modification, allowed the disease to persist with a carrying capacity of 1500.

Two modifications allowed the disease to persist within a grey-only population, with a carrying capacity of 1500. These, were an increased recovery time and spatial structure, and both modifications were then considered in a red/grey/squirrelpox model framework. The disease did not persist in the "full" system when the recovery time was increased, but it did when a one-dimensional spatial framework was adopted. Therefore, the only suitable modification to the model to allow disease to persist is the spatial framework.

Our spatial structure transforms the population into a metapopulation, consisting of subpopulations with migration between neighbouring patches. Harrison and Taylor (1997) stated metapopulation theory was based on "the fundamental theory that the persistence of species depends on their existence as sets of local populations largely independent yet interconnected by migration". The metapopulation, as a whole, persists as a result of migration between subpopulations. There are "local" extinctions, within subpoulations, followed by recolonisation from neighbouring patches (Begon *et al.*, 1996).

The dispersal rate, is an important parameter within a metapopulation model as it governs the ability of individuals to move between patches. If the dispersal parameter is increased, recolonisation following local extinction will happen faster; this may, in turn, improve the persistence chances of the metapopulation. However, there are negative effects of increased dispersal, as discussed by Hess (1996) in relation to corridors between patches. One of the negative impacts, outlined by Hess (1996), is the increased spread of infectious diseases (see Grenfell and Harwood (1997) for a review of disease dynamics within metapopulations).

A relevant example, to our work, of a metapopulation framework was used by Foley *et al.*

(1999) to model feline enteric coronavirus dynamics in domestic cats. Their framework differs from ours as there is no recovered class and infecteds can recover back to the susceptible class (SIS). However, they too considered a stochastic model framework and found that the disease did not persist in an isolated population but did within a metapopulation.

The spatial structure, showed the disease enabling the greys to replace the reds faster (approximately 15 years without disease and 8 years with the disease, figure 4.22). These findings are very similar to those of Tompkins *et al.* (2003), whose deterministic model showed a replacement without disease taking 15 years and replacement with disease taking 6 years. Tompkins *et al.* (2003) also highlighted that the disease was only present in small numbers, and offered this as a reason why disease may be overlooked in observational studies. Our results also highlight this, as there is small oscillations, near zero, of the infected class seen in our spatial framework.

Our spatial results also show the disease spreading, across the landscape, into the red squirrel populations in advance of the greys. This agrees with evidence collected from the field by Reynolds (1985) (replacement of red squirrels by greys in East Anglia between 1960 and 1981). Diseased red squirrels were found in spatial locations, before any grey squirrels. These findings were assumed, at the time, to show that the disease was not connected to the invasion of grey squirrels. However, our models show that this is not the case and the disease is a result of the grey invasion. This phenomenon was also seen in our spatial deterministic results, reaction-diffusion equations, in Chapter 3. These findings indicate the importance of considering individuals to be a discrete entity; they also highlight how useful deterministic approaches can be in laying down the key mechanisms that determine the population dynamics.

In the next chapter, we hope to build a "realistic" model of a refuge for red squirrels similar to the refuge in Formby, Merseyside. Based on the findings above, we will use a spatial stochastic model framework as the foundation from which to build the refuge model.

Chapter 5

A Stochastic Model of a Red Squirrel Refuge

5.1 Introduction

In this chapter we will develop the spatial stochastic model, seen in Chapter 4, to represent a variety of strategies for red squirrel conservation. One conservation strategy employed for red squirrels is the establishing of red squirrel refuges with surrounding buffer zones. The aim of a refuge and buffer zone is to isolate the red squirrel population from greys found in the wider population. We wish to develop a model encompassing a refuge, buffer zone and wider population; this model will allow analysis into the effectiveness of buffer zones and also of further conservation efforts such as culling. Our model will be based on the refuge at Formby, Merseyside but is applicable to general refuges and strategies.

The United Kingdom has seen its native red squirrel, *Sciurus vulgaris*, replaced by the introduced North American grey squirrel, *Sciurus carolinensis*, since its first introduction in 1876 (Middleton, 1930; Lloyd, 1983; Reynolds, 1985). It is now widely acknowledged that the replacement of red squirrels by greys has been aided by the greys acting as a reservoir host for squirrelpox (Sainsbury *et al.*, 2000; Tompkins *et al.*, 2003). There are now over 2.5 million grey squirrel widespread throughout Britain (Harris *et al.*, 1995). However, there are believed to be only 160,000 red squirrels left in Britain with 75% of these found in Scotland, 19% in England and 6% in Wales (Harris *et al.*, 1995; Battersby and Partnership, 2005).

The Forestry Commission Scotland has undertaken a consultation process to identify 18 red squirrel "strongholds" throughout Scotland (Forestry Commision Scotland, 2009). It is currently seeking formal agreements with relevant landowners. This forms part of the "Red Squirrel Action Plan 2006–2011", which gives details of squirrel conservation plans for Scotland. These plans in-

clude grey control programs throughout Scotland, forest management to promote habitat suitable for red squirrels and the formation of red squirrel refuges or "strongholds" (Forestry Commision Scotland *et al.*, 2006). The proposed 18 strongholds are all forests between 2,400 and 14,400 hectares, meaning 100,000 hectares of woodlands would be allocated to red squirrel conservation in Scotland. The forests would be improved for red squirrels within the strongholds, threats from greys would be minimised and continual research and monitoring carried out. They are not intending to provide buffer zones around the strongholds but recognise that site-specific measures may be needed. The proposed strongholds are located in the following woodlands:

1. Morangie Forest (Highland)
2. Glen Glass (Highland)
3. Culbin (Grampian and Moray / Highland)
4. Black Isle (Highland)
5. Ordiequish, Whiteash, Ben Aigan (Grampian and Moray)
6. Daviot Loch Moy (Highland)
7. Abernethy, Nethy Bridge (Highland)
8. Inshriach and Glenfeshie (Highland)
9. Glentochty (Grampian and Moray)
10. Balmoral to Inver (Grampian and Moray)
11. Leanachan (Highland)
12. South Rannoch (Tayside)
13. Inverliever (Argyll)
14. Eredine (Argyll)
15. Kilmichael (Argyll)
16. Eskdalemuir(Dumfries and Galloway)
17. Fleet Basin (Dumfries and Galloway)
18. Glenbranter (Argyll)

The strongholds are being proposed as a contingency plan in case the ongoing forestry management to favour red squirrels and grey culling in Scotland does not prevent the greys spreading through Scotland. The Isle of Arran is the only Scottish island with a resident red squirrel population. Although it has not been specifically named as a stronghold site, measures are being put in place on the island to protect the reds from invading greys and forests are being managed to provide a red refuge in the future if necessary (Forestry Commision Scotland, 2009).

The Welsh population is confined to Tywi, Crychan, Irfon, Brechfa and the island of Angle-

sey (there are also two small populations believed to exist near Bala and Dolgellau) (Cartmel, 2003). The Island of Anglesey lies off the North Wales coast, it is separated from the mainland by the narrow Menai Straits and is linked by two bridges. Although red squirrels were once widespread on the island, the population had decreased to approximately 40 red squirrels in 1998 as a result of grey squirrel invasion. Due to the near extinction of the red population, a local conservation group "The Friends of the Anglesey Red Squirrels" was formed and grey squirrel control implemented (approximately 8,000 greys were removed from the island of Anglesey between 1998 and 2009). The grey control strategies were followed by a successful reintroduction programme (six red squirrels were released between 2006 and 2008). The grey squirrel control and reintroduction of red squirrels continues in Anglesey with positive results for red squirrels (see `http://www.redsquirrels.info/index.html`).

The majority of the English red squirrel population are found in the North of the country with only small populations, isolated from greys, in the South. These pockets of remaining red squirrels can be found in Cannock Chase the Isle of Wight and three small islands in Poole Harbour (Kenward and Holm, 1993). There was a small population of red squirrels surviving in Thetford Chase, Norfolk until recent years. A refuge was set up and grey squirrel control along with red squirrel reintroductions implemented; however, the reintroductions were unsuccessful as a result of squirrelpox (Gurnell *et al.*, 2002). It is now believed that there are no red squirrels left in this area (Carroll *et al.*, 2009). It is estimated that 85% of the remaining population in England is found in Cumbria, North Lancashire and Northumberland (Harris *et al.*, 1995). Following an assessment of all the forests in Cumbria, Lancashire, Northumberland, Yorkshire and Durham in 2001–2004, the following 16 sites were chosen as "National Squirrel Refuge and Buffer Zones" (SAVE OUR SQUIRRELS, 2005):

1. Kielder (Northumberland / Cumbria)
2. Kidland (Northumberland)
3. Uswayford (Northumberland)
4. Harwood (Northumberland)
5. Kyloe (Northumberland)
6. Raylees (Northumberland)
7. Greystoke (Cumbria)
8. Garsdale/Mallerstang (Cumbria)
9. Widdale (North Yorkshire)
10. Thirlmere (Cumbria)
11. Sefton (Merseyside)

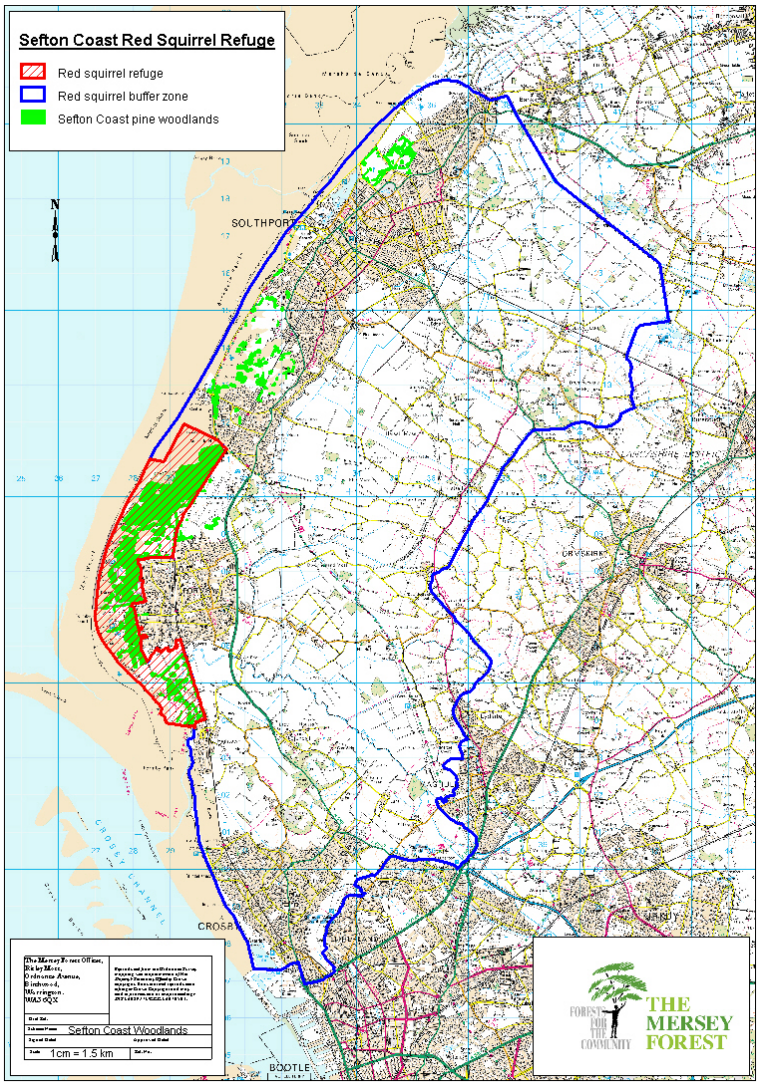

Figure 5.1 Map outlining Sefton Coast Refuge and Buffer Zone, courtesy of Sefton Council (available from http://sefton.gov.uk).

12. Whinfell (Cumbria)
13. Dipton/Dukeshouse Wood (Northumberland)
14. Healey/Kellas (Northumberland)
15. Slaley/Dukesfield (Northumberland)
16. Whinlatter (Cumbria).

The National Trust site at Formby is one of the remaining red squirrel populations in Northern England; the squirrels have been a tourist attraction for many years with organised red squirrel walks and peanuts sold for feeding. It officially became a refuge in 2005 when the Sefton Coast Woodlands became one of the 16 National Squirrel Refuge and Buffer Zones (Burkmar, 2006). The woodlands consist of mainly conifers making them well suited for red squirrels; they are actively managed to ensure they are suited to red squirrels by the Sefton Coast Woodlands Forest

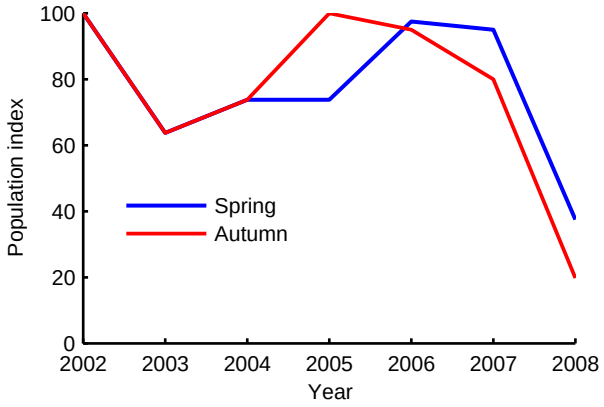

Figure 5.2 Population trends of red squirrel population within Sefton Coast Red Squirrel Refuge. These results are reproduced from White (2009b)

.

Plan (Whitfield, 2008). There are small pockets of woodlands within the buffer zone, as well as agricultural and urban areas (figure 5.1 shows a map outlining refuge and buffer zones).

Red squirrels occupy both the refuge and buffer zone; they are a vulnerable population and considerable conservation efforts are carried out to protect and maintain the populations within the refuge and buffer zone. A large number of organisations are involved in the conservation, with the majority of the work being carried out by volunteers and coordinated by Red Alert (as part of the, The Heritage Lottery funded, "SAVE OUR SQUIRRELS" project) (Burkmar, 2006). The main threat to the Formby populations is the spread of grey squirrels into the refuge and resulting outbreaks of squirrelpox. Other potential threats include road mortalities and over-mature woodlands no longer providing suitable food resources (Whitfield, 2008).

The squirrel population in the refuge and buffer zone, have been monitored since 2002 using line transect surveys White (2009b). This data is used to produce a population index, highlighting the population trends since 2002 (figure 5.2). The red squirrel population in the refuge suffered declines in 2003, following the first reported squirrelpox outbreak in Formby. The population did show signs of recovering following this outbreak; unfortunately another outbreak of squirrelpox occurred in 2006 and major declines followed. As a result, by Autumn 2008 the red squirrel population within the refuge had declined by 80% (compared to 2002) (White, 2009b). Prior to the squirrelpox outbreaks, the refuge was believed to carry a population of up to 1500 red squirrels with a minimum spring population of between 800 and 1000 squirrels. In July 2009, the population was estimated to be between 150 and 200 red squirrels although thought to be recovering (White, 2009a). There was a confirmed case of squirrelpox in October 2009, although this is not thought to have spread (Lancashire Wildlife Trust, 2009).

Squirrelpox will be a major consideration in our model as it is not only one of the main threats

to the red squirrel population at Formby but also to the other British red squirrel refuges. Following the analysis in Chapter 4, we will develop a refuge model that is represented by an array of patches connected by dispersal between neighbouring patches.

5.2 Model

We will consider a spatial stochastic framework, with three regions: refuge, buffer zone and landscape. The refuge and buffer zone will both be single patches and the landscape an array of 11 locally connected patches (see figure 5.3). We showed in Chapter 4 the 11 patch spatial arrangement allows persistence of squirrelpox, across the landscape, in the grey population. The refuge and buffer zone are connected, and the buffer zone is connected to one of the landscape patches. Therefore, the only route for a squirrel to enter the refuge is through the buffer zone, and there is only one route from the landscape to the buffer zone (see figure 5.3). This allows comparison with the Formby refuge, where the sea is located on one side and the buffer zone on the other.

The model framework consists of each patch being modelled in an identical manner to the stochastic model used in chapter 4 (see section 4.2 for a description). We will undertake the following analysis to assess a variety of conservation and management strategies:

- Baseline scenario

  In this scenario the refuge and buffer zone are identical and there are no management strategies in place. Therefore, this scenario models the red/grey/squirrelpox system if there is no effective refuge or buffer zone in place. We will use this scenario as a baseline to compare the various conservation and management strategies.

- Buffer zone characteristics

  We consider the effect, on the red squirrel population within the refuge, of the level of

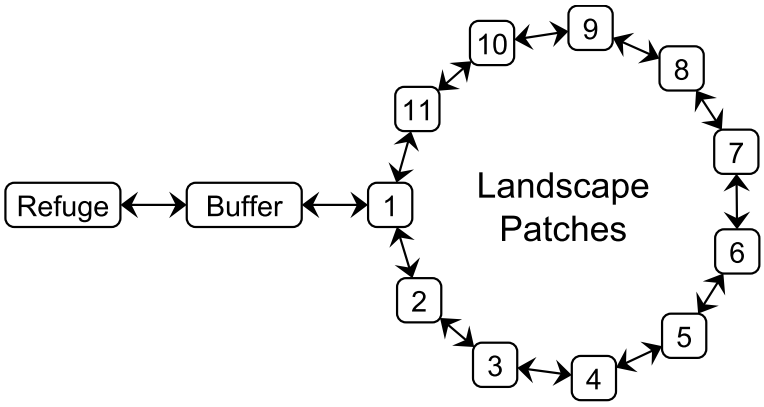

Figure 5.3 A schematic representation of the spatial stochastic model involving refuge, buffer zone and landscape patches.

connectivity between the buffer zone and the landscape. We also assess the effect of varying habitat suitability, for squirrels, within the buffer zone.

- Management strategies

  Grey squirrel control is a common management strategy used in red squirrel refuge and buffer zones. We analyse the effect of two different control strategies on red squirrel populations within refuges.

5.3 Results

Baseline scenario

We will initially consider a baseline scenario in which no conservation strategies are applied. To allow comparison with the Formby refuge, the red carrying capacity is taken to be 1125 and grey carrying capacity 1500 (Whitfield, 2008). The disease transmission rate is determined using the methods outlined in Chapter 4. Following a comparison of simulations using a range of spatial parameters, a spatial parameter of 0.2 has been chosen as a baseline as this corresponds to a value that allows grey squirrel and disease persistence in the spatial model. All other parameters are the same as those used by Tompkins *et al.* (2003) and can be found in table 4.1. As in Chapter 4, we carry out a default number of 10,000 simulations in each scenario. The initial conditions consist of the reds alone, at their carrying capacity, in the refuge and buffer zone and the greys at "realistic" endemic levels, across the landscape. Our work in Chapter 4 suggested squirrelpox persists, amongst the greys, by spreading in waves across the landscape. To allow us to capture these waves within the initial conditions, we ran a grey-only simulation in the 11 landscape patches for a long time period (a spin-up phase). The final densities of susceptible, infected and recovered greys in each patch were recorded and used as initial conditions for the baseline scenario.

In the baseline scenario, the susceptible and recovered greys disperse into the buffer zone almost immediately, with a squirrelpox epidemic occurring amongst the reds within a year. The invasion of greys and the squirrelpox epidemic result in the reds being replaced by the greys, in the buffer zone, within five years (we ran multiple simulations, figure 5.4b plots a simulation with representative behaviour). A similar pattern is observed in the refuge, however the presence of the buffer zone delays the process meaning the invasion, squirrelpox epidemic and replacement occur later (figure 5.4). The reds are replaced and the greys establish themselves, within the refuge and buffer zone, with squirrelpox at endemic levels (figure 5.4). Thus, in a situation with no intervention our model predicts that the reds would be replaced (as they have been in most regions

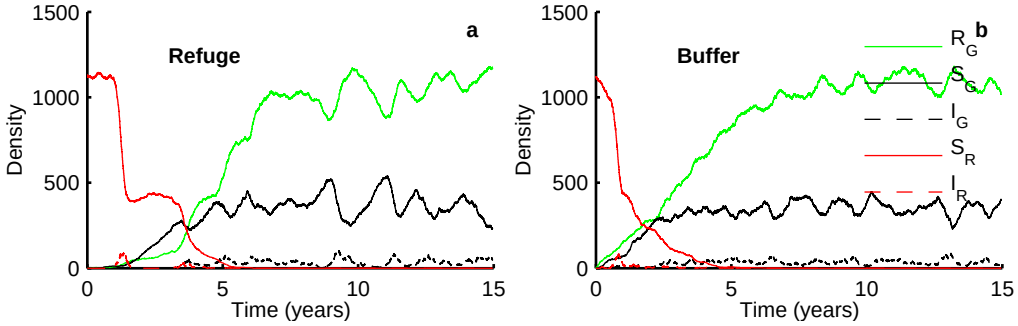

Figure 5.4 Population densities in refuge and buffer with no conservation strategies in place (baseline scenario). Panel **a** shows the densities in the refuge and panel **b** the densities in the buffer zone from. The carrying capacities are set as $K_R = 1125$ and $K_G = 1500$ with a spatial parameter of 0.2. All other parameters are identical to those used by Tompkins *et al.* (2003) and can be found in table 4.1. The initial conditions are the reds alone in the refuge and buffer zone and the greys at a pseudo endemic level across the landscape (obtained from a grey-only simulation involving only the landscape patches). This single realisation is representative of behaviour seen in the majority or simulations.

of the UK).

5.3.1 Buffer zone characteristics

The characteristics of the buffer zone, will have a great effect on the success of the refuge in protecting the red squirrels. We will investigate three different factors:

- The connectivity of the buffer zone, will affect grey dispersal rate into the buffer zone and hence the refuge. We expect low connectivity to have a positive effect on the red squirrel population densities within the buffer zone and refuge.
- It is a common conservation policy, for the buffer zone to provide an unsuitable habitat for squirrels (both red and grey). An example of this would be a buffer zone consisting of farmland or urban areas.
- If the buffer zone contains woodlands, an alternative conservation strategy is to provide a habitat suitable for red squirrels but unsuitable for greys. This could be implemented by, woodland management within the buffer zone, ensuring only tree species favouring red squirrels are planted.

Connectivity

The connectivity of the buffer zone, affects the dispersal of the squirrels from the landscape to the buffer zone and vice versa. If the connectivity is lowered between the buffer zone and the rest of the landscape, we expect to observe less invasions by the greys. The connectivity of the

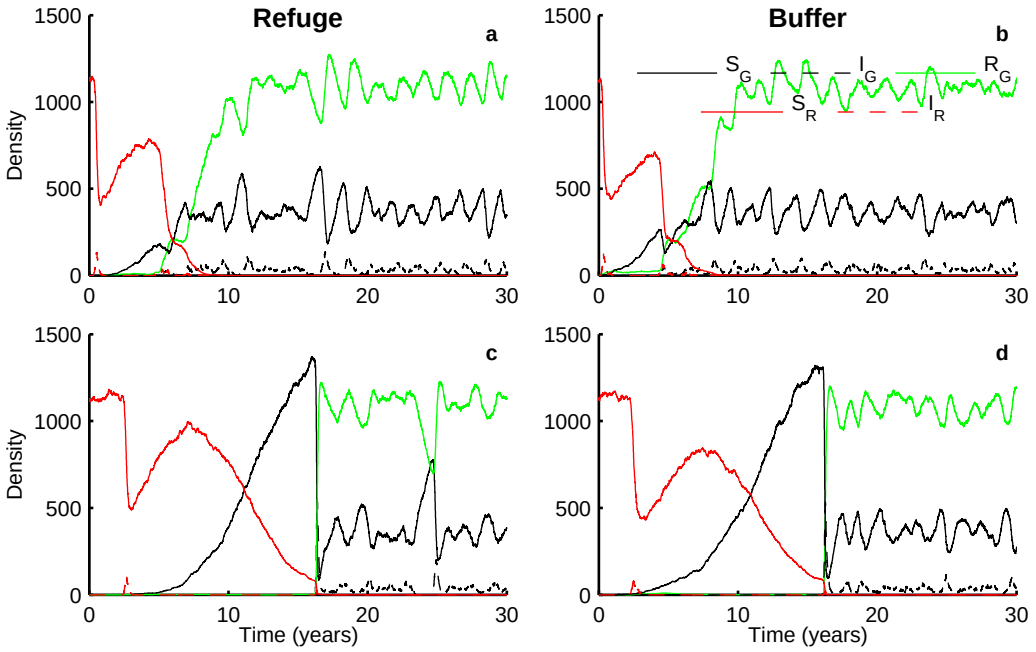

Figure 5.5 Population densities within refuge and buffer zone with lowered connectivity between buffer zone and landscape. Panels **a** and **c** show the densities in the refuge and panels **b** and **d** the densities in the buffer zone. The probability of dispersal between the buffer zone and landscape is lowered from 0.2 to 0.02 in panels **a**–**b** and 0.002 in panels **c**–**d**. All other parameters and initial conditions are identical to the baseline scenario (figure 5.4). This single realisation is representative of behaviour seen in the majority or simulations.

buffer zone is lowered, by reducing the probability of dispersal between the buffer zone and the landscape.

A reduction in the connectivity of the buffer zone reduces the number of attempted invasions, from the landscape, by the greys and hence outbreaks of squirrelpox. Figure 5.5a–b shows densities of the red and grey populations, in the refuge and buffer zone, following a reduction in the connectivity to 10% of its previous level. There are two outbreaks of squirrelpox within the buffer zone, and consequently the refuge, resulting in large reductions in the red populations. Squirrelpox dies out, following the first epidemic, as there are insufficient greys to sustain squirrelpox. However, following the second outbreak the grey population has increased to sufficient levels to allow squirrelpox to remain at endemic levels within the population and the reds do not recover. This reduction in connectivity protected the reds for a further 4 years (see figure 5.5a–b).

A further reduction in the connectivity, to 1% of its original connectivity, protects the reds for a longer period (figure 5.5c–d). The lower the connectivity, the longer the red population in the refuge will be protected. Regardless of the length of protection, the result is always replacement of the reds by the greys. The only exception to this, is if there is no connectivity between the buffer zone and the landscape (for example an island, with no entry method for the greys or squirrelpox).

Reduced habitat suitability in the buffer zone

We next consider the effect of a reduction in the habitat suitability for (*i*) both red and grey squirrels and (*ii*) grey squirrels only in the buffer zone. To represent a reduction in habitat suitability, we lower the carrying capacities within the buffer zone. In (*i*) we reduce both carrying capacities by 75% to give $\widetilde{K_R} = 0.25K_R$ and $\widetilde{K_G} = 0.25K_G$ (figure 5.6a–b). While, in (*ii*) we use the original red carrying capacity and reduce the grey carrying capacity by 75% to give $\widehat{K_R} = K_R$ and $\widehat{K_G} = 0.25K_G$ (figure 5.6c–d).

(*i*) There is no epidemic observed in the buffer zone when habitat suitability of both reds and greys is reduced. The greys and squirrelpox enter the buffer zone almost immediately and replacement of the red population occurs within 12 years (figure 5.6b). However, there is an epidemic observed within the refuge resulting in a rapid decline of the red population and a replacement of the red population in approximately 11 years (figure 5.6a).

(*ii*) A reduction in habitat suitability for the grey squirrels sees the initial large population of red squirrels in the buffer zone suffer a decline following a squirrelpox epidemic (figure 5.6d). This squirrelpox outbreak spreads into the refuge, causing an epidemic and rapid decline in the red and grey populations. However, squirrelpox does not persist within the grey population until there is a second epidemic approximately 5 years later. The reds are replaced within the refuge within approximately 12 years and the buffer zone within 15 years (figure 5.6c–d).

A reduction in habitat suitability within the buffer zone, for red and grey squirrels or greys only, greatly reduces the influx of greys but squirrelpox will always invade unless the carrying capacity is reduced to very low levels. If the carrying capacity is reduced to zero, we create a disconnected refuge with similar results as the disconnected buffer zone described above. In both cases, if the buffer zone provides a harsher environment than that of the refuge, the number of attempted invasions is decreased leading to protection for the red squirrel population in the refuge. A buffer zone consisting of no trees, for example agricultural fields or urban environments, would provide a harsh environment for both reds and grey squirrels. If the forestry, within the buffer zone, is managed to provide trees preferable to reds but not greys, a harsh environment for greys is created.

All the strategies considered here that relate to the buffer zone characteristics fail to protect the red population within the refuge. They act to reduce the amount of invasions of greys into the refuge, by limiting connectivity or restricting the pool of potential dispersers. This prolongs the time in which the reds can be maintained in the refuge but cannot ultimately prevent their replacement.

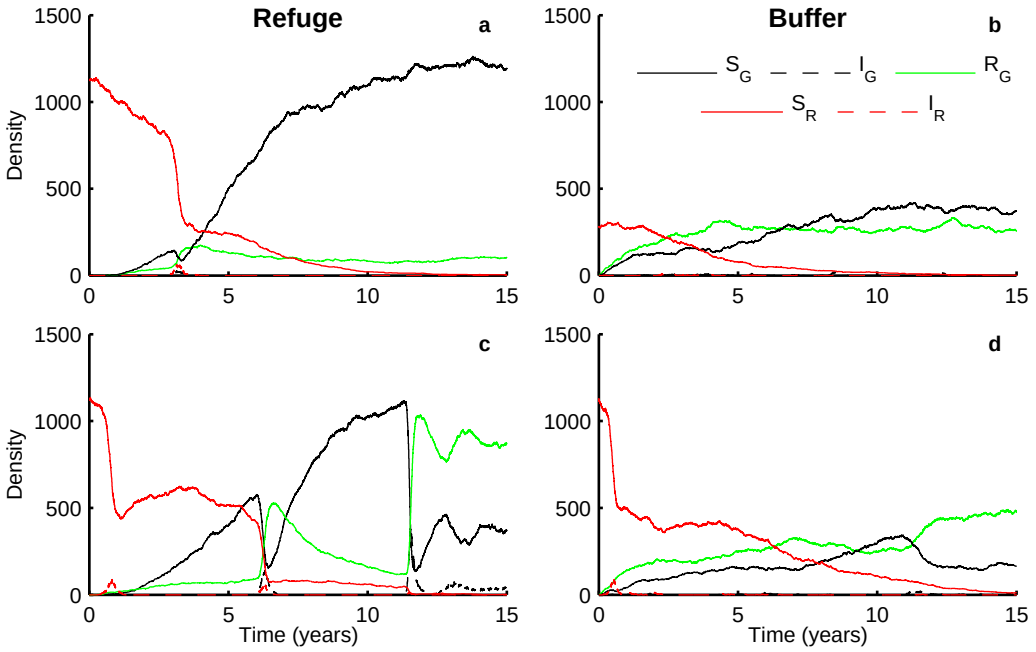

Figure 5.6 Population densities in refuge and buffer zone with reduced habitat suitability for squirrels in the buffer zone. In panels **a**–**b** the carrying capacity of the reds and greys, in the buffer zone, are reduced by 75% ($\widetilde{K_R} = 0.25K_R = 281$ and $\widetilde{K_G} = 0.25K_G = 375$). In panels **c**–**d** the carrying capacity of greys, in the buffer zone, is reduced by 75% ($\widetilde{K_R} = K_R = 1125$ and $\widetilde{K_G} = 0.25K_G = 375$). All other parameters and initial conditions are identical to the baseline scenario (figure 5.4). This single realisation is representative of behaviour seen in the majority or simulations.

5.3.2 Management strategies

A common strategy employed within red squirrel refuges and buffer zones is the culling of grey squirrels. We will investigate the effectiveness of two culling strategies: (*i*) culling the greys at given points in time and (*ii*) culling them when their population reaches a certain level. In both (*i*) and (*ii*) the parameters are identical to those used in the baseline scenario, except we include a culling strategy. In (*i*) we reduce the grey population in the refuge and buffer zone by a given proportion twice each year. We examine the effectiveness of this control measure and compare different culling proportions. Grey squirrel culling is carried out in the refuge and buffer zone at Formby twice a year White (2009b).

If all the greys in the buffer zone and refuge are culled twice a year, the red population in the buffer zone and refuge is protected. The refuge and buffer zone still suffer from squirrelpox outbreaks, but manage to recover; in our representative simulation we see four epidemics within the refuge and at least seven within the buffer zone (figure 5.7 a–b). Similar results are seen for culling levels of 90% and 50%, although the level of greys in the refuge is greater with 50% culling (figure 5.7 c–f). If the level of culling is lowered to 25%, the refuge and buffer zone are protected for a prolonged period but not indefinitely and the greys invade and replace the reds (figure 5.7

g–h). Therefore, culling twice a year can protect the red squirrel population within the refuge if carried out at sufficient levels and continued indefinitely.

The second culling strategy, (*ii*), instruments culling whenever the grey population, within the buffer zone reaches a given level. This given level is a percentage of the grey carrying capacity and denoted by $\overline{K_G}$ (for example, if we are considering a given level of 50%, $\overline{K_G} = 0.5K_G$). If the total grey population within the buffer zone reaches this level, $\overline{K_G}$, a proportion of the grey population in the refuge and buffer zone is culled (if $S_G + I_G + R_G \geqslant \overline{K_G}$ then S_G, I_G and R_G are all reduced). This strategy simulates the culling of greys when they become visible in the buffer zone.

If 20% of the greys in the refuge and buffer zone are culled whenever the grey population reaches 10% of its carrying capacity ($\overline{K_G} = 0.1K_G$), the red population is protected from replacement by the greys. The greys have to be repeatly culled within the buffer zone but the reds in the buffer zone are not replaced by the greys. However, squirrelpox is present and they suffer from many small declines but always recover (figure 5.8b). As a result of this culling there are only a low number of greys observed within the refuge. The red squirrel population within the refuge is protected from grey replacement but not outbreaks of squirrelpox; the population suffers from rapid declines after each outbreak but then manages to recover (we observe four such declines and recoveries within 30 years in figure 5.8a). If the proportion of the grey population culled is increased or decreased from 20%, we see a very similar pattern within the buffer zone and refuge. However, the larger the proportion culled, the shorter the time period between necessary culls.

An increase in the level determining culling, ($\overline{K_G}$), reduces the effectiveness of this control measure. If the level is increased to 50%, $\overline{K_G} = 0.5K_G$, the reds are no longer protected from replacement (figure 5.8c–d). An initial epidemic followed by a rapid decline in red squirrels allows replacement by the greys within the buffer zone. The squirrelpox outbreak spreads into the refuge and again causes a rapid decline of reds followed by replacement by the greys. Although, the greys continue to be culled, the reds never manage to recover. This culling strategy can protect the population of red squirrels within the refuge and buffer zone, but it must be carried out at suitable levels.

Culling, using either strategy, can result in the red squirrel population in the refuge and buffer zone being protected from grey invasion. However, they will not be protected from squirrelpox, with the buffer zone suffering from more outbreaks, but they should recover if culling is carried out at sufficient levels. If the culling is carried out at given time intervals, there will be a minimum required threshold to ensure success. If the culling is carried out whenever the grey populations reaches a certain level ($\overline{K_G}$) there is a minimum threshold for the level, and the higher the proportion culled the less frequently the culling will need to be carried out. Theoretically, either strategy

will be effective if carried out at the required levels but in practice culling twice a year is more manageable.

5.4 Discussion

This chapter examined some of the common strategies employed in planning and managing red squirrel refuges in the UK. Our model is based on the Sefton Coast Woodlands National Squirrel Refuge and Buffer Zone at Formby, Merseyside but can be applied to general refuge strategies. We initially examined a baseline scenario, with no conservation strategies in place, and observed squirrelpox spreading through the buffer zone and refuge causing rapid declines in the red populations followed by replacement of the red squirrels by greys. We compared the following design and management strategies to the baseline scenario to examine their effectiveness:

- Buffer zone characteristics

  We considered three different buffer zone characteristics to assess their influence on protecting the red squirrel population in the refuge from grey replacement and disease. The effect of reduced connectivity, reduced habitat suitability in the buffer zone for both the red and grey squirrels and reduced habitat suitability for greys. All three approaches prolonged the time the red squirrels were maintained in the refuge, but none of them protected the reds indefinitely unless the refuge was completely isolated from the landscape (was effectively an island). In each scenario, the red squirrels suffered rapid declines as a result of squirrelpox outbreaks, followed by replacement by the greys.

- Management strategies

  The two management strategies we considered involved culling grey squirrels in the refuge and the buffer zone. We examined culling a proportion of the grey squirrels in the refuge and buffer zone twice a year and culling when the population of grey squirrels in the buffer zone reached a certain level. Both control strategies can protect the red squirrel population within the refuge, but in both cases there is a minimum level of effort required and the culling must continue indefinitely. Although, culling of greys at sufficient levels protects the red squirrel populations from replacement, they suffer repeated squirrelpox outbreaks but manage to recover.

Except for extreme strategies (full continual culling, isolation of the refuge) no single strategy could protect the red population in the refuge from periods of population decline. If a refuge and buffer zone is completely disconnected or isolated from any surrounding grey squirrel populations, it will be protected indefinitely. There is evidence to support this in the UK, as the only

remaining populations of red squirrels in Southern England are found either on islands or in areas isolated from greys (Kenward and Holm, 1993). The Isle of Wight is one of these last remaining strongholds, and recognised as a priority area for red squirrels in the UK. The Isle of Wight is a small island 3km off the South coast of England, and boasts an estimated summer population of 3,330 red squirrels (Harris *et al.*, 1995; Pope and Grogan, 2003).

It is widely acknowledged that this isolated population of red squirrels have survived because there are no greys on the island. An accidental or deliberate introduction of grey squirrels to the island is regarded as the greatest threat to the Isle of Wight red squirrel population. This is not only because of squirrelpox but it is also feared grey squirrels would replace the reds very quickly as a result of the habitat on the island being better suited to greys than reds (Rushton *et al.*, 1999). As a result of this threat, English Nature, Forestry Commission and Isle of Wight Council have formed a "Grey Squirrel Contingency Plan" in case of any grey squirrel sightings on the island (Pope and Grogan, 2003). The contingency plan was put into operation in 2002, with the help of Wight Squirrel Project, Wight Wildlife and Forest Enterprise, following a grey squirrel corpse being found on the island in July 2001, and three further sightings in 2002. The emergency measures include trapping and humanely killing greys, monitoring using hair tubes and public awareness campaigning. The contingency plan in 2002, or "Operation Squirrel" as it became known, did not find any more greys on the island and concluded there was no resident grey squirrel population (Isle of Wight Council, 2002). The contingency plan is an ongoing initiative, and reviewed regularly as part of the "Isle of Wight Biodiversity Action Plan", to ensure all required measures can be carried out quickly if needed (Pope and Grogan, 2003).

Unlike the Isle of Wight, the red squirrel refuge and buffer zone at Formby is not isolated from surrounding greys and as a result has suffered from disease outbreaks and invasions (Whitfield, 2008). The Formby buffer zone characteristics consist of natural reduced connectivity due to the shoreline but not isolation (see figure 5.1). The buffer zone offers habitat with reduced suitability for both red and grey squirrels as it consists of woodland, agricultural and urban areas. There are grey squirrels in the buffer zone and refuge; a management strategy is in place involving culling of grey squirrels twice a year (in 2002–2004, 118 grey squirrels were culled while it is estimated approximately 500 were present in the refuge and buffer zone (Whitfield, 2005)).

The red squirrel population in the refuge, at Formby, suffered rapid declines in 2003, 2007 and 2008 as a result of squirrelpox outbreaks (White, 2009b). The population showed signs of recovery following the declines in 2003 and is believed to recovering following the later outbreak with no new cases of squirrelpox recorded between December 2008 and July 2009 (White, 2009a). This is analogous to our findings when considering the management strategy of culling twice a year (see

figure 5.7). The red squirrel population within the refuge is protected from grey replacement but it suffers and recovers from repeated squirrelpox outbreaks. Our results, closely match the observed pattern of population densities observed in Formby (see figures 5.2 and 5.7). If the current culling strategy is continued indefinitely, the reds within the refuge should be protected from replacement by the greys but will continue to suffer from periodic outbreaks of squirrelpox resulting in low densities of reds within the refuge.

Our results, when considering grey culling twice a year, showed that culling levels above 50% are effective at protecting the red squirrels within the refuge from replacement but not squirrelpox outbreaks. This agrees, in principal, with Rushton *et al.* (2006)'s results, that suggest a grey squirrel control strategy using a cull level of 60% would have prevented the decline of red squirrels within Cumbria. Although it is diffficult to compare our findings accurately as it is not clear from their paper which culling strategy they were modelling. Our results also show that an increase from 50% to 90% or 100% has little effect on the length of time between squirrelpox epedemics within the refuge (see figure 5.8). Therefore, an increased effort will not neccesarily provide better protection for the red squirrels within the refuge.

We have not considered, here, the effect of supplementary feeding that occurs at Formby, this supplementary feeding could act to increase the carrying capacity of red squirrels within the refuge. Although, it could also increase the carrying capacity of the grey squirrels if they have access to the food or steal it from a red squirrel cache. Supplementary feeding could potentially increase the spread of squirrelpox if both red and grey squirrels are present. Following a study at Formby, it is recommended that any supplementary feeding programmes are accompanied by grey control strategies Shuttleworth (2000).

This chapter not only offers insight into the refuge and buffer zone at Formby, the results can be extended to consider other refuge and buffer zones. It not only reminds us of the importance of squirrelpox in the replacement of red squirrels by greys, it also shows the difficulty in trying to protect red squirrels within refuge and buffer zones from it. Squirrelpox is a major factor in the replacement of reds when we consider different buffer characteristics (see figures 5.5 and 5.6). Management strategies can protect the red squirrels from replacement by the greys but it cannot protect them from squirrelpox (see figures 5.7 and 5.8). Therefore all refuges, except those isolated from all surrounding populations, are constantly at risk of a squirrelpox outbreak. This difficulty in protecting red populations from squirrelpox needs to be considered in all conservation strategy planning for red squirrel refuges in the UK.

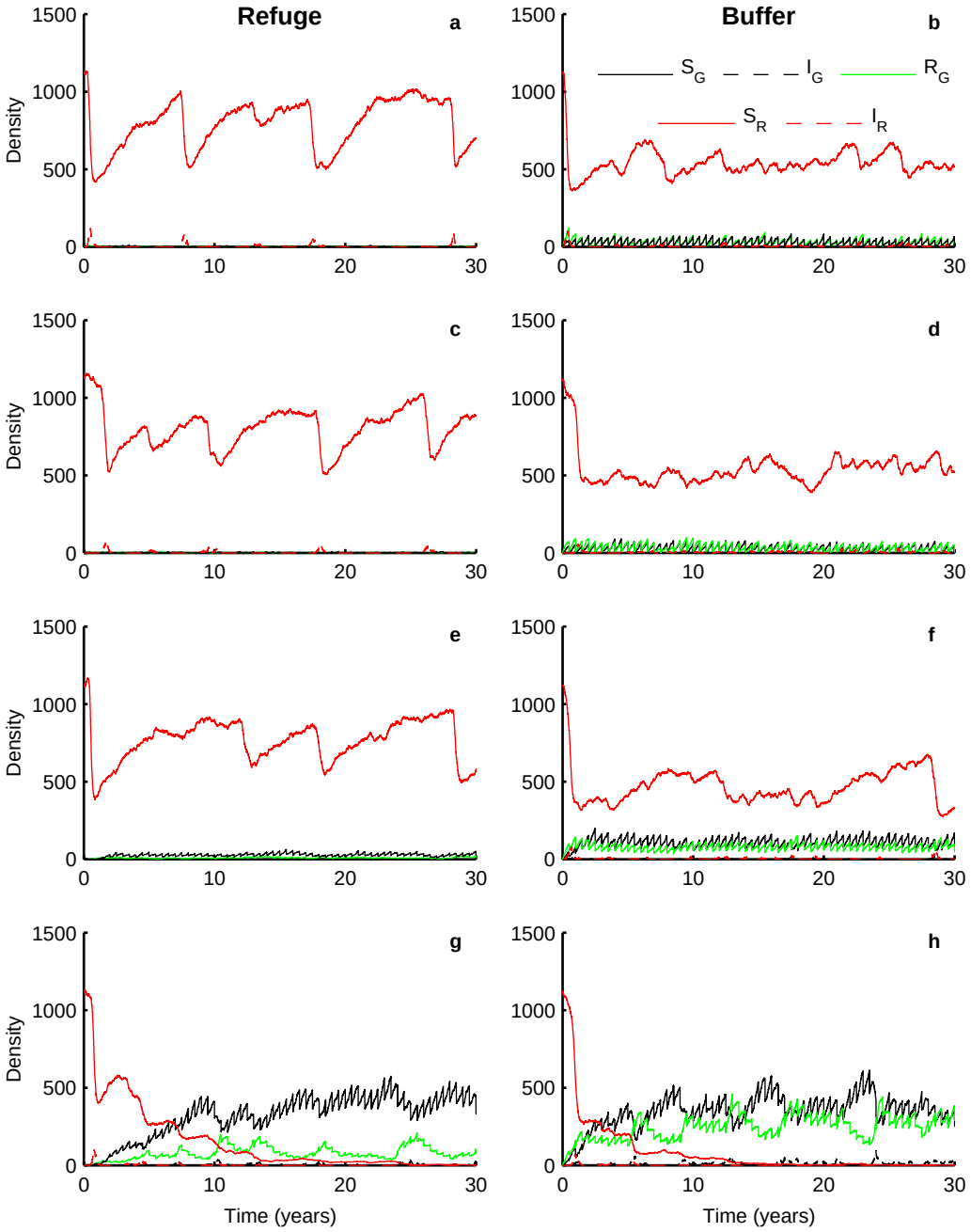

Figure 5.7 Refuge and buffer zone, with management strategy of culling 100% (panels **a**–**b**), 90% (panels **c**–**d**), 50% (panels **e**–**f**), 25% (panels **g**–**h**) of greys, in both buffer zone and refuge, twice a year. All parameters and initial conditions are identical to the baseline scenario (figure 5.4). This single realisation is representative of behaviour seen in the majority or simulations.

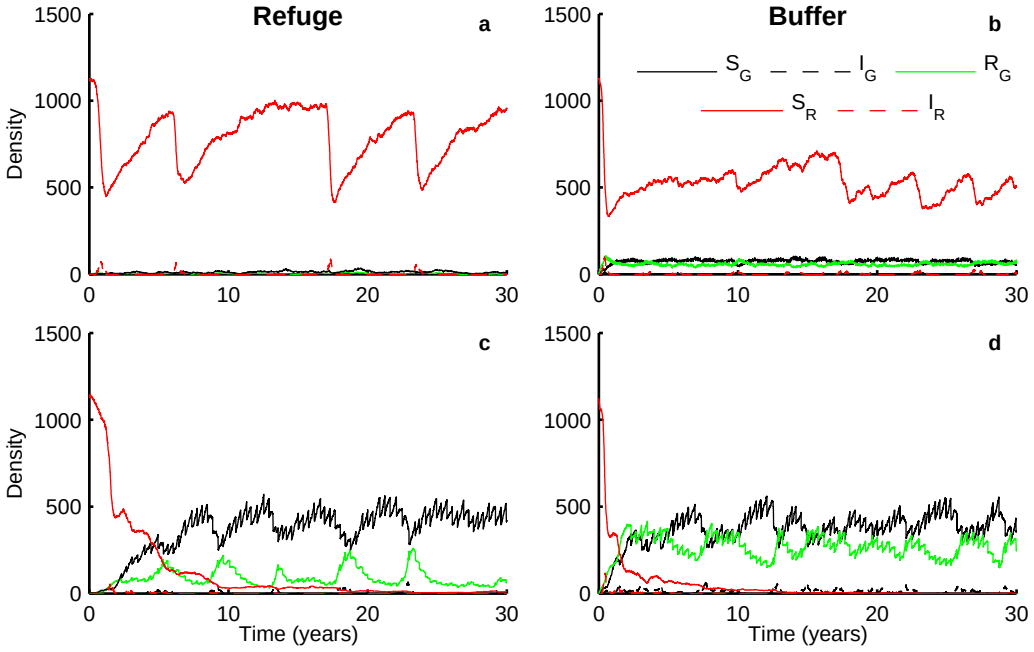

Figure 5.8 Population densities in the refuge and buffer zone, with culling occurring when the total grey population reaches 10% (panels **a**–**b**) and 50% (panels **c**–**d**) of K_G, in buffer zone. Culling is being carried out in both the refuge and buffer zone and 20% of all greys present are being removed. All parameters and initial conditions are identical the baseline scenario (figure 5.4). This single realisation is representative of behaviour seen in the majority or simulations.

Chapter 6

Discussion

This thesis has aimed to broaden our theoretical understanding of the role of disease, combined with competition, in ecological invasions. The effect of disease on ecological invasions is widely recognised, although our theoretical knowledge on the underlying effects of disease is still lacking (Prenter *et al.*, 2004). The need for a deep understanding of ecological invasions is not only driven by their adverse effects on native biodiversity, community structure and ecosystem function but also their economic repercussions (Sala *et al.*, 2000; Kolar and Lodge, 2001).

6.1 The impact of disease on ecological invasions

The first main objective of this thesis was to use mathematical models to help understand the spread of disease in invasive systems. We set up a continuous time deterministic model in Chapter 2 to address this objective, with a focus on situations where the disease acts as a "biological weapon". Our modelling framework was based on classical competition (Lotka-Volterra) and epidemiological (Anderson and May) modelling frameworks, and allowed us to analyse the effect of different disease parameters on the replacement time of a native by an alien invader.

We analysed the effect of disease-induced fecundity loss, additional mortality through disease and recovery from disease. Our findings showed a shared disease passed from an alien to a native species does not always have beneficial effects on the attempted invasion. If the disease has a similar effect on both species, it will not decrease the replacement time and in many scenarios it will increase the replacement time compared to when the disease is not present. The invader must have a sufficient relative advantage over the native species for the disease to be beneficial to the invader.

Our work is focussed on invasion and the effect on replacement time and this sets our work apart from previous studies that focus on a steady-state and stability analysis (Holt and Pickering,

1985; Begon *et al.*, 1992; Bowers and Turner, 1997). Holt and Pickering (1985) described a disease-only model with two species and a shared disease, and identified that the exclusion of one species by another may occur as a result of a difference in tolerance to a shared disease. They further defined this higher tolerance to the disease as potentially resulting from "their faster recovery, lower death rates, or higher reproductive rates" (Holt and Pickering, 1985). Our work is in agreement with the findings of Holt and Pickering (1985) – and also the study of Begon *et al.* (1992) who additionally include intraspecific competition – but our study additionally includes the effect of interspecific competition between species. We also highlight the key result that the invader must possess a sufficient relative advantage, over the native species, for disease to enhance the replacement process.

Our work also builds on the study of Bowers and Turner (1997) who consider intraspecific competition, interspecific competition and disease since our model additionally includes fecundity loss as a result of disease. Their study focuses on the conditions for coexistence of the two species with the disease whereas our focus is on the effect of disease on replacement time.

Our modelling framework has added to the knowledge of the underlying parameters affecting the replacement of native species. It is a very flexible framework and can be used to examine individual case-studies including SI and SIS frameworks, lethal and non-lethal diseases, a castrating parasite or a disease which has no effect on the fecundity of infected individuals. This flexibility allows the examination of a wide range of ecological examples, allowing us to increase our theoretical understanding of invasion, competition and disease dynamics within an ecosystem.

We discussed a selection of ecological examples in Chapter 2; examined how our model would relate to them and compared this to evidence from the literature. These examples included: (1) the effect of squirrelpox on the replacement of red squirrels by greys in the UK, (2) the effect of crayfish plague on the replacement of white-clawed crayfish by introduced North American signal crayfish and (3) the replacement of the UK's native pedunculate oak by the introduced Turkey oak. We showed in each of the examples how our modelling framework can help inform our understanding of the invasion process.

Although this work offers good insight into the effect of disease on the replacement time of a native by alien species, it offers no insight into the spatial effects. This leads us to our next objective, which is to extend the work to include the effects of space and compared our findings to the temporal results.

6.2 The spatial spread of invading species

The temporal findings of Chapter 2 are extended to include spatial effects by considering random movement in the form of diffusion. Such systems of reaction-diffusion equations have a long history in modelling movement in ecological systems that include competition and/or infectious diseases (for example Murray (2002); Cantrell and Cosner (2003); De Vries *et al.* (2006) all give excellent introductions to the subject).

Our findings showed that the temporal and spatial models have similar properties; if the disease caused the temporal replacement time to slow, it would also cause the spatial spread to slow. Conversely, if the disease hastened the temporal replacement, it also hastened spatial replacement. In the absence of disease there was one wave of replacement spreading across the landscape transforming the population from the native carrying capacity, in front of the wave, to the alien carrying capacity behind. When the disease was present, we observed two waves, a wave of disease spreading across the landscape transforming the population from the native carrying capacity to the native at endemic levels. This was followed by a wave of replacement transforming the population from the native at its endemic levels to the alien at its endemic levels.

The wave of replacement occurring behind the wave of disease is an important finding that had not been reported in other studies. It increases our understanding of the replacement of native species by alien invaders and highlights the subtle impact of disease. This phenomenon occurs regardless of whether disease increased or decreased the temporal and spatial replacement time and may be wrongly overlooked or discounted as a contributing factor to the replacement of a native species. This is the case with red squirrels in the UK, squirrelpox was discounted as a contributing factor to their replacement by greys in East Anglia as diseased red squirrels were found well in advance of the greys (Reynolds, 1985). In fact, the observation of disease may act as an early warning of imminent invasion. We also examined the effect of disease on the spatial dynamics and disease can allow an invader to increase the range of its spatial spread. These are important findings when considering the conservation implications of ecological invaders and show disease must not be ignored as a factor in invasion success, speed and spatial range.

There is scope to extend the mathematical analysis of the spatial results in our study and in particular to gain a better understanding of the disease and replacement waves. This could also include relaxing the assumption that susceptible and infected individuals disperse at the same rate. These findings would have general implications for the spatial spread of disease in interacting species.

Chapters 2 and 3 studied general theoretical frameworks, and we wish to use the frameworks and insights gained here as a baseline from which to consider the specific ecological system of the

invasion and replacement of red squirrels by greys.

6.3 Red squirrels, grey squirrels and squirrelpox

The third main objective of this thesis was to develop a red/grey/squirrelpox model to allow investigation into different conservation and management strategies. To do this, we extended the continuous-time frameworks examined in Chapters 2 and 3 (and in Tompkins *et al.* (2003)) and developed an individual-based, probabilistic model of the UK squirrel population.

The probabilistic model allowed us to examine the effect of stochasticity, and the chance of persistence of the disease at low endemic levels in the red/grey/squirrelpox system. A direct analogue of the Tompkins *et al.* (2003) model did not allow disease persistence; spatial structure in the form of a set of linked sub-populations was required to allow disease persistence (see Chapter 4 for a discussion and related literature). Following the inclusion of this metapopulation structure, the results from the probabilistic model are in agreement with the findings of Tompkins *et al.* (2003). The probabilistic model displayed the key result of squirrelpox reducing replacement time for the grey squirrel and also indicated that a wave of disease would spread ahead of a wave of replacement. This highlights the importance of deterministic models as a key to increasing our theoretical knowledge and understanding of ecological systems.

The red squirrel has been replaced throughout much of the UK, as a result there are a range of conservation and management strategies in place. The development of this stochastic model framework allowed us to model and examine the effectiveness of these strategies within a red squirrel refuge.

6.4 Red squirrel conservation

The final objective of this thesis was to evaluate the effectiveness of current conservation and management strategies that are used to protect remaining populations of red squirrels. We developed a modelling framework that encompassed the refuge, buffer zone and wider population using the spatial probabilistic framework developed in Chapter 4. The framework was developed to incorporate some of the key properties of a red squirrel refuge in Formby, Merseyside.

We considered a range of different strategies employed in the red squirrel refuges within the UK to examine their effectiveness at maintaining red squirrel numbers. Buffer zones of "unfavourable" habitat around red squirrel refuges have been suggested as a way of protecting red populations (Forestry Commision Scotland *et al.*, 2006). Our study indicates that such buffer

zones alone cannot protect the refuge from invasion of grey squirrels unless buffer zones are so "harsh" that they fully isolate the refuge. We evaluated the replacement of red squirrels and found buffer zones can slow down the replacement of reds within the refuge.

Another strategy that is employed is the culling of grey squirrels in the refuge and buffer zone (Rushton *et al.*, 2006). Providing the culling effort exceeds a threshold (and is maintained periodically) it can be effective at protecting the red population in the refuge. Such culling protects the red population, in the refuge, from replacement but does not protect the reds from infection. Our model predicts the reds will suffer from regular outbreaks of squirrel pox in the refuge. This is analogous to observations at Formby where a culling strategy is employed and the the red population has exhibited several population crashes as a result of squirrel infection (Burkmar, 2006; Whitfield, 2008; White, 2009a,b). Out theoretical study indicates that it is difficult to impose a conservation strategy that will prevent disease outbreaks in the refuge.

We compared our results to those of Rushton *et al.* (2006), whose findings suggested that a 60% culling level would have prevented the decline of red squirrels within Cumbria. It is difficult to compare our findings as their strategy is not explained in detail; however, we found that cull levels above 50% are effective controls against replacement when culling twice a year. Our results are similar, although we further build on this by showing that an increase in the culling level above 50% has little effect on the period of time between suirrelpox outbreaks and is therefore not neccesary.

Although, this model is based on the red squirrel refuge and buffer zone in Formby, its results are useful when considering red squirrel refuges in general and could easily be adapted to another specific site. There are potential extensions to this work including the investigation of supplementary feeding of the reds, vaccination of the reds and sterilisation of the greys. Another conservation strategy not discussed here but being considered as an option, within refuges and buffer zones, is the culling of any diseased reds or reds found in the vicinity of a confirmed squirrelpox case. This could also be included as an extension to our work and the results would be useful in examining the usefulness of this strategy as a conservation tool.

The model could also be adapted for other species, we know of a similar example involving the replacement of white-clawed crayfish throughout the UK by North American signal crayfish. The native species suffers as a result of a shared disease (crayfish plague), while the invading species is resistant to it (Holdich, 2003; Bubb *et al.*, 2004). This framework may be adaptable to the crayfish example by considering an individual watercourse, as opposed to a refuge, and its connecting sites.

6.5 The future of red squirrels in the UK

It is estimated that 75% of Britain's remaining red squirrels are found in Scotland (Harris *et al.*, 1995; Battersby and Partnership, 2005). The Scottish population is threatened by replacement from greys spreading North from England and through released populations in the Central Belt and Aberdeen City. It is believed the Scottish population will be replaced in the next 50–100 years if measures are not taken to stop the spread of greys (Forestry Commision Scotland *et al.*, 2006).

Our spatial spread model described in Chapter 3 gives insight into the spread of disease ahead of an invading species and also the potential increase in spatial range as a result of disease. This is of major importance in the planning of conservation measures for Scotland. If the grey squirrels have been kept out of Scotland as a result of differences in habitat, squirrelpox may allow them to invade. Hence, it is important to either stop the spread of squirrelpox through Scotland or to ensure the wave of replacement, behind, is halted. It may be possible to halt the wave of replacement using culling as shown, for a refuge, in Chapter 5.

A potential extension to our work described in Chapters 4 and 5 would be to adapt our refuge model to investigate the spread of grey squirrels into and through Scotland. The stochastic modelling framework described in Chapter 4 could be used as a basis for a larger model to analyse the situation in Scotland as a whole with particular consideration to natural corridors available to the greys for dispersal. There are currently some conservation efforts in place including a consultation to identify squirrel strongholds. The design of these strongholds could be greatly improved if theoretical models, similar to the model described in Chapter 5, were used to examine the effectiveness of different sites and relevant conservation and management strategies available.

It is essential that conservation strategies continue to be implemented to try and protect the UK's remaining red squirrels. Theoretical modelling techniques, like those described in this thesis, can help find the most beneficial conservation strategies and ensure the best use of skills, time and money. The use of theoretical modelling can not only help us plan the conservation of red squirrels but can also be extended to other animals suffering from the threat of an alien invader.

REFERENCES

Aliabadi, B. W. & Juliano, S. A. (2002). Escape from gregarine parasites affects the competitive interactions of an invasive mosquito. *Biological Invasions*, 4: 283–297.

Anderson, R. C. (1972). The ecological relationships of meningeal worm and native cervids in North America. *Journal of Wildlife Diseases*, 8: 304–310.

Anderson, R. M., Jackson, H. C., May, R. M. & Smith, A. M. (1981). Population dynamics of fox rabies in Europe. *Nature, London*, 289: 765–771.

Anderson, R. M. & May, R. M. (1978). Regulation and stability of host-parasite population interactions: I. regulatory processes. *Journal of Animal Ecology*, 47(1): 219–247.

Anderson, R. M. & May, R. M. (1981). The population dynamics of microparasites and their invertebrate hosts. *Philosophical Transactions of the Royal Society of London. Series B*, 291(1054): 451–524.

Anderson, R. M. & May, R. M. (1991). *Infectious Diseases of Humans: Dynamics and Control*. Oxford University Press, Oxford and New York.

Battersby, J. & Partnership, T. M. (Eds.) (2005). *UK mammals: species status and population trends. First report by the Tracking Mammals Partnership*. JNCC/Tracking Mammals Partnership, Peterborough, UK.

Begon, M., Bowers, R. G., Kadianakis, N. & Hodgkinson, D. E. (1992). Disease and community structure: the importance of host-regulation in a host-host-pathogen model. *The American Naturalist*, 139(6): 1131–1150.

Begon, M., Harper, J. L. & Townsend, C. R. (1996). *Ecology*. Blackwell Science Ltd, Oxford, 3rd edn.

Bell, S. S., White, A., Sherratt, J. A. & Boots, M. (2009). Invading with biological weapons: the role of shared disease in ecological invasion. *Theoretical Ecology*, 2(1): 53–66.

Bergerud, A. T. & Mercer, W. E. (1989). Caribou introductions in Eastern North America. *Wildlife Society Bulletin*, 17(2): 111–120.

Boots, M. & Norman, R. (2000). Sublethal infection and the population dynamics of host-microparasite interactions. *Journal of Animal Ecology*, 69(3): 517–524.

Bowers, R. G. & Turner, J. (1997). Community structure and the interplay between interspecific infection and competition. *Journal of Theoretical Biology*, 187(1): 95–109.

Brauer, F. (2005). The Kermack-McKendrick epidemic model revisited. *Mathematical Biosciences*, 198(2): 119 –131.

Bryce, J. M., Speakman, J. R., Johnson, P. J. & Macdonald, D. W. (2001). Competition between Eurasian red and introduced Eastern grey squirrels: the energetic significance of body-mass differences. *Proceedings: Biological Sciences*, 268(1477): 1731–1736.

Bubb, D. H., Thom, T. J. & Lucas, M. C. (2004). Movement and dispersal of the invasive signal crayfish *Pacifastacus leniusculus* in upland rivers. *Freshwater Biology*, 49: 357–368.

Burkmar, R. (Ed.) (2006). *The North Merseyside Biodiversity Action Plan: the first five years 2001–2006*, p. 45. MERSEYSIDE Biodiversity Group.

Cannon, R. J. C., Baker, R. H. A., Taylor, M. C. & Moore, J. P. (1999). A review of the status of the New Zealand flatworm in the UK. *Annals of Applied Biology*, 135: 597–614.

Cantrell, R. S. & Cosner, C. (2003). *Spatial Ecology via Reaction-Diffusion Equations*. John Wiley and Sons, Chichester, UK.

Carroll, B., RUSSELL, P., GURNELL, J., NETTLETON, P. & SAINSBURY, A. W. (2009). Epidemics of squirrelpox virus disease in red squirrels (*Sciurus vulgaris*): temporal and serological findings. *Epidemiology and Infection*, 137(02): 257–265.

Cartmel, S. (2003). *Species Action Plan: Red Squirrel*. Denbighshire County Council, Wales.

Cerenius, L., Bangyeekhun, E., Keyser, P., Soderhall, I. & Soderhall, K. (2003). Host prophenoloxidase expression in freshwater crayfish is linked to increased resistance to the crayfish plague fungus, *Aphanomyces astaci*. *Cellular Microbiology*, 5(5): 353–357.

Cook, A., Marion, G., Butler, A. & Gibson, G. (2007). Bayesian inference for the spatio-temporal invasion of alien species. *Bulletin of Mathematical Biology*, 69(6): 2005–2025.

Daszak, P., Cunningham, A. A. & Hyatt, A. D. (2000). Emerging infectious diseases of wildlife – threats to biodiversity and human health. *Science*, 287: 443–449.

De Vries, G., Hillen, T., Lewis, M., Muller, J. & Schoenfisch, B. (2006). *A Course in Mathematical Biology: Quantitative Modelling with Mathematical and Computational Methods*. Society for Industrial and Applied Mathematics, Philadelphia.

Dobson, A. P. & Hudson, P. J. (1986). Parasites, disease and the structure of ecological communities. *TRENDS in Ecology & Evolution*, 1(1): 11–15.

Dukes, J. S. & Mooney, H. A. (1999). Does global change increase the success of biological invaders? *TRENDS in Ecology & Evolution*, 14(4): 135–139.

Fisher, R. A. (1937). The wave of advance of advantageous genes. *Annals of Eugenics*, 7: 353–369.

Foley, J., Foley, P. & Pedersen, N. C. (1999). The persistence of a SIS disease in a metapopulation. *Journal of Applied Ecology*, 36(4): 555–563.

Forestry Commision Scotland (2009). Red squirrel strongholds consultation. Available from http://www.forestry.gov.uk/strongholdsconsultation.

Forestry Commision Scotland, Scottish Natural Heritage & Scottish Executive (2006). Scottish Red Squirrel Action Plan: 2006–2011. Available from http://www.snh.org.uk/.

Greenman, J. V. & Hudson, P. J. (1997). Infected coexistence instability with and without density-dependent regulation. *Journal of Theoretical Biology*, 185(3): 345–356.

Grenfell, B. T. & Dobson, A. P. (1995). *Ecology of Infectious Diseases in Natural Populations*. Cambridge University Press, Cambridge.

Grenfell, B. T. & Harwood, J. (1997). (Meta)population dynamics of infectious diseases. *TRENDS in Ecology & Evolution*, 12: 395–399.

Gurnell, J. (1987). *The Natural History of Squirrels*. Christopher Helm, London.

Gurnell, J., Clark, M. J., Lurz, P. W. W., Shirley, M. D. F. & Rushton, S. P. (2002). Conserving red squirrels (*Sciurus vulgaris*): mapping and forecasting habitat suitability using a Geographic Information Systems Approach. *Biological Conservation*, 105(1): 53–64.

Hails, R. S. & Crawley, M. J. (1991). The population dynamics of an alien insect: *Andricus quercuscalicis* (Hymenoptera: Cynipidae). *The Journal of Animal Ecology*, 60(2): 545–561.

Hanski, I. (1998). Metapopulation dynamics. *Nature*, 396: 41–49.

Hanski, I. A. & Gilpin, M. E. (Eds.) (1997). *Metapopulation Biology: Ecology, Genetics, and Evolution*. Academic Press, London.

Harris, S., Morris, P., Wray, S. & Yalden, D. (1995). *A review of British mammals: population estimates and conservation status of British mammals other than cetaceans*. Joint Nature Conservation Committee, Peterborough, UK.

Harrison, S. & Taylor, A. D. (1997). Empirical evidence for metapopulation dynamics. In: Hanski, I. A. & Gilpin, M. E. (Eds.), *Metapopulation Biology: Ecology, Genetics, and Evolution*, pp. 27–42. Academic Press, London.

Hess, G. (1996). Disease in metapopulation models: implications for conservation. *Ecology*, 77(5): 1617–1632.

Hethcote, H. W., Wang, W. & Li, Y. (2005). Species coexistence and periodicity in host-host-pathogen Models. *Journal of Mathematical Biology*, 51(6): 629–660.

Hilker, F. M., Lewis, M. A., Seno, H., Langlais, M. & Malchow, H. (2005). Pathogens can slow down or reverse invasion fronts of their hosts. *Biological Invasions*, 7(5): 817–832.

Holdich, D. (2003). *Ecology of the White-clawed Crayfish.* Conserving Natura 2000 Rivers Ecology Series No. 1. English Nature, Peterborough.

Holt, R. D. & Pickering, J. (1985). Infectious disease and species coexistence: A model of Lotka-Volterra form. *The American Naturalist*, 126(2): 196–211.

Hoogendoorn, M. & Heimpel, G. E. (2002). Indirect interactions between an introduced and a native ladybird beetle species mediated by a shared parasitoid. *Biological Control*, 25(3): 224–230.

Hosono, Y. (1998). The minimal speed of traveling fronts for a diffusive Lotka-Volterra competition model. *Bulletin of Mathematical Biology*, 60: 435–448.

Hudson, P. & Greenman, J. (1998). Competition mediated by parasites: biological and theoretical progress. *TRENDS in Ecology & Evolution*, 13(10): 387–390.

Hudson, P. J., Dobson, A. P. & Newborn, D. (1998). Prevention of population cycles by parasite removal. *Science*, 282: 2256–2258.

Ims, R. A., Henden, J.-A. & Killengreen, S. T. (2008). Collapsing population cycles. *Trends in Ecology & Evolution*, 23(2): 79 – 86.

Isle of Wight Council (2002). Operation Squirrel. Information available from http://www.iwight.com.

Kenward, R. E. & Holm, J. L. (1993). On the replacement of the red squirrel in Britain. A phytotoxic explanation. *Proceedings of the Royal Society of London Series B*, 251(1332): 187–194.

Kermack, W. O. & McKendrick, A. G. (1927). A contribution to the mathematical theory of epidemics. *Proceedings of the Royal Society of London. Series A, Containing Papers of a Mathematical and Physical Character*, 115(772): 700–721.

Kidd, H. (2000). Japanese knotweed – the world's largest female! *Pesticide outlook*, 11: 99–100.

Kolar, C. S. & Lodge, D. M. (2001). Progress in invasion biology: predicting invaders. *TRENDS in Ecology & Evolution*, 16(4): 199–204.

Kolmogorov, A., Petrovsky, I. & Piscounoff, N. (1937). Étude de l'équation de la diffusion avec croissance de la quantité de matière et son application à un problème biologique. *Moscow University, Bulletin of Mathematics*, 1: 1–25.

Kot, M. (2001). *Elements of Mathematical Ecology*, vol. l. Cambridge University Press, Cambridge, UK.

Lancashire Wildlife Trust (2009). Sefton Red squirrels bounce back after huge decline. Available from http://www.wildlifeextra.com/go/news/sefton-squirrels.html.

Levins, R. (1969). Some demographic and genetic consequences of environmental heterogeneity for biological control. *Bulletin of the Entomological Society of America*, 15: 237–240.

Lloyd, H. G. (1983). Past and present distribution of red and grey squirrels. *Mammal Review*, 13: 69–80.

Lodge, D. M. (1993). Biological invasions: lessons for ecology. *TRENDS in Ecology & Evolution*, 8(4): 133–137.

Malchow, H., Petrovskii, S. & Venturino, E. (2008). *Spatiotemporal Patterns in Ecology and Epidemiology: Theory, Models, Simulations.* Chapman & Hall / CRC Press, Boca Raton. Mathematical and Computational Biology Series.

Manchester, S. J. & Bullock, J. M. (2000). The impacts of non-native species on UK biodiversity and the effectiveness of control. *Journal of Applied Ecology*, 37: 845–864.

May, R. M. & Anderson, R. M. (1978). Regulation and stability of host-parasite population interactions: II. destabilizing processes. *Journal of Animal Ecology*, 47(1): 249–267.

Middleton, A. D. (1930). Ecology of the American gray squirrel in the British Isles. *Proceedings of the Zoological Society of London*, 2: 809–843.

Middleton, A. D. (1932). The grey squirrel (*Sciurus carolinensis*) in the British Isles,1930–1932. *Journal of Animal Ecology*, 1(2): 166–167.

Mollison, D. (1991). Dependence of epidemic and population velocities on basic parameters. *Math Biosci*, 107(2): 255–287.

Murray, J. D. (2002). *Mathematical Biology. I: An Introduction*. Springer-Verlag, Berlin, 3rd edn.

Murray, J. D., Stanley, E. A. & Brown, D. L. (1986). On the spatial spread of rabies among foxes. *Proceedings of the Royal Society of London. Series B, Biological Sciences*, 229(1255): 111–150.

Oates, D. W., Sterner, M. C. & Boyd, E. (2000). Meningeal worm in deer from western Nebraska. *Journal of Wildlife Diseases*, 36(2): 370–373.

Okubo, A., Hastings, A. & Powell, T. (2001). Population dynamics in temporal and spatial domains. In: Okubo, A. & Levin, S. A. (Eds.), *Diffusion and Ecological Problems: Modern Perspectives*, chap. 10. Springer-Verlag, New York, 2nd edn.

Okubo, A., Maini, P. K., Williamson, M. H. & Murrayk, J. D. (1989). On the spatial spread of the grey squirrel in Britain. *Proceedings of the Royal Society of London Series B*, 238(1291): 113–125.

Petrovskii, S. V., Malchow, H., Hilker, F. M. & Venturino, E. (2005). Patterns of patchy spread in deterministic and stochastic models of biological invasion and biological control. *Biological Invasions*, 7: 771–793.

Pimentel, D., McNair, S., Janecka, J., Wightman, J., Simmonds, C., O'Connell, C., Wong, E., Russel, L., Zern, J., Aquino, T. & Tsomondo, T. (2001). Economic and environmental threats of alien plant, animal, and microbe invasions. *Agriculture, Ecosystems and Environment*, 84: 1–20.

Pope, C. & Grogan, R. (2003). *Isle of Wight Biodiversity Action Plan*, chap. Red squirrel species action plan. Isle of Wight Biodiversity Action Plan Steering Group.

Prenter, J., MacNeil, C., Dick, J. T. A. & Dunn, A. M. (2004). Roles of parasites in animal invasions. *TRENDS in Ecology & Evolution*, 19(7): 385–390.

Pybus, M. J., Samuel, W. M., Welch, D. A. & Wilke, C. J. (1990). *Parelaphostrongylus andersoni* (Nematoda: Protostrongylidae) in white-tailed deer from Michigan. *Journal of Wildlife Diseases*, 26(4): 535–537.

Renshaw, E. (1991). *Modelling Biological Populations in Space and Time*. Cambridge University Press, Cambridge.

Reynolds, J. C. (1985). Details os the geographic replacement of the red squirrel (*Sciurus vulgaris*) by the grey squirrel (*Sciurus carolinensis*) in Eastern England. *Journal of Animal Ecology*, 54: 149–162.

Rohde, K. (1984). Ecology of marine parasites. *Helgoland Marine Research*, 37(1): 5–33.

Rushton, S. P., Lurz, P. W. W., Fuller, R. & Garson, P. J. (1997). Modelling the distribution of the red and grey squirrel at the landscape scale: a combined GIS and population dynamics approach. *Journal of Applied Ecology*, 34(5): 1137–1154.

Rushton, S. P., Lurz, P. W. W., Gurnell, J. & Fuller, R. (2000). Modelling the spatial dynamics of parapoxvirus disease in red and grey squirrels: a possible cause of the decline in the red squirrel in the UK? *Journal of Applied Ecology*, 37(6): 997–1012.

Rushton, S. P., Lurz, P. W. W., Gurnell, J., Nettleton, P., Bruemmer, C., Shirley, M. D. F. & Sainsbury, A. W. (2006). Disease threats posed by alien species: the role of a poxvirus in the decline of the native red squirrel in Britain. *Epidemiol Infect*, 134(3): 521–533.

Rushton, S. P., Lurz, P. W. W., South, A. B. & Mitchell-Jones, A. (1999). Modelling the distribution of red squirrels (*Sciurus vulgaris*) on the Isle of Wight. *Animal Conservation*, 2: 111–120.

Saenz, R. A. & Hethcote, H. W. (2006). Competing species models with an infectious disease. *Mathematical Biosciences and Engineering*, 3(1): 219–235.

Sainsbury, A. W., Nettleton, P., Gilray, J. & Gurnell, J. (2000). Grey squirrels have high seroprevalence to a parapoxvirus associated with deaths in red squirrels. *Animal Conservation*, 3(3): 229–233.

Sala, O. E., Chapin, F. S. l., Armesto, J. J., Berlow, E., Bloomfield, J., Dirzo, R., Huber-Sanwald, E., Huenneke, L. F., Jackson, R. B., Kinzig, A., Leemans, R., Lodge, H. A., D. M.and Mooney, Oesterheld, M., LeRoy Poff, N., Sykes, M. T., Walker, B. H., Walker, M. & Wall, D. H. (2000). Global Biodiversity Scenarios for the Year 2100. *Science*, 287: 1770–1774.

SAVE OUR SQUIRRELS (2005). Red squirrel reserves – an overview. Available from http://saveoursquirrels.org.

Shigesada, N. & Kawasaki, K. (1997). *Biological Invasions: Theory and Practice*. Oxford University Press, New York.

Shuttleworth, C. M. (2000). The foraging behaviour and diet of red squirrels *Sciurus vulgaris* receiving supplemental feeding. *WILDLIFE BIOLOGY*, 6: 149–156.

Skellam, J. G. (1951). Random dispersal in theoretical populations. *Biometrika*, 38(1/2): 196–218.

Tiley, G. E. D., Dodd, F. S. & Wade, P. M. (1996). emphHeracleum mantegazzianum Sommier & Levier. *Journal of Ecology*, 84(2): 297–319.

Tompkins, D., White, A. R. & Boots, M. (2003). Ecological replacement of native red squirrels by invasive greys driven by disease. *Ecology Letters*, 6(3): 189–196.

Tompkins, D. M., Sainsbury, A. W., Nettleton, P., Buxton, D. & Gurnell, J. (2002). Parapoxvirus causes a deleterious disease in red squirrels associated with UK population declines. *Proceedings of the Royal Society of London Series B*, 269(1490): 529–533.

http://www.redsquirrels.info/index.html (). Friends of Anglesey Red Squirrels.

Vitousek, P. M., D'Antonio, C. M., Loope, L. L., Rejmanek, M. & Westbrooks, R. (1997). Introduced species: a significant component of human-caused global change. *New Zealand Journal of Ecology*, 21(1): 1–16.

Vitousek, P. M., D'Antonio, C. M., Loope, L. L. & Westbrooks, R. (1996). Biological invasions as global environmental change. *American Scientist*, 84: 468–478.

Wauters, L. A., Lurz, P. W. W. & Gurnell, J. (2000). Interspecific effects of grey squirrels (*Sciurus carolinensis*) on the space use and population demography of red squirrels (*Sciurus vulgaris*) in conifer plantations. *Ecological Research*, 15: 271–284.

White, A., Bowers, R. G. & Begon, M. (1999). The spread of infection in seasonal insect-pathogen systems. *Oikos*, 85(3): 487–498.

White, S. (2009a). Formby's red squirrels fighting back from verge of extinction. Available from www.formbytimes.co.uk. Written by Steve Orme, Formby Times (Jul 15).

White, S. (2009b). Monitoring red squirrel numbers in Sefton, Annual Report 2008. Lancashire Wildlife Trust.

Whitfield, F. (2005). Sefton Coast Woodlands Refuge and Buffer Zone launch (Information Sheet).

Whitfield, F. (Ed.) (2008). *North Merseyside Biodiversity Action Plan*. MERSEYSIDE Biodiversity Group.